

Search for flavour-changing neutral current interactions of the top quark and the Higgs boson in events with a pair of τ -leptons in pp collisions at $\sqrt{s} = 13$ TeV with the ATLAS detector



The ATLAS collaboration

E-mail: atlas.publications@cern.ch

ABSTRACT: A search for flavour-changing neutral current (FCNC) tqH interactions involving a top quark, another up-type quark ($q = u, c$), and a Standard Model (SM) Higgs boson decaying into a τ -lepton pair ($H \rightarrow \tau^+\tau^-$) is presented. The search is based on a dataset of pp collisions at $\sqrt{s} = 13$ TeV that corresponds to an integrated luminosity of 139 fb^{-1} recorded with the ATLAS detector at the Large Hadron Collider. Two processes are considered: single top quark FCNC production in association with a Higgs boson ($pp \rightarrow tH$), and top quark pair production in which one of top quarks decays into Wb and the other decays into qH through the FCNC interactions. The search selects events with two hadronically decaying τ -lepton candidates (τ_{had}) or at least one τ_{had} with an additional lepton (e, μ), as well as multiple jets. Event kinematics is used to separate signal from the background through a multivariate discriminant. A slight excess of data is observed with a significance of 2.3σ above the expected SM background, and 95% CL upper limits on the $t \rightarrow qH$ branching ratios are derived. The observed (expected) 95% CL upper limits set on the $t \rightarrow cH$ and $t \rightarrow uH$ branching ratios are 9.4×10^{-4} ($4.8_{-1.4}^{+2.2} \times 10^{-4}$) and 6.9×10^{-4} ($3.5_{-1.0}^{+1.5} \times 10^{-4}$), respectively. The corresponding combined observed (expected) upper limits on the dimension-6 operator Wilson coefficients in the effective tqH couplings are $C_{c\phi} < 1.35$ (0.97) and $C_{u\phi} < 1.16$ (0.82).

KEYWORDS: Flavour Changing Neutral Currents, Hadron-Hadron Scattering, Higgs Physics, Top Physics

ARXIV EPRINT: [2208.11415](https://arxiv.org/abs/2208.11415)

Contents

1	Introduction	1
2	ATLAS detector	4
3	Event reconstruction	4
4	Data sample and event preselection	7
5	Simulated events	8
6	Analysis strategy	11
7	Background estimation	12
7.1	Backgrounds with fake τ -leptons	13
7.2	Background with fake light leptons	14
8	Multivariate discriminant	14
9	Systematic uncertainties	19
9.1	Luminosity	19
9.2	Reconstructed objects	19
9.3	Background modelling	20
9.4	Signal modelling	21
10	Statistical analysis	21
11	Results	22
12	Conclusion	28
A	Fake-τ_{had} scale factor calibration in the CRtt	29
	The ATLAS collaboration	38

1 Introduction

Since the discovery of the Higgs boson in 2012 at the Large Hadron Collider (LHC) by the ATLAS [1] and CMS [2] collaborations, a comprehensive programme of measurements has been conducted to explore this particle. Measurements so far have proved to be consistent with the Standard Model (SM) predictions. The programme is ongoing and precision measurements as well as searches for rare new-physics processes beyond the Standard Model

(BSM) are underway. One such possibility is flavour-changing neutral current (FCNC) interactions between the Higgs boson, the top quark, and an up-type quark, tqH ($q = u, c$), which have been searched for by the ATLAS and CMS collaborations. Since the Higgs boson is lighter than the top quark [3], such interactions could manifest themselves as FCNC top-quark decays ($t \rightarrow qH$) [4].

In the Standard Model (SM), the FCNC interaction is forbidden at tree level and suppressed at higher orders through the Glashow–Iliopoulos–Maiani (GIM) mechanism [5]. An observation of an enhanced rate of this decay would be clear evidence of new physics. Furthermore, if the tqH interaction exists, the associated single-top and Higgs production process through this interaction would enhance the total production cross section of $pp \rightarrow tH$. The $t \rightarrow qH$ branching fraction in the SM is calculated to be exceedingly small, $\mathcal{B}(t \rightarrow qH) \approx 10^{-15}$ [6–9]. However, these branching ratios can be large enough to be observed at LHC when processes beyond the SM are included. Examples of these processes include: quark-singlet models [10], two-Higgs-doublet models (2HDMs) [11] with or without flavour violation, the minimal supersymmetric SM (MSSM) [12–15], supersymmetric models with R-parity violation [16], composite Higgs models with partial compositeness [17], and warped extra dimensions models with SM fermions in the bulk [18]. An even larger branching ratio of $\mathcal{B}(t \rightarrow cH) \sim 10^{-3}$ can be reached in 2HDMs without explicit flavour conservation, since in these models the tree-level FCNC coupling is no longer forbidden by any symmetry [19–26]. The study of $pp \rightarrow tH$ processes will also contribute to the FCNC interaction searches [27]. In the SM, associated production of tH in pp collisions is expected to have a cross section of $\sigma_{tH} = 92_{-12}^{+7}$ fb at a centre-of-mass energy of $\sqrt{s} = 13$ TeV [28].

Searches for $t \rightarrow qH$ decays have been performed by the ATLAS and CMS collaborations, taking advantage of the large samples of top-quark pair ($t\bar{t}$) events collected in proton–proton (pp) collisions at centre-of-mass energies of $\sqrt{s} = 7$ TeV and 8 TeV [29–31] during Run 1 of the LHC, as well as at $\sqrt{s} = 13$ TeV [32] using early Run 2 data. In these searches, one of the top quarks is required to decay into Wb , while the other top quark decays into qH with a small branching ratio $\mathcal{B}(t \rightarrow qH)$, a process denoted by $t\bar{t} \rightarrow WbHq$.¹ The Higgs boson is assumed to have a mass of $m_H = 125$ GeV and to decay as predicted by the SM. Compared to Run 1, the Run 2 searches, summarised in table 1, benefit from the increased $t\bar{t}$ cross section at $\sqrt{s} = 13$ TeV, as well as the larger integrated luminosity. Using 36.1 fb^{-1} of data at $\sqrt{s} = 13$ TeV, the ATLAS Collaboration has derived upper limits at 95% confidence level (CL) on the $t \rightarrow cH$ branching ratio: $\mathcal{B}(t \rightarrow cH) < 0.22\%$ using $H \rightarrow \gamma\gamma$ decays [33] and $\mathcal{B}(t \rightarrow cH) < 0.16\%$ based on multi-lepton (electron or muon) signatures resulting from $H \rightarrow WW^*, ZZ^*, \tau^+\tau^-$ in which both τ -leptons decay leptonically [34]. ATLAS also set upper limits of $\mathcal{B}(t \rightarrow cH) < 0.42\%$ using $H \rightarrow b\bar{b}$ decay [32] and $\mathcal{B}(t \rightarrow cH) < 0.19\%$ using $H \rightarrow \tau^+\tau^-$ decays in which at least one of the τ -leptons decays hadronically [32]. These upper limits are derived assuming that the branching ratio $\mathcal{B}(t \rightarrow uH) = 0$. Similar upper limits are obtained for $\mathcal{B}(t \rightarrow uH)$ when assuming $\mathcal{B}(t \rightarrow cH) = 0$. Combining all of the ATLAS searches using 36.1 fb^{-1} of Run 2 data, upper limits at 95% CL on the branching fractions are set at $\mathcal{B}(t \rightarrow cH) < 0.11\%$ assuming $\mathcal{B}(t \rightarrow uH) = 0$, and at $\mathcal{B}(t \rightarrow uH) < 0.12\%$ assuming $\mathcal{B}(t \rightarrow cH) = 0$ [32].

¹In the following, $WbHq$ is used to denote both $W^+bH\bar{q}$ and its charge conjugate, $HqW^-\bar{b}$. Similarly, $WbWb$ is used to denote $W^+bW^-\bar{b}$.

		\mathcal{L} [fb $^{-1}$]	95% CL observed upper limits	
			on $\mathcal{B}(t \rightarrow cH)$	on $\mathcal{B}(t \rightarrow uH)$
ATLAS	$H \rightarrow b\bar{b}$ [32]	36.1	4.2×10^{-3}	5.2×10^{-3}
	$H \rightarrow \gamma\gamma$ [33]	36.1	2.2×10^{-3}	2.4×10^{-3}
	$H \rightarrow \tau\tau$ ($\tau_{\text{lep}}\tau_{\text{had}}, \tau_{\text{had}}\tau_{\text{had}}$) [32]	36.1	1.9×10^{-3}	1.7×10^{-3}
	$H \rightarrow WW^*, \tau\tau, ZZ^* (2\ell\text{SS}, 3\ell)$ [34]	36.1	1.6×10^{-3}	1.9×10^{-3}
	Combination [32]	36.1	1.1×10^{-3}	1.2×10^{-3}
CMS	$H \rightarrow b\bar{b}$ [35]	35.9	4.7×10^{-3}	4.7×10^{-3}
	$H \rightarrow b\bar{b}$ [36]	137	9.4×10^{-4}	7.9×10^{-4}
	$H \rightarrow \gamma\gamma$ [37]	137	7.3×10^{-4}	1.9×10^{-4}

Table 1. Summary of 95% CL upper limits on $\mathcal{B}(t \rightarrow cH)$ and $\mathcal{B}(t \rightarrow uH)$ obtained by the ATLAS and CMS collaborations with Run 2 data. Each limit is obtained assuming the other branching ratio is zero.

The CMS Collaboration performed a similar search using $H \rightarrow b\bar{b}$ decays [35] with 35.9 fb $^{-1}$ of data at $\sqrt{s} = 13$ TeV, resulting in upper limits of $\mathcal{B}(t \rightarrow cH) < 0.47\%$ and $\mathcal{B}(t \rightarrow uH) < 0.47\%$, in each case neglecting the other decay mode. The search in ref. [35] also considers the contribution to the signal from $pp \rightarrow tH$ production [27]. CMS subsequently updated their search for tqH in the $H \rightarrow b\bar{b}$ channel using the full Run 2 dataset, obtaining observed (expected) upper limits of $\mathcal{B}(t \rightarrow cH) < 9.4 \times 10^{-4}$ (8.6×10^{-4}) and $\mathcal{B}(t \rightarrow uH) < 7.9 \times 10^{-4}$ (1.1×10^{-3}) [36]. CMS also recently reported a search for tqH in the $H \rightarrow \gamma\gamma$ mode using the full Run 2 data and set observed (expected) upper limits on $\mathcal{B}(t \rightarrow Hu)$ of 1.9×10^{-4} (3.1×10^{-4}) and $\mathcal{B}(t \rightarrow Hc)$ of 7.3×10^{-4} (5.1×10^{-4}) [37].

The analysis reported here targets Higgs boson decays into τ -leptons in the complete Run 2 dataset collected by ATLAS in 2015–2018. The corresponding integrated luminosity is 139 fb $^{-1}$. Both $t\bar{t} \rightarrow WbHq$ decays and $pp \rightarrow tH$ production are sought. The dataset is divided into several final states depending on the production mode and the W boson and τ -lepton decays. Top quark pair production events where the W boson decays hadronically (leptonically) are denoted by t_h (t_ℓ). The decays $\tau \rightarrow \ell\nu_\ell\nu_\tau$ are denoted by τ_{lep} , while the decays $\tau \rightarrow \text{hadrons} + \nu_\tau$ are denoted by τ_{had} . The contribution of $W \rightarrow \tau\nu$ is included as τ_{lep} in t_ℓ when the τ -lepton decays into a light lepton (electron or muon) or as τ_{had} in t_h when the τ -lepton decays hadronically. The $H \rightarrow \tau\tau$ decay is detected in either the $\tau_{\text{lep}}\tau_{\text{had}}$ or $\tau_{\text{had}}\tau_{\text{had}}$ final states when the top quark decays hadronically (t_h), but only the $\tau_{\text{had}}\tau_{\text{had}}$ final state is considered when the top quark decays leptonically (t_ℓ), in order to avoid overlaps with other ATLAS searches [34]. In this search, events with two hadronically decaying τ -leptons and no electron or muon define the hadronic channel. Events with at least one τ_{had} and an additional electron or muon (corresponding to t_ℓ or τ_{lep} events) are assigned to leptonic channels. More signal regions (with the top quark decaying leptonically) are exploited here than in the previous FCNC $tqH(\tau\tau)$ search, which was conducted using the partial Run 2 dataset [32]. In addition, an improved treatment of misidentified τ -leptons (‘fakes’) in simulation and in data-driven estimations of fakes from

multi-jet background is implemented. Finally, a multivariate technique based on boosted decision trees is used to discriminate between the signal and the background on the basis of their different kinematical distributions.

2 ATLAS detector

The ATLAS detector [38] at the LHC covers almost the entire solid angle around the collision point,² and it consists of an inner tracking detector surrounded by a thin superconducting solenoid producing a 2 T axial magnetic field, electromagnetic and hadronic calorimeters, and a muon spectrometer incorporating three large toroid magnet assemblies with eight coils each. The inner detector contains a high-granularity silicon pixel detector, including the insertable B-layer [39–41] added as a new innermost layer in 2014, and a silicon microstrip tracker, together providing precise reconstruction of tracks of charged particles in the pseudorapidity range $|\eta| < 2.5$. The inner detector also includes a transition radiation tracker that provides tracking and electron identification for $|\eta| < 2.0$. The calorimeter system covers the pseudorapidity range $|\eta| < 4.9$. Within the region $|\eta| < 3.2$, electromagnetic (EM) calorimetry is provided by barrel and endcap high-granularity lead/liquid-argon (LAr) sampling calorimeters, with an additional thin LAr presampler covering $|\eta| < 1.8$ to correct for energy loss in material upstream of the calorimeters. Hadronic calorimetry is provided by a steel/scintillator-tile calorimeter, segmented into three barrel structures within $|\eta| < 1.7$, and two copper/LAr hadronic endcap calorimeters. The solid angle coverage is completed with forward copper/LAr and tungsten/LAr calorimeter modules optimised for electromagnetic and hadronic measurements, respectively. The calorimeters are surrounded by a muon spectrometer within a magnetic field provided by air-core toroid magnets with a bending integral of about 2.5 T m in the barrel and up to 6.0 T m in the endcaps. The muon spectrometer measures the trajectories of muons with $|\eta| < 2.7$ using multiple layers of high-precision tracking chambers, and it is instrumented with separate trigger chambers covering $|\eta| < 2.4$. A two-level trigger system [42], consisting of a hardware-based level-1 trigger followed by a software-based high-level trigger, is used to reduce the event rate to a maximum of around 1 kHz for offline storage. An extensive software suite [43] is used in the reconstruction and analysis of real and simulated data, in detector operations, and in the trigger and data acquisition systems of the experiment.

3 Event reconstruction

Events are selected from pp collisions at $\sqrt{s} = 13$ TeV recorded by the ATLAS detector during 2015–2018 [44]. Only events for which all relevant subsystems were operational are considered. Events are required to have at least one primary vertex with two or more tracks

²ATLAS uses a right-handed coordinate system with its origin at the nominal interaction point (IP) in the centre of the detector. The x -axis points from the IP to the centre of the LHC ring, the y -axis points upward, and the z -axis coincides with the axis of the beam pipe. Cylindrical coordinates (r, ϕ) are used in the transverse plane, ϕ being the azimuthal angle around the beam pipe. The pseudorapidity is defined in terms of the polar angle θ as $\eta = -\ln \tan(\theta/2)$. Angular separation is measured in units of $\Delta R \equiv \sqrt{(\Delta\eta)^2 + (\Delta\phi)^2}$.

with transverse momentum (p_T) larger than 500 MeV that are consistent with originating from the beam collision region in the x - y plane. If more than one primary vertex candidate is found, the candidate whose associated tracks form the largest sum of squared p_T [45] is selected as the hard-scatter primary vertex.

Electron candidates [46] are reconstructed from energy clusters in the EM calorimeter that are matched to reconstructed tracks in the inner detector; electron candidates in the transition region between the EM barrel and endcap calorimeters ($1.37 < |\eta_{\text{cluster}}| < 1.52$) are excluded. Electron candidates are required to have $|\eta_{\text{cluster}}| < 2.47$, and to satisfy ‘tight’ likelihood-based identification criteria [47] based on calorimeter, tracking and combined variables that provide separation between electrons and jets.

Muon candidates [48] are reconstructed by matching track segments in different layers of the muon spectrometer to tracks found in the inner detector; the resulting muon candidates are re-fitted using the complete track information from both detector systems. Muon candidates are required to have $|\eta| < 2.5$, and to satisfy ‘medium’ identification criteria [49].

Electron (muon) candidates are matched to the primary vertex by requiring that the significance of their transverse impact parameter, d_0 , satisfies $|d_0/\sigma(d_0)| < 5$ (3), where $\sigma(d_0)$ is the measured uncertainty in d_0 , and by requiring that their longitudinal impact parameter, z_0 , satisfies $|z_0 \sin \theta| < 0.5$ mm. To further reduce the background from non-prompt leptons, which originate mostly from heavy-flavour hadron decays, photon conversions and misidentified hadrons, lepton candidates are also required to be isolated in the tracker and in the calorimeter. A track- and cluster-based lepton isolation criterion is defined by placing requirements on the quantities $I_R = \sum p_T^{\text{trk}}$ and $E_R = \sum E^{\text{clst}}$, where the scalar sum runs over all tracks p_T^{trk} or cluster energy deposits E^{clst} (excluding the lepton candidate itself) within the cone defined by $\Delta R < 0.2$ (0.3) around the direction of the electron (muon). The electron (muon) candidates are required to satisfy both $I_R/p_T^\ell < 0.2$ (0.3) and $E_R/p_T^\ell < 0.2$ (0.3), where $\ell = e$ or μ .

‘Tight’ isolation working points are also applied in some channels to reduce fake and non-prompt lepton contributions by using a trained isolation boosted decision tree (BDT) **PromptLeptonVeto** (PLIV), which identifies non-prompt light leptons by using lifetime information associated with a track-jet that matches the selected light lepton. These additional reconstructed charged-particle tracks inside the jet can be used to increase the efficiency for identifying the displaced decay vertices of heavy-flavour (b , c) hadrons that produced non-prompt leptons. The ‘tight’ working points are used for leptons with high p_T (> 20 GeV). Simulation-to-data scale factors for the efficiencies of the ‘tight’ PLIV working points are measured using the tag-and-probe method [47] with $Z \rightarrow \ell^+ \ell^-$ events. These scale factors were checked for electrons or muons from the τ -lepton decays using $Z \rightarrow \tau\tau \rightarrow e\mu 4\nu$ samples, and are consistent at the 2% level. To be conservative, an additional uncertainty of $\pm 2\%$ is considered for the PLIV efficiency for the τ -lepton in the lepton+ τ_{had} channels.

Candidate jets are reconstructed using the anti- k_t algorithm [50, 51] with a radius parameter $R = 0.4$ applied to topological energy clusters [52] and charged-particle tracks, processed using a particle-flow algorithm [53]. The reconstructed jets are then calibrated

to the particle level by the application of a jet energy scale derived from simulation and in situ corrections based on $\sqrt{s} = 13$ TeV data [54]. After being calibrated, the jets are required to have $p_T > 25$ GeV and $|\eta| < 2.5$. The four-momentum of each jet is corrected for pile-up effects using the jet-area method [55].

Quality criteria are imposed to reject events that contain any jets arising from non-collision sources or detector noise [56]. To reduce the contamination due to jets originating from pile-up interactions, additional requirements are imposed on the jet vertex tagger (JVT) [57] output for jets with $p_T < 60$ GeV and $|\eta| < 2.4$.

Jets containing b -hadrons are identified (b -tagged) via the DL1r tagger [58, 59], which uses multivariate techniques to combine information about the impact parameters of displaced tracks and the topological properties of secondary and tertiary decay vertices reconstructed within the jet. For each jet, a value for the multivariate b -tagging discriminant is calculated. A jet is considered b -tagged if this value is above the threshold corresponding to an average 70% efficiency to tag a b -quark jet, with a light-jet³ rejection factor of about 385 and a charm-jet rejection factor of about 12, as determined for jets with $p_T > 20$ GeV and $|\eta| < 2.5$ in simulated $t\bar{t}$ events [58].

Hadronically decaying τ -lepton (τ_{had}) candidates are reconstructed from calorimeter energy clusters and associated inner-detector tracks [60]. Candidates are required to have either one or three associated tracks, with a total charge of ± 1 , and to have $p_T > 25$ GeV with $|\eta| < 2.5$, excluding the EM calorimeter's transition region. A recurrent neural network (RNN) [61] using calorimeter- and tracking-based variables is used to identify τ_{had} candidates and reject jet backgrounds. Three working points, labelled 'loose', 'medium' and 'tight', are defined and correspond to different τ_{had} identification efficiency values, with the efficiency designed to be independent of p_T . The $tqH(\tau\tau)$ search uses the 'medium' working point for the τ_{had} selection. The 'medium' working point has a combined reconstruction and identification efficiency of 75% (60%) for one-prong (three-prong) τ_{had} decays, and an expected rejection factor of 35 (240) against light jets [60]. Electrons that are reconstructed as one-prong τ_{had} candidates are removed via a BDT trained to reject electrons. Events are rejected if the jet seeding the τ_{had} candidate is b -tagged.

To avoid double-counting of reconstructed objects, an overlap removal procedure is applied. Electron candidates that lie within $\Delta R = 0.01$ of a muon candidate are removed to suppress contributions from muon bremsstrahlung. Energy clusters from identified electrons are not excluded during jet reconstruction. In order to avoid double-counting of electrons as jets, the closest jet whose axis is within $\Delta R = 0.2$ of an electron is discarded if the jet is not b -tagged; otherwise the electron is removed. If the electron is within $\Delta R = 0.4$ of the axis of any jet after this initial removal, the jet is retained and the electron is removed. The overlap removal procedure between the remaining jet candidates and muon candidates is designed to remove those muons that are likely to have arisen in the decay of hadrons and to retain the overlapping jet instead. Jets and muons may also appear in close proximity when the jet results from high- p_T muon bremsstrahlung, and in such cases the jet is removed and the muon retained. Such jets are characterised by having very few

³A 'light jet' refers to a jet originating from the hadronisation of a light quark (u, d, s) or a gluon.

matching inner-detector tracks. Selected muons that satisfy $\Delta R(\mu, \text{jet}) < 0.2$ are rejected if the jet is either b -tagged or has at least three tracks originating from the primary vertex; otherwise the jet is removed and the muon is kept. The τ_{had} within a $\Delta R = 0.2$ cone around an electron or muon are removed. In order to avoid double-counting of τ_{had} as jets, the closest jet whose axis is within $\Delta R = 0.2$ of a τ_{had} is discarded if the jet is not b -tagged; otherwise the τ_{had} is removed.

The missing transverse momentum $\vec{p}_{\text{T}}^{\text{miss}}$ (with magnitude $E_{\text{T}}^{\text{miss}}$) is defined as the negative vector sum of the p_{T} of all selected and calibrated objects in the event, including a term to account for momentum from soft particles in the event which are not associated with any of the selected objects. This soft term is calculated from inner-detector tracks matched to the selected primary vertex to make it more resilient to contamination from pile-up interactions [62].

4 Data sample and event preselection

The search is based on a dataset of pp collisions at $\sqrt{s} = 13$ TeV with 25 ns bunch spacing collected from 2015 to 2018, corresponding to an integrated luminosity of 139 fb^{-1} . Only events recorded with a single-electron trigger, a single-muon trigger, or a di- τ -lepton trigger [63–66] under stable beam conditions and for which all detector subsystems were operational are considered for analysis. The events recorded by dilepton triggers that fall into the control regions are used for fake- τ -lepton background estimation as discussed in section 7. The number of pp interactions per bunch crossing in this dataset ranges from about 8 to 45, with an average of 24.

Single-electron and single-muon triggers with low p_{T} thresholds and lepton isolation requirements are combined in a logical OR with higher-threshold triggers that have a looser identification criterion and no isolation requirement. The lowest p_{T} threshold used for muons is 20 (26) GeV in 2015 (2016–2018), while for electrons the threshold is 24 (26) GeV. For di- τ triggers, the p_{T} threshold for the leading (subleading) τ_{had} candidate is 35 (25) GeV. To reduce the impact of the trigger efficiency uncertainty around the threshold, the leptons are required to have a p_{T} that is at least 1 GeV above the threshold. The reconstructed τ -leptons are required to have a p_{T} at least 5 GeV higher than the trigger threshold. The events in the leptonic channels are recorded by a single-electron or single-muon trigger, and are required to have exactly one electron or muon that matches, within $\Delta R < 0.15$, the lepton reconstructed by at least one of the possible triggers. The following additional requirements are applied.

- $t_h \tau_{\text{lep}} \tau_{\text{had}}$: To enhance selection of the $t_h H$ and $t_h t(qH)$ final states with a $H \rightarrow \tau_{\text{lep}} \tau_{\text{had}}$ decay, exactly one τ_{had} with opposite-sign charge to τ_{lep} is required, plus at least three jets with exactly one b -jet.
- $t_{\ell} \tau_{\text{had}} \tau_{\text{had}}$: To enhance selection of $t_{\ell} H$ and $t_{\ell} t(qH)$ final states with a $H \rightarrow \tau_{\text{had}} \tau_{\text{had}}$ decay, exactly one light lepton and two opposite-sign τ_{had} are required, plus jets with exactly one b -jet.

Requirement	Leptonic channels			Hadronic channel
	$t_h \tau_{\text{lep}} \tau_{\text{had}}$	$t_\ell \tau_{\text{had}} \tau_{\text{had}}$	$t_\ell \tau_{\text{had}}$	$t_h \tau_{\text{had}} \tau_{\text{had}}$
Trigger	single-lepton trigger			di- τ trigger
Leptons	=1 isolated e or μ			=0 isolated e or μ
τ_{had}	=1 τ_{had}	=2 τ_{had}	=1 τ_{had}	=2 τ_{had}
Electric charge (Q)	$Q_\ell \times Q_{\tau_{\text{had}1}} = -1$	$Q_{\tau_{\text{had}1}} \times Q_{\tau_{\text{had}2}} = -1$	$Q_\ell \times Q_{\tau_{\text{had}1}} = 1$	$Q_{\tau_{\text{had}1}} \times Q_{\tau_{\text{had}2}} = -1$
Jets	≥ 3 jets	≥ 1 jets	≥ 2 jets	≥ 3 jets
b -tagging		=1 b -jets		=1 b -jets

Table 2. Summary of the preselection requirements. The leading and subleading τ_{had} candidates are denoted by $\tau_{\text{had}1}$ and $\tau_{\text{had}2}$ respectively.

- $t_\ell \tau_{\text{had}}$: This channel enhances the selection of $t_\ell H$ and $t_\ell t(qH)$ final states with a $H \rightarrow \tau_{\text{had}} \tau_{\text{had}}$ decay where one τ_{had} fails the applied reconstruction or identification criterion so that there is only one reconstructed τ_{had} candidate. To reduce the SM backgrounds and avoid overlaps with the final states used in other ATLAS searches, exactly one τ_{had} with the same charge as that assigned to the light lepton is required. In addition, at least two jets including exactly one b -jet are required.

The events in the hadronic channel are selected by a di- τ trigger. Further requirements are:

- $t_h \tau_{\text{had}} \tau_{\text{had}}$: The $t_h H$ and $t_h t(qH)$ final states with $H \rightarrow \tau_{\text{had}} \tau_{\text{had}}$ decay are targeted. Exactly two τ_{had} with opposite-sign charge and at least three jets, including exactly one b -jet, are required.

The above requirements apply to the reconstructed objects defined in section 3. These requirements are referred to as the preselection and are summarised in table 2.

5 Simulated events

An overview of the Monte Carlo (MC) generators used for the main signal and background samples is summarised in table 3. Samples of simulated $t\bar{t} \rightarrow WbHq$ ($t\bar{t}(qH)$) events were generated with the next-to-leading-order (NLO) generator⁴POWHEG BOX v2 [67–70] with the NNPDF3.0NLO [71] parton distribution function (PDF) set and interfaced to PYTHIA 8.212 [72] with the NNPDF2.3LO [73] PDF set for the modelling of the parton showers (PS), hadronisation, and underlying event. A set of tuned parameters called the A14 tune [74] was used in PYTHIA to control the modelling of multi-parton interactions and initial- and final-state radiation. The signal sample is normalised to the same total cross section as is used for the inclusive $t\bar{t} \rightarrow WbWb$ sample (see discussion below) assuming a benchmark branching ratio of $\mathcal{B}_{\text{ref}}(t \rightarrow qH) = 0.1\%$. The case of both top quarks decaying into qH is neglected in the analysis given the existing upper limits on $\mathcal{B}(t \rightarrow qH)$ (section 1).

⁴In the following, the order of a generator should be understood as referring to the order in the strong coupling constant at which the matrix-element (ME) calculation is performed.

The tH signal events were generated by MADGRAPH5_AMC@NLO 2.6.2 [75] (referred to in the following as MG5_AMC) with the NNPDF3.0NLO parton distribution function (PDF) set. The parton showers, hadronisation, and underlying event were modelled by PYTHIA 8.212 with the NNPDF2.3LO PDF set in combination with the A14 tune. Depending on whether the up quark or the charm quark is involved in the FCNC production process, the effective Lagrangian of the tqH interaction is parameterised using dimension-6 operators [76]. The cross sections $\sigma(ug \rightarrow tH) = 0.711$ pb and $\sigma(cg \rightarrow tH) = 0.103$ pb were obtained using $\mathcal{B}_{\text{ref}}(t \rightarrow qH) = 0.1\%$ as the benchmark.

The sample used to model the $t\bar{t}$ background was generated with the NLO generator POWHEG BOX v2 using the NNPDF3.0NLO PDF set. The POWHEG BOX model parameter h_{damp} , which controls matrix element to parton shower matching and regulates the high- p_T radiation, was set to 1.5 times the top-quark mass. The parton showers, hadronisation, and underlying event were modelled by PYTHIA 8.210 with the NNPDF2.3LO PDF set in combination with the A14 tune. Alternative $t\bar{t}$ simulation samples used to derive parton shower systematic uncertainties are described in section 9.3. The generated $t\bar{t}$ samples are normalised to a theoretical cross section of $\sigma_{t\bar{t}} = 832^{+46}_{-51}$ pb, computed using TOP++ 2.0 [77] at next-to-next-to-leading order (NNLO), including resummation of next-to-next-to-leading logarithmic (NNLL) soft gluon terms [78–82].

Samples of single-top-quark events corresponding to the t -channel production mechanism were generated with the POWHEG BOX v2 generator [83], using the four-flavour scheme for the NLO matrix-element calculations and the corresponding NNPDF3.0NLO set of PDFs. Samples corresponding to the tW - and s -channel production mechanisms were generated with POWHEG BOX v2 using the five-flavour scheme. Overlaps between the $t\bar{t}$ and tW final states were avoided by using the diagram removal scheme [84]. The parton showers, hadronisation and underlying event were modelled using PYTHIA 8.230 [85] with the A14 tune and the NNPDF2.3LO PDF set. The single-top-quark samples are normalised to the approximate NNLO theoretical cross sections [86–88].

Samples of W/Z +jets events were generated with the SHERPA 2.2.1 [89] generator. The matrix element was calculated for up to two partons at NLO and up to four partons at LO using COMIX [90] and OPENLOOPS [91]. The matrix-element calculation was merged with the SHERPA parton shower [92] using the MEPS@NLO prescription [93]. The PDF set used for the matrix-element calculation is NNPDF3.0NNLO [71] with a dedicated parton shower tune developed for SHERPA. Separate samples were generated for different W/Z +jets categories using filters for a b -jet ($W/Z+\geq 1b$ +jets), a c -jet and no b -jet ($W/Z+\geq 1c$ +jets), and with a veto on b - and c -jets (W/Z +light-jets), and were combined into the inclusive W/Z +jets samples. The W +jets and Z +jets samples are normalised to their respective inclusive NNLO theoretical cross sections calculated with FEWZ [94].

Samples of $WW/WZ/ZZ$ +jets events were generated with SHERPA 2.2.1 using the CT10 PDF set and include processes containing up to four electroweak vertices. In the case of WW/WZ +jets (ZZ +jets) the matrix element was calculated for zero (up to one) additional partons at NLO and up to three partons at LO using the same procedure as for the W/Z +jets samples. The final states that were simulated require one of the bosons to decay leptonically and the other hadronically. All diboson samples are normalised to their NLO theoretical cross sections provided by SHERPA.

Process	Generator		PDF set		Tune	Order
	ME	PS	ME	PS		
$t\bar{t}(qH)$ signal	POWHEG BOX	PYTHIA 8	NNPDF3.0NLO	NNPDF2.3LO	A14	NLO
tH signal	MADGRAPH5_AMC@NLO	PYTHIA 8	NNPDF3.0NLO	NNPDF2.3LO	A14	NLO
W/Z +jets	SHERPA 2.2.1		NNPDF3.0NNLO		SHERPA	NLO/LO
$t\bar{t}$	POWHEG BOX	PYTHIA 8	NNPDF3.0NLO	NNPDF2.3LO	A14	NLO
Single top	POWHEG BOX	PYTHIA 8	NNPDF3.0NLO	NNPDF2.3LO	A14	NLO
$t\bar{t}X$	MADGRAPH5_AMC@NLO	PYTHIA 8	NNPDF3.0NLO	NNPDF2.3LO	A14	NLO
VH	POWHEG BOX	PYTHIA 8	PDF4LHC15	CTEQ6L1	AZNLO	NLO
tH	MADGRAPH5_AMC@NLO	PYTHIA 8	CT10		A14	NLO
Diboson	SHERPA 2.2.1		NNPDF3.0NNLO		SHERPA	NLO/LO

Table 3. Overview of the MC generators used for the main signal and background samples, including the matrix element (ME), parton shower (PS), parton distribution function set (PDF), and cross-section calculation order (Order).

Samples of $t\bar{t}V$ ($V = W, Z$ boson) and $t\bar{t}H$ events were generated with MG5_AMC 2.2.1, using NLO matrix elements and the NNPDF3.0NLO PDF set, and interfaced to PYTHIA 8.210 with the NNPDF2.3LO PDF set and the A14 tune. The $t\bar{t}V$ samples are normalised to the NLO cross section computed with MG5_AMC, while the $t\bar{t}H$ sample is normalised using the NLO cross section recommended in ref. [28].

Samples of WH and ZH , collectively referred to as VH , were generated using POWHEG BOX v2 [67–70] and interfaced to PYTHIA 8.210 with the PDF4LHC15 PDF set and the AZNLO tune. The contribution of tH associated production is also considered as part of the SM Higgs background. The sample was generated using MADGRAPH5_AMC@NLO 2.6.2 [75] and interfaced to PYTHIA 8.210 with the CT10 PDF set and the A14 tune. The MC predictions are normalised using the NLO cross section recommended in ref. [28]. The contribution of triboson production is found to be negligible.

All generated samples, except those produced with the SHERPA [89] event generator, utilise EVTGEN 1.2.0 [95] to model the decays of heavy-flavour hadrons. The effects of multiple interactions in the same and nearby bunch crossings (pile-up) were modelled by overlaying minimum-bias events, simulated using the soft QCD processes of PYTHIA 8.186 [85] with the A3 tune [96] and NNPDF2.3LO PDF set [73].

The generated events were processed through a simulation [97] of the ATLAS detector geometry and response using GEANT4 [98]. A faster simulation, where the full GEANT4 simulation of the calorimeter response is replaced by a detailed parameterisation of the shower shapes [99], was adopted for some of the samples used to estimate systematic uncertainties in background modelling. Simulated events were processed through the same reconstruction software as the data, and corrections were applied so that the object identification efficiencies, energy scales and energy resolutions match those determined from data control samples.

	Regions	b -jets	Light-flavour jets	Leptons	Hadronic τ decays	Charge
SR	$t_\ell \tau_{\text{had}} \tau_{\text{had}}$	1	≥ 0	1	2	$\tau_{\text{had}} \tau_{\text{had}}$ OS
	$t_\ell \tau_{\text{had}}\text{-1j}$	1	1	1	1	$t_\ell \tau_{\text{had}}$ SS
	$t_\ell \tau_{\text{had}}\text{-2j}$	1	2	1	1	$t_\ell \tau_{\text{had}}$ SS
	$t_h \tau_{\text{lep}} \tau_{\text{had}}\text{-2j}$	1	2	1	1	$\tau_{\text{lep}} \tau_{\text{had}}$ OS
	$t_h \tau_{\text{lep}} \tau_{\text{had}}\text{-3j}$	1	≥ 3	1	1	$\tau_{\text{lep}} \tau_{\text{had}}$ OS
	$t_h \tau_{\text{had}} \tau_{\text{had}}\text{-2j}$	1	2	0	2	$\tau_{\text{had}} \tau_{\text{had}}$ OS
	$t_h \tau_{\text{had}} \tau_{\text{had}}\text{-3j}$	1	≥ 3	0	2	$\tau_{\text{had}} \tau_{\text{had}}$ OS
VR	$t_\ell \tau_{\text{had}} \tau_{\text{had}}\text{-SS}$	1	≥ 0	1	2	$\tau_{\text{had}} \tau_{\text{had}}$ SS
	$t_h \tau_{\text{had}} \tau_{\text{had}}\text{-3j SS}$	1	≥ 3	0	2	$\tau_{\text{had}} \tau_{\text{had}}$ SS
CRtt	$t_\ell t_\ell 1b \tau_{\text{had}}$	1	≥ 0	2	1	$t_\ell t_\ell$ OS
	$t_\ell t_\ell 2b \tau_{\text{had}}$	2	≥ 0	2	1	$t_\ell t_\ell$ OS
	$t_\ell t_h 2b \tau_{\text{had}}\text{-2jSS}$	2	2	1	1	$t_\ell \tau_{\text{had}}$ SS
	$t_\ell t_h 2b \tau_{\text{had}}\text{-2jOS}$	2	2	1	1	$t_\ell \tau_{\text{had}}$ OS
	$t_\ell t_h 2b \tau_{\text{had}}\text{-3jSS}$	2	≥ 3	1	1	$t_\ell \tau_{\text{had}}$ SS
	$t_\ell t_h 2b \tau_{\text{had}}\text{-3jOS}$	2	≥ 3	1	1	$t_\ell \tau_{\text{had}}$ OS

Table 4. Overview of the signal regions (SR), validation region (VR), and $t\bar{t}$ control regions (CRtt) used for the fake- τ -lepton scale factor derivation in the leptonic channels. Leptons are required to have either same-sign (SS) or opposite-sign (OS) charges in each region.

6 Analysis strategy

The analysis strategy adopted in this FCNC $tqH(\tau\tau)$ search is similar to the one used in refs. [32, 100] but extended to more search channels. The $t\bar{t}(qH)$ and tH signal being probed is characterised by the presence of τ -leptons from the decay of the Higgs boson, where the remaining top quark decays into Wb . There is an additional q -jet from the FCNC $t \rightarrow qH$ decay in the top pair production. If the W boson or one of the τ -leptons decays leptonically, an isolated electron or muon, together with significant $E_{\text{T}}^{\text{miss}}$, is also expected. In a significant fraction of the events, the lowest- p_{T} jet from the hadronic W boson decay fails the minimum p_{T} requirement of 25 GeV, resulting in only three reconstructed jets where the production mode is dominant. In order to optimise the sensitivity of the search, the selected events are categorised into seven signal regions (SRs) based on the numbers of light leptons, τ_{had} candidates, and light-flavour jets: $t_\ell \tau_{\text{had}} \tau_{\text{had}}$, $t_\ell \tau_{\text{had}}$ (1j and 2j), $t_h \tau_{\text{lep}} \tau_{\text{had}}$ (2j and 3j), $t_h \tau_{\text{had}} \tau_{\text{had}}$ (2j and 3j), as shown in table 4.

This event categorisation is primarily used to optimise the sensitivity in each signal region that targets either leptonic or hadronic top-quark decays as well as the Higgs boson decays into either the $\tau_{\text{lep}} \tau_{\text{had}}$ or $\tau_{\text{had}} \tau_{\text{had}}$ final state. The contribution of background to the signal regions of the $t_h \tau_{\text{had}} \tau_{\text{had}}$ and $t_h \tau_{\text{lep}} \tau_{\text{had}}$ channels is reduced by placing kinematic constraints on the di- τ mass and the $E_{\text{T}}^{\text{miss}}$ in the event [100].

For the $t_h t(qH)$ events, the jet from $t \rightarrow qH$, referred to as the FCNC jet (q -jet), should be a high- p_{T} jet from the decay chain $t \rightarrow qH \rightarrow q\tau\tau$, with τ -leptons reconstructed as $\tau_{\text{lep}} \tau_{\text{had}}$ or $\tau_{\text{had}} \tau_{\text{had}}$. Events should contain four jets, with the one having the smallest

angular separation from the visible di- τ system being labelled the q -jet since the FCNC top-quark decay products are likely to be boosted closer together. If there are more than two jets besides the q -jet and b -jet, the jets from the W boson decay are chosen to be those from the combination with an invariant mass closest to the W boson mass. It is possible that one of the jets fails the p_T requirement and is not reconstructed. Events of this kind produce the $t_h H$ final state. When both the t_h and H can be reconstructed, three jets come from the top quark's hadronic decay, including a b -jet, and a pair of opposite-sign τ_{had} come from the Higgs boson decay.

The four-momenta of the invisible decay products from the decay of the τ -leptons are estimated using a kinematic fit and assuming a collinear approximation for the τ decay products. The fit is done by minimising a χ^2 function based on the Gaussian constraints placed on the Higgs boson mass ($m_H = 125$ GeV) and the measured $E_{x,y}^{\text{miss}}$ within their expected resolutions ($\sigma_{E_{x,y}^{\text{miss}}}$), defined as

$$\chi^2 = \left(\frac{m_{\tau\tau,\text{fit}} - m_H}{\sigma_{\tau\tau}} \right)^2 + \left(\frac{E_{x,\text{fit}}^{\text{miss}} - E_x^{\text{miss}}}{\sigma_{E_x^{\text{miss}}}} \right)^2 + \left(\frac{E_{y,\text{fit}}^{\text{miss}} - E_y^{\text{miss}}}{\sigma_{E_y^{\text{miss}}}} \right)^2. \quad (6.1)$$

The Higgs boson mass resolution ($\sigma_{\tau\tau}$) is estimated to be 20 GeV from a fit of the mass distribution of the simulated tqH signal events, while the E_T^{miss} measurement's resolution is parameterised as a linear function of $\sqrt{\sum E_T}$, where $\sum E_T$ is the scalar sum of the E_T values of all physics objects contributing to the E_T^{miss} reconstruction [62]. After the χ^2 minimisation, both the Higgs boson p_T and the p_T values of the parent top quarks are determined with better resolution in the signal events.

For the $t_\ell t(qH)$ and $t_\ell H$ events where the W boson from $t \rightarrow Wb$ decay decays leptonically, the kinematic fit is no longer feasible due to the neutrino from the $W \rightarrow \ell\nu$ decay. The kinematic variables are calculated using the visible objects only. After the event reconstruction, a number of these variables are used in a multivariate analysis to discriminate the signal from the background, as described in section 8.

7 Background estimation

Most background processes are modelled using MC simulation. After the event preselection, the main background is $t\bar{t}$ production, often in association with jets, denoted by $t\bar{t}+\text{jets}$ in the following. Small contributions arise from single-top-quark, $W/Z+\text{jets}$, multi-jet and diboson (WW, WZ, ZZ) production, as well as from the associated production of a vector boson V ($V = W, Z$) or a Higgs boson and a $t\bar{t}$ pair ($t\bar{t}V$ and $t\bar{t}H$). All backgrounds with prompt leptons, i.e. those originating from the decay of a W boson, a Z boson, or a τ -lepton, are estimated using samples of simulated events and are initially normalised to their theoretical cross sections. In the simulation, the top-quark and SM Higgs boson masses are set to 172.5 GeV and 125 GeV, respectively, and the Higgs boson is forced to decay via $H \rightarrow \tau\tau$ with a branching ratio calculated using HDECAY [101]. Backgrounds with non-prompt light leptons (electron or muon), with photons or jets misidentified as electrons, or with jets misidentified as τ -lepton candidates, generically referred to as fake leptons,

are estimated using data-driven methods. The background prediction is improved during the statistical analysis by performing a likelihood fit to data using several signal-depleted control regions as shown in table 4. The events with one light lepton, two same-sign τ_{had} , and one b -jet, are also selected, providing a validation region (VR) for the background estimation in the leptonic channels.

7.1 Backgrounds with fake τ -leptons

The background with one or more fake τ candidates arises mainly from $t\bar{t}$ or multi-jet production, depending on the search channel. Studies based on simulation show that, for all the above processes, fake τ candidates primarily result from the misidentification of light jets and b -quark jets. It is also found that the fake rate decreases for all jet flavours as the τ candidate's p_T increases.

In the leptonic channels, the events with a prompt electron or muon and fake τ -leptons are modelled by calibrating the MC samples with scale factors (SF) derived from the dedicated $t\bar{t}$ control regions (CR $_{t\bar{t}}$) using dileptonic decays of $t\bar{t}$ pairs and semileptonic decays of $t\bar{t}$ pairs with two b -jets, as is summarised in table 4. The control regions are defined similarly to the signal regions but with an additional b -jet or light lepton. There are four kinds of fake τ -leptons that need to be calibrated: Type-1 fake τ -leptons from hadronic W boson decay (τ_W) with opposite-sign (OS) charge relative to the light lepton; Type-2 τ_W 's with same-sign (SS) charge relative to the light lepton; Type-3 fake τ -leptons originating from b -hadron decays; and Type-4 fake τ -leptons from light-flavour hadron decays. The dilepton regions ($t_\ell t_\ell 1b\tau_{\text{had}}$ and $t_\ell t_\ell 2b\tau_{\text{had}}$) are used to calibrate Type-3 and Type-4 fake τ -leptons. The semileptonic regions ($t_\ell t_h 2b\tau_{\text{had}}\text{-2jOS}$ and $t_\ell t_h 2b\tau_{\text{had}}\text{-3jOS}$), where the τ_{had} and light lepton have opposite charges, are used to calibrate Type-1 fake τ -leptons. Similarly for Type-2, the semileptonic regions ($t_\ell t_h 2b\tau_{\text{had}}\text{-2jSS}$ and $t_\ell t_h 2b\tau_{\text{had}}\text{-3jSS}$), where the τ_{had} and light lepton have same charges, are used. A simultaneous fit to data is made to derive the scale factors for fake τ -leptons in the MC samples. These consist of a total of 24 parameters depending on four types of fake τ -leptons, three p_T bins, and two bins for 1- and 3-prong τ decays separately. The post-fit distributions of the leading τ_{had} p_T and measured τ scale factors are presented in appendix A. The values of these scale factors range from 0.3 to 1.28 and are used to correct the MC-estimated fakes in the corresponding signal regions with a single b -jet. In the $t_\ell \tau_{\text{had}} \tau_{\text{had}}$ channel, both τ candidates can be misidentified, so the calibration is applied to each τ candidate separately, following the same procedure used in the $\tau_{\text{lep}} \tau_{\text{had}}$ channel. The central values of the scale factors vary according to their uncertainties in the final fit. A closure test is made for the fake- τ estimates, using the same procedure as in the $t_\ell \tau_{\text{had}} \tau_{\text{had}}\text{-SS}$ validation region, and it shows good agreement between data and the background prediction.

In the hadronic channels, the contribution of fakes is estimated from data using the fake-factor (FF) method to derive the transfer functions from the background-enriched control regions (CR) to the SR [102]. These CRs do not overlap with the main signal regions discussed in section 6. The CR selection requirements are analogous to those used to define signal regions, except that the subleading τ candidate is required to fail the ‘medium’ τ identification while still passing a loose requirement. The contribution of

fakes with subleading τ candidates can be calculated by rescaling the templates for ‘loose’ τ candidates in the CR with the FFs. The templates are produced by subtracting all MC background contributions with real subleading τ -leptons from the data. The FFs are computed as the ratio of misidentified τ_{had} candidates that either pass or fail the ‘medium’ τ ID selection in regions enriched in events originating from W +jets processes [102]. FFs obtained from the W +jets events are compared with those from the same-sign $\tau_{\text{had}}\tau_{\text{had}}$ control regions and the differences are treated as systematic uncertainties.

7.2 Background with fake light leptons

The background originating from non-prompt or misidentified light leptons is primarily from multi-jet production. The contribution from these events is estimated with a data-driven method called ABCD. The estimate is based on the numbers of ‘tight’ and ‘loose’ light leptons that passed and failed the PLIV cut in the low (< 25 GeV) and high (> 25 GeV) $E_{\text{T}}^{\text{miss}}$ regions. The number of fake light leptons in the signal region is evaluated by scaling the number of ‘loose’ leptons in the high $E_{\text{T}}^{\text{miss}}$ region by the ratio of ‘tight’ leptons to ‘loose’ leptons in the low $E_{\text{T}}^{\text{miss}}$ region. The contributions of prompt leptons and calibrated fake τ -leptons to the numbers of ‘tight’ and ‘loose’ leptons are subtracted using MC simulation. A closure test is made for the background estimates in the signal-depleted low-BDT-score (< -0.6) regions, defined in section 8. The data are in good agreement with the background prediction in the $t_{\ell}\tau_{\text{had}}$ channels, while the fake light leptons are negligible in other leptonic channels.

8 Multivariate discriminant

Boosted decision trees implemented in the TMVA framework [103] are used in each SR to improve the separation between signal and background. In the training process, all signal events from $tt(qH)$ and tH are combined for tuH and tcH . All background sources from SM processes (including both the real and fake τ contributions) are also used in the training.

Many potential variables were investigated in each SR separately. The discrimination of a given variable is quantified by the ‘separation’ (which measures the degree of overlap between background and signal distribution shape) and ‘importance’ (which ranks the power of the variable in the classification of the events) provided by the TMVA package. The BDT discriminant is trained for each SR starting from a large list of variables; then the least important variables are removed sequentially, and the BDT is retrained until the receiver operating characteristic (ROC) score, the area under the ROC curve, drops by more than 2%. The final BDT input variables in each SR and their importance ranking are listed in table 5. The discriminating variables are as follows:

- $E_{\text{T}}^{\text{miss}}$ is the missing transverse momentum.
- $p_{\text{T}\tau 1}$ is the transverse momentum of the leading τ -lepton candidate.
- $\max(\eta_{\tau})$ is the maximum η of the τ_{had} candidate(s).
- p_{T}^{ℓ} is the transverse momentum of the leading light lepton.

	$t_\ell\tau_{\text{had-1j}}$	$t_h\tau_{\text{lep}}\tau_{\text{had-2j}}$	$t_\ell\tau_{\text{had-2j}}$	$t_h\tau_{\text{lep}}\tau_{\text{had-3j}}$	$t_\ell 2\tau_{\text{had}}$	$t_h 2\tau_{\text{had-2j}}$	$t_h 2\tau_{\text{had-3j}}$
Total variables (n)	12	15	12	17	15	12	12
$E_{\text{T}}^{\text{miss}}$	5	11	10	13	6	7	13
$p_{\text{T}\tau 1}$	1	4	1	1	5	11	10
$\max(\eta_\tau)$	4		4		10		
p_{T}^ℓ	12	15	12	17			
χ^2				14			
m_{bjj}		1		2		3	4
m_{T}^W	11		8		13		
$m_{\tau\tau, \text{fit}}$		2		3		1	1
m_{jj}				9		6	7
$m_{\tau\tau\text{q}, \text{fit}}$						10	6
$m_{\tau\tau}$	10	14	11	6	1	2	2
$p_{\text{T}\tau^+\tau^-}$					9		
$m_{\tau\tau\text{q}}$					3		
$m_{\ell\text{b}}$	3		5		4		
$\min(m_{\tau\tau\text{j}})$	9		3		14		
$\min(m_{\text{jj}})$		12		11			
$E_{\text{T}}^{\text{miss}}$ centrality		13		15		12	9
$E_{\tau 1}/E_{\tau 1, \text{fit}}$		10		12		8	8
$E_{\tau 2}/E_{\tau 2, \text{fit}}$		7		4		9	11
$\Delta\phi(\tau\tau, E_{\text{T}}^{\text{miss}})$		6		16		13	12
$\min(\Delta R(\ell, \tau))$	8	9	9	10	15		
$\Delta R(\tau, \tau)$					2	4	3
$\Delta R(\ell, b\text{-jet})$	2	3	2	8	12		
$\Delta R(\tau 1, b\text{-jet})$	6	5	6	7	11		
$\Delta R(\ell + b\text{-jet}, \tau\tau)$					7		
$\Delta R(\tau 1, \text{light-jet})$	7	8	7	5	8	5	5

Table 5. Discriminating variables (n) used in the training of the BDT of each SR. The ranking of the input variables according to their importance in the training is reported from highest (1) to lowest (n). Variables whose ranking is missing are not included in the training of that SR. The description of each variable is provided in the text.

- χ^2 of the kinematic fit of the momentum of the invisible decay products of the τ -leptons as defined in eq. (6.1).
- m_{bjj} is the invariant mass of the b -jet and the two jets from the W boson decay, and reflects the top-quark mass in the decay $t \rightarrow Wb \rightarrow j_1 j_2 b$. This variable is only defined for the 4-jet $t_h H$ and $t_h t(qH)$ events.
- m_{T}^W is the transverse mass calculated from the lepton and $E_{\text{T}}^{\text{miss}}$ in the leptonic channels, defined as

$$m_{\text{T}}^W = \sqrt{2p_{\text{T}\ell} E_{\text{T}}^{\text{miss}} (1 - \cos \Delta\phi_{\ell, \text{miss}})},$$

where $\Delta\phi_{\ell, \text{miss}}$ is the azimuthal angle between the light lepton and $E_{\text{T}}^{\text{miss}}$.

- $m_{\tau\tau,\text{fit}}$ is the fitted invariant mass of the τ candidates and reconstructed neutrinos for the $t_h H$ and $t_h t(qH)$ events.
- m_{jj} is the reconstructed invariant mass of two light jets from the W decay with a mass closest to the known W boson mass.
- $m_{\tau\tau q,\text{fit}}$ is the fitted invariant mass of the FCNC-decaying top quark reconstructed from the di- τ candidates, q -jet and reconstructed neutrinos.
- $m_{\tau\tau}$ is the visible invariant mass of the di- τ system (including the light lepton when there is only one τ_{had} candidate).
- $p_{T\tau\tau}$ is the visible p_T of the di- τ system.
- $m_{\tau\tau q}$ is the reconstructed visible mass of the FCNC-decaying top quark.
- $m_{\ell b}$ is the invariant mass of the lepton and the b -jet, which reflects the visible top-quark mass.
- $\min(m_{\tau\tau j})$ is the minimum value of the visible mass of the di- τ candidates (including leptonically decaying τ candidates) and the light-flavour jet, reflecting the invariant mass of the visible FCNC top-quark decay products.
- $\min(m_{jj})$ is the minimum value of the invariant mass of all the light-flavour jet pairs, reflecting the invariant mass of the W boson candidate.
- E_T^{miss} centrality is a measure of how centrally the E_T^{miss} lies between the two τ candidates in the transverse plane, and is defined as

$$E_T^{\text{miss}} \text{ centrality} = (x + y) / \sqrt{x^2 + y^2},$$

$$\text{with } x = \frac{\sin(\phi_{\text{miss}} - \phi_{\tau_1})}{\sin(\phi_{\tau_2} - \phi_{\tau_1})}, \quad y = \frac{\sin(\phi_{\tau_2} - \phi_{\text{miss}})}{\sin(\phi_{\tau_2} - \phi_{\tau_1})},$$

- $E_{\tau i} / E_{\tau i,\text{fit}}$ ($i = 1, 2$) is the momentum fraction carried by the visible decay products from the leading and subleading τ decays. It is based on the best fit of the four-momentum of the neutrino(s) according to the event reconstruction algorithm in this section. For the τ_{had} decay mode, the visible decay products carry most of the τ -lepton's energy since there is only a single neutrino in the final state.
- $\Delta\phi(\tau\tau, E_T^{\text{miss}})$ is the azimuthal angle between the E_T^{miss} and di- τ system's p_T .
- $\Delta R(a, b)$ is the angular distance between the a and b objects in the event.

Comparisons between the data and the predicted background for the distributions of leading τ_{had} p_T and visible invariant mass of the di- τ system ($m_{\tau\tau}$) in SRs and VRs, after applying fake factors, are shown in figures 1 and 2, respectively. The data are well described by the background model in all cases. The final observable used to extract the signal contribution is the BDT distribution in each SR corresponding to either the tuH or tcH signal.

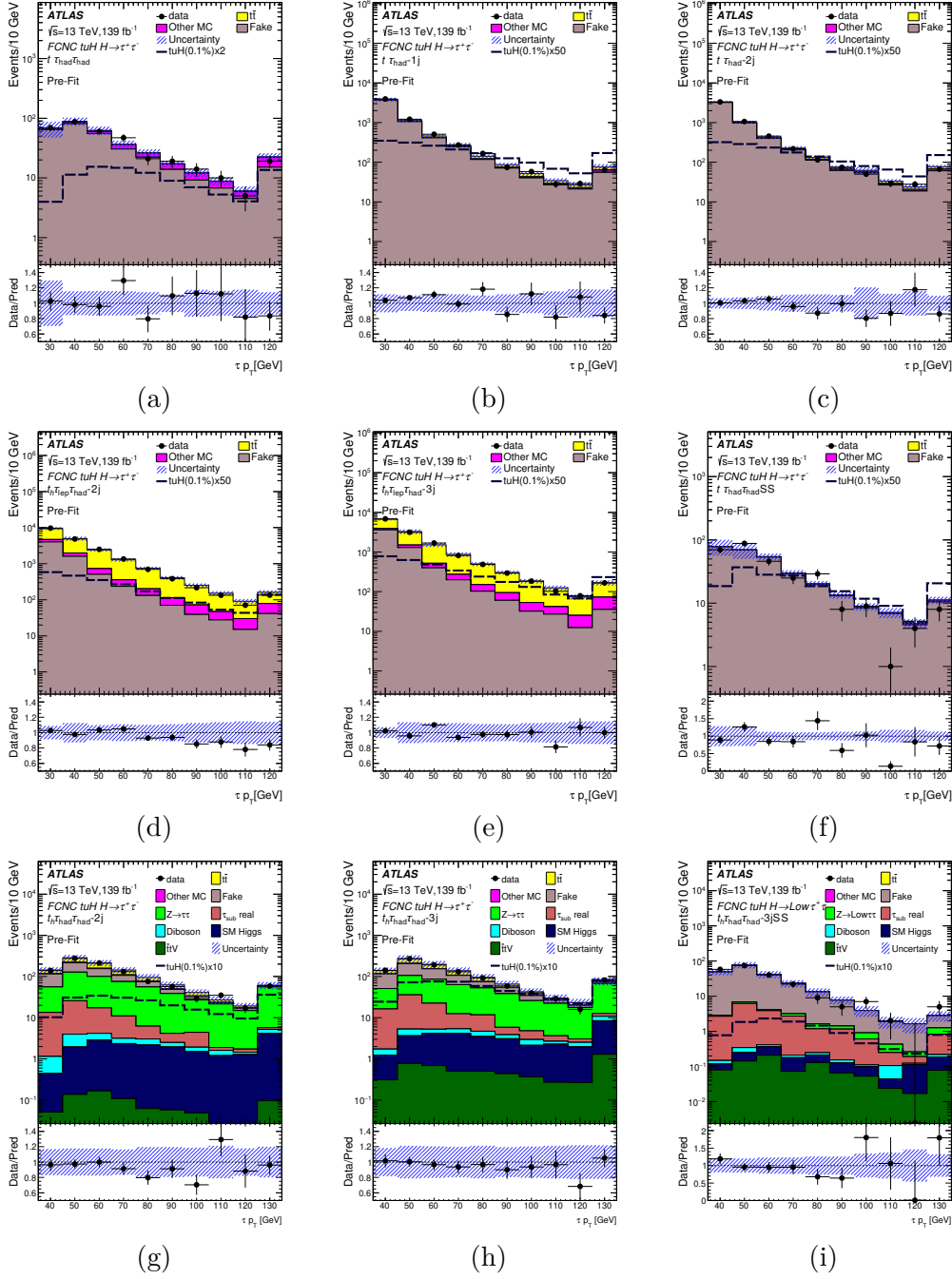


Figure 1. Leading τ_{had} p_T distributions obtained before the fit to data (‘Pre-Fit’) showing the expected background and tuH signals after applying fake factors in the following regions: (a) $t_{\ell}\tau_{\text{had}}\tau_{\text{had}}$, (b) $t_{\ell}\tau_{\text{had}}\text{-1j}$, (c) $t_{\ell}\tau_{\text{had}}\text{-2j}$, (d) $t_h\tau_{\text{lep}}\tau_{\text{had}}\text{-2j}$, (e) $t_h\tau_{\text{lep}}\tau_{\text{had}}\text{-3j}$, (f) $t_{\ell}\tau_{\text{had}}\tau_{\text{had}}\text{-SS}$, (g) $t_h\tau_{\text{had}}\tau_{\text{had}}\text{-2j}$, (h) $t_h\tau_{\text{had}}\tau_{\text{had}}\text{-3j}$ and (i) $t_h\tau_{\text{had}}\tau_{\text{had}}\text{-3j SS}$. The total statistical and systematic uncertainty of the background prediction is indicated by the hatched band. Overflow events are included in the last bin. ‘Other MC’ includes single-top, V +jets, and other small backgrounds in the leptonic and hadronic channel. The tuH signal is scaled by a normalisation factor of either 2, 10, or 50. The lower panels show the ratio of data to prediction.

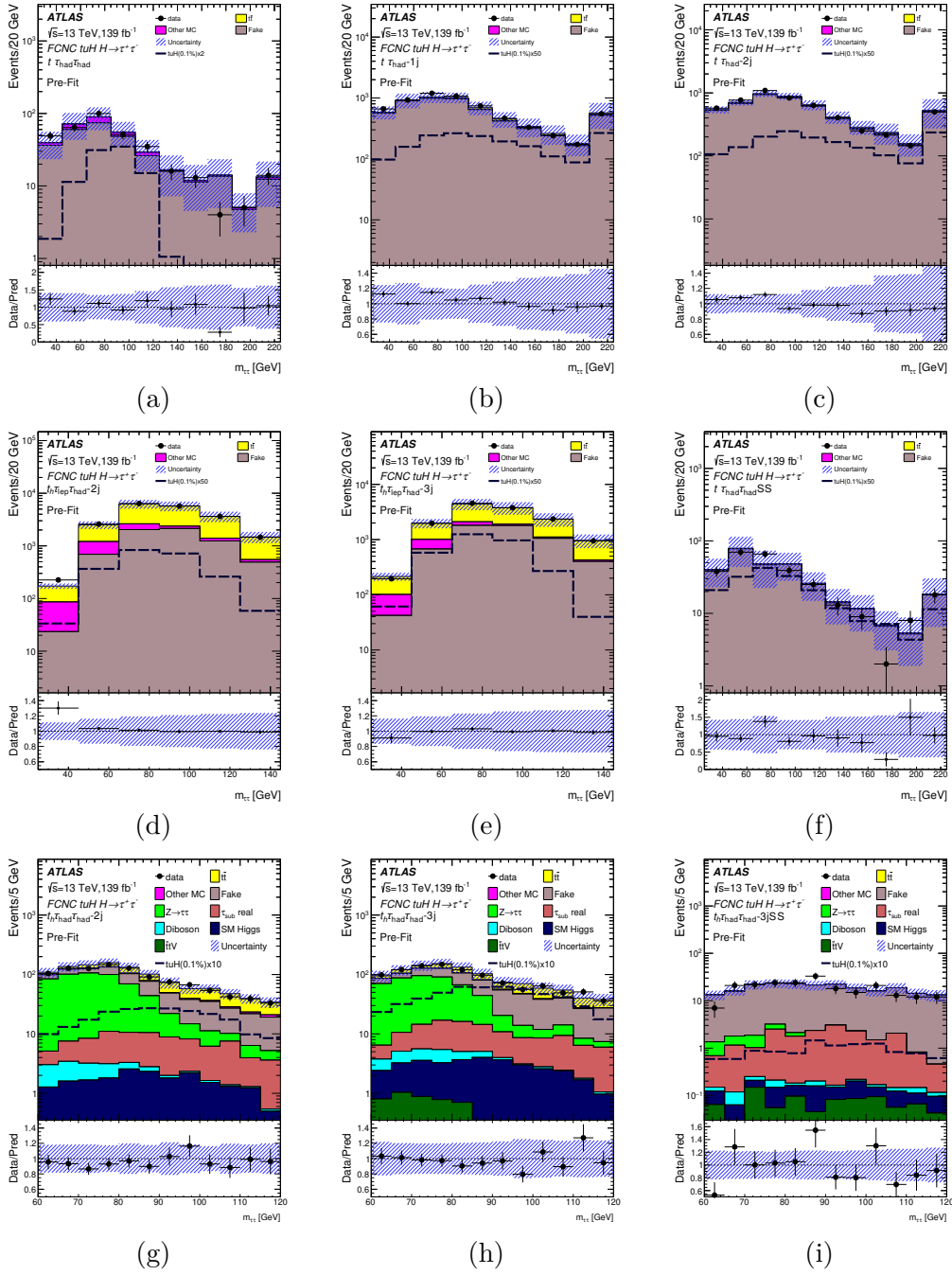


Figure 2. Distributions of the visible invariant mass of the di- τ system ($m_{\tau\tau}$) obtained before the fit to data (‘Pre-Fit’) showing the expected background and tuH signals after applying fake factors in the following regions: (a) $t\ell\tau_{\text{had}}\tau_{\text{had}}$, (b) $t\ell\tau_{\text{had}}-1j$, (c) $t\ell\tau_{\text{had}}-2j$, (d) $t_h\tau_{\text{lep}}\tau_{\text{had}}-2j$, (e) $t_h\tau_{\text{lep}}\tau_{\text{had}}-3j$, (f) $t\ell\tau_{\text{had}}\tau_{\text{had}}\text{-SS}$, (g) $t_h\tau_{\text{had}}\tau_{\text{had}}-2j$, (h) $t_h\tau_{\text{had}}\tau_{\text{had}}-3j$ and (i) $t_h\tau_{\text{had}}\tau_{\text{had}}-3j$ SS. The total statistical and systematic uncertainty of the background prediction is indicated by the hatched band. Overflow events are included in the last bin. ‘Other MC’ includes single-top, and V +jets and other small backgrounds in the leptonic and hadronic channels. The tuH signal is scaled by a normalisation factor of either 2, 10, or 50. The lower panels show the ratio of data to prediction.

9 Systematic uncertainties

Several sources of systematic uncertainty that can affect the normalisation of signal and background and/or the shape of their corresponding discriminant distributions are considered. Each source is considered to be uncorrelated with the other sources. Correlations of a given systematic uncertainty are maintained across processes and channels as appropriate. The following sections describe the systematic uncertainties considered. Table 7 shows a summary of the dominant systematic uncertainties in the measured $\mathcal{B}(t \rightarrow qH)$ branching ratio resulting from the fits to the data in the signal regions as described in section 11.

9.1 Luminosity

The uncertainty in the integrated luminosity is 1.7%, affecting the overall normalisation of all processes estimated from the simulation. It is derived, following a methodology similar to that detailed in ref. [104] and using the LUCID-2 detector for the baseline luminosity measurements [105], from a calibration of the luminosity scale using x - y beam-separation scans.

9.2 Reconstructed objects

Uncertainties associated with electrons, muons, and τ_{had} candidates arise from the trigger, reconstruction, identification and, in the case of electrons and muons, isolation efficiencies, as well as the momentum scale and resolution. These are measured using $Z \rightarrow \ell^+\ell^-$ and $J/\psi \rightarrow \ell^+\ell^-$ events ($\ell = e, \mu$) [47, 49] in the case of electrons and muons, and using $Z \rightarrow \tau^+\tau^-$ events in the case of τ_{had} candidates [106].

Uncertainties associated with jets arise from the jet energy scale (JES) and resolution (JER), and the efficiency to pass the JVT requirements. The largest contribution comes from the jet energy scale, whose uncertainty dependence on jet p_T and η , jet flavour, and pile-up treatment is split into 43 uncorrelated components that are treated independently [54]. The total JES uncertainty is below 5% for most jets and below 1% for central jets with p_T between 300 GeV and 2 TeV. The difference between the JER values in data and MC events is represented by one nuisance parameter (NP). It is applied to the MC events by smearing the jet p_T within the prescribed uncertainty.

Uncertainties associated with energy scales and resolutions of leptons and jets are propagated to E_T^{miss} . Additional uncertainties originating from the modelling of the underlying event, in particular its impact on the p_T scale and resolution of unclustered energy, are negligible.

Efficiencies to tag b -jets and c -jets in the simulation are corrected by p_T -dependent factors to match the efficiencies in data, while the light-jet efficiency is scaled by p_T - and η -dependent factors. The b -jet efficiency is measured in a data sample enriched in $t\bar{t}$ events [58], while the c -jet efficiency is measured using $t\bar{t}$ events [107] or $W+c$ -jet events [108]. The light-jet efficiency is measured in a multi-jet data sample enriched in light-flavour jets [109]. The uncertainties in these scale factors come from a total of 44 independent sources affecting b -jets, 19 sources affecting c -jets, and 19 sources affecting light jets. These systematic uncertainties are taken to be uncorrelated between b -jets, c -jets,

and light jets. Scale factors are applied to reweight simulated events in order to obtain the pile-up distribution corresponding to the data. An uncertainty in these reweighting scale factors is estimated by reweighting the profile in data while keeping it within its uncertainties.

9.3 Background modelling

A number of sources of systematic uncertainty affecting the modelling of $t\bar{t}$ +jets are considered: the choice of renormalisation and factorisation scale in the matrix-element calculation, the choice of matching scale when matching the matrix elements to the parton shower generator, the uncertainty in the value of α_s when modelling initial-state radiation (ISR), and the choice of renormalisation scale when modelling final-state radiation (FSR).

The h_{damp} parameter, which controls the amount of radiation produced by the parton shower in POWHEG BOX v2, is set to $1.5m_t$ in the $t\bar{t}$ sample. An alternative sample was generated with $h_{\text{damp}} = 3m_t$. The difference between the two samples is treated as a systematic uncertainty called ‘ $t\bar{t}$ h_{damp} ’.

The uncertainty due to the choice of parton shower and hadronisation (PS & Had) model is derived by comparing the predictions from POWHEG BOX interfaced either to PYTHIA 8 or HERWIG 7. The latter uses the MMHT2014LO [110] PDF set in combination with the H7UE tune [111]. The uncertainty in the modelling of additional radiation from the PS is assessed by varying the corresponding parameter of the A14 set [112] and by varying the radiation renormalisation and factorisation scales by a factor of 2.0 and 0.5, respectively.

Another significant background in the hadronic channel stems from the $Z \rightarrow \tau\tau$ samples. Several sources of uncertainty are considered for these samples: the PDF variation, which is evaluated by considering the standard deviation produced by the event weights from the 100 NNPDF replicas for the NNPDF3.0NNLO [113] PDF set used in SHERPA, the renormalisation (μ_r) and factorisation (μ_f) scales, the jet-to-parton matching uncertainty, the resummation scale uncertainty, the variation in the choice of α_s , and the use of alternative PDFs, which is evaluated by comparing predictions from the NNPDF3.0NNLO PDF set (nominal) with those from the MMHT2014NNLO68CL and CT14NNLO [114, 115] PDF sets.

Uncertainties affecting the normalisation of the V +jets background are estimated separately for V +light-jets, $V+\geq 1c$ +jets, and $V+\geq 1b$ +jets subprocesses. The total normalisation uncertainty of V +jets processes is estimated to be approximately 30% by taking the maximum difference between the data and the total background prediction in the different analysis regions considered, but requiring exactly zero, one, and two b -jets. This is driven mainly by differences between MC simulations in the V +jets regions with a high multiplicity of jets.

Uncertainties affecting the modelling of the single-top-quark background include a $+5\%/-4\%$ uncertainty in the total cross section, which is estimated as a weighted average of the theoretical uncertainties in t -, tW - and s -channel production [86–88]. Additional uncertainties associated with the parton shower, hadronisation and ISR/FSR are also considered by using the same procedure as for $t\bar{t}$. Uncertainties in the diboson background

normalisation include those estimated from variations of the renormalisation and factorisation scales, NNPDF3.0NNLO variations and α_s variations. Uncertainties in the $t\bar{t}V$ and $t\bar{t}H$ cross sections are estimated to be 12% and $[+5.8\% / -9.2\%]$, respectively, from the uncertainties in their respective NLO theoretical cross sections [116].

The statistical uncertainties of the fake- τ -background calibration in the leptonic channels are applied with uncorrelated uncertainties for different sources of fake τ -leptons and different p_T slices. The uncertainties in the MC modelling of the various processes used for evaluation of the fake factors in the CRtt are treated as fully correlated in the fit. The uncertainty in the ABCD method is applied to the normalisation factors for muons and electrons, including both its statistical fluctuation and the differences between the normalisation factors for the various leptonic channels. The uncertainties in the fake-factor method applied to the hadronic channel includes the statistical uncertainty of each fake factor and differences between the sets of fake factors derived from different signal-depleted CRs.

9.4 Signal modelling

Several normalisation and shape uncertainties are taken into account and are treated as fully correlated for the $t\bar{t} \rightarrow WbHq$ and $pp \rightarrow tH$ signals. Uncertainties in the Higgs boson branching ratios are taken into account by following the recommendation in ref. [28]. The uncertainties due to ISR, FSR, the scales, and the PDFs, are considered and are treated as fully correlated in all SRs. The parton shower uncertainties are estimated by comparing the nominal sample with an alternative sample interfaced with HERWIG 7.

10 Statistical analysis

The final discriminant distributions are the BDT outputs from all the considered analysis regions. They are jointly analysed for the presence of a signal. The BDT distributions are binned to maximise sensitivity to the signal. The statistical analysis uses a binned likelihood function $\mathcal{L}(\mu, \theta)$ constructed as a product of Poisson probability terms over all bins considered in the search. This function depends on the signal-strength parameter μ , defined as a factor multiplying the expected yield of tH and $t\bar{t}(qH)$ signal events normalised to a reference branching ratio $\mathcal{B}_{\text{ref}}(t \rightarrow qH) = 0.1\%$, and on θ , a set of nuisance parameters that encode the effect of systematic uncertainties on the signal and background expectations. The $pp \rightarrow tH$ production cross section is related to $\mathcal{B}(t \rightarrow qH)$ through their dimension-6 operators [76]. It follows that the expected total number of events in a given bin depends on μ and θ . All nuisance parameters are subject to Gaussian constraints in the likelihood function. For a given value of μ , the nuisance parameters θ allow variations of the expectations for signal and background consistent with the corresponding systematic uncertainties, and their fitted values result in the deviations from the nominal expectations that globally provide the best fit to the data. This procedure reduces the impact of systematic uncertainties on the search's sensitivity by taking advantage of the highly populated background-dominated bins included in the likelihood fit. Statistical uncertainties in each bin of the predicted final discriminant distributions are taken into account through dedicated parameters in the fit. The best-fit $\mathcal{B}(t \rightarrow qH)$ is obtained by performing a binned

likelihood fit to the data under the signal-plus-background hypothesis, and maximising the likelihood function $\mathcal{L}(\mu, \theta)$ over μ and θ .

The fitting procedure was initially validated through extensive studies using pseudo-data (which is defined as the sum of all predicted backgrounds plus an injected signal of variable strength) as well as by performing fits to real data where bins of the final discriminating variable with an expected signal contamination above 10%, assuming $\mathcal{B}_{\text{ref}}(t \rightarrow qH) = 0.1\%$, are excluded (referred to as ‘blinding’ requirements). In both cases, the robustness of the model with respect to systematic uncertainties is established by verifying the stability of the fitted background when varying assumptions about some of the leading sources of uncertainty. After this, the blinding requirements are removed in the data and a fit under the signal-plus-background hypothesis is performed. Further checks involve the comparison of the fitted nuisance parameters before and after removal of the blinding requirements, and their values are found to be consistent. In addition, it is verified that the fit is able to determine the strength of a simulated signal injected into the real data.

The test statistic q_μ is defined as the profile likelihood ratio, $q_\mu = -2\ln(\mathcal{L}(\mu, \hat{\theta}_\mu)/\mathcal{L}(\hat{\mu}, \hat{\theta}))$, where $\hat{\mu}$ and $\hat{\theta}$ are the values of the parameters that maximise the likelihood function (subject to the constraint $\hat{\mu} \geq 0$), and the $\hat{\theta}_\mu$ are the values of the nuisance parameters that maximise the likelihood function for a given value of μ . The test statistic q_μ is evaluated with the RooFit package [117, 118].

Exclusion limits are set on μ and thus on $\mathcal{B}(t \rightarrow qH)$, derived by using q_μ in the CL_s method [119, 120]. For a given signal scenario, values of $\mathcal{B}(t \rightarrow qH)$ yielding CL_s < 0.05, where CL_s is computed using the asymptotic approximation [121], are excluded with at least 95% confidence.

11 Results

This section presents the results obtained from the individual channels, as well as their combination, by following the statistical analysis discussed in section 10.

A binned likelihood fit under the signal-plus-background hypothesis is performed on the BDT discriminant distributions in the seven signal regions. The unconstrained parameter of the fit is the signal strength. No significant pulls or constraints are obtained for the fitted nuisance parameters, resulting in a post-fit background prediction in each analysis region that is very close to the pre-fit prediction, albeit with reduced uncertainties resulting from the fit. Figures 3 and 4 show the BDT output distributions after the signal-plus-background fit to the data for the tcH and tuH searches, respectively. The observed and predicted yields after a background-only fit to the data are summarised in table 6. A slight excess of data events, with a significance of 2.3σ , is observed above the expected background. This is mainly in the high BDT-score region of the most sensitive channel, $t_\ell\tau_{\text{had}}\tau_{\text{had}}$, as shown in figures 3(a) and 4(a). The kinematic distributions for the observed excess in the high BDT-score region were checked. Within the large statistical uncertainty, the observed distributions are compatible with the background shapes, but also with a small signal contribution. There is no indication that the excess is from a specific data period. The background modelling in this signal region was also checked using the VR in which both

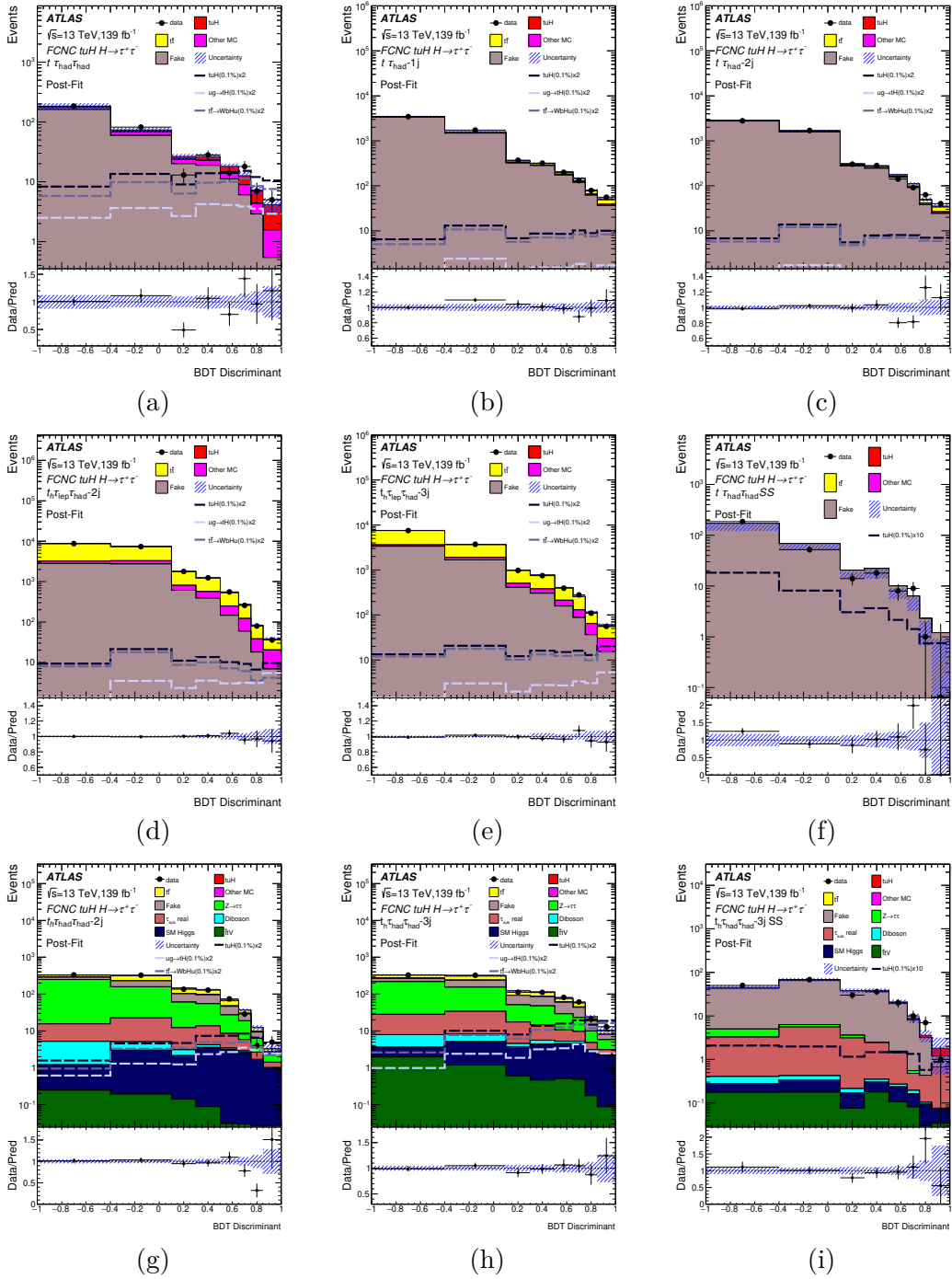


Figure 3. BDT output distributions obtained from a signal+background fit to the data for the tuH search: (a) $t_\ell \tau_{\text{had}} \tau_{\text{had}}$, (b) $t_\ell \tau_{\text{had}}-1j$, (c) $t_\ell \tau_{\text{had}}-2j$, (d) $t_h \tau_{\text{lep}} \tau_{\text{had}}-2j$, (e) $t_h \tau_{\text{lep}} \tau_{\text{had}}-3j$, (f) $t_\ell \tau_{\text{had}} \tau_{\text{had}}-SS$, (g) $t_h \tau_{\text{had}} \tau_{\text{had}}-2j$, (h) $t_h \tau_{\text{had}} \tau_{\text{had}}-3j$ and (i) $t_h \tau_{\text{had}} \tau_{\text{had}}-3j$ SS. The total statistical and systematic uncertainty is indicated by the hatched band. The signal shapes of $tt(uH)$, tH , and their sum are also shown using a normalisation of $2 \times \mathcal{B}(t \rightarrow uH)$ of 0.1%.

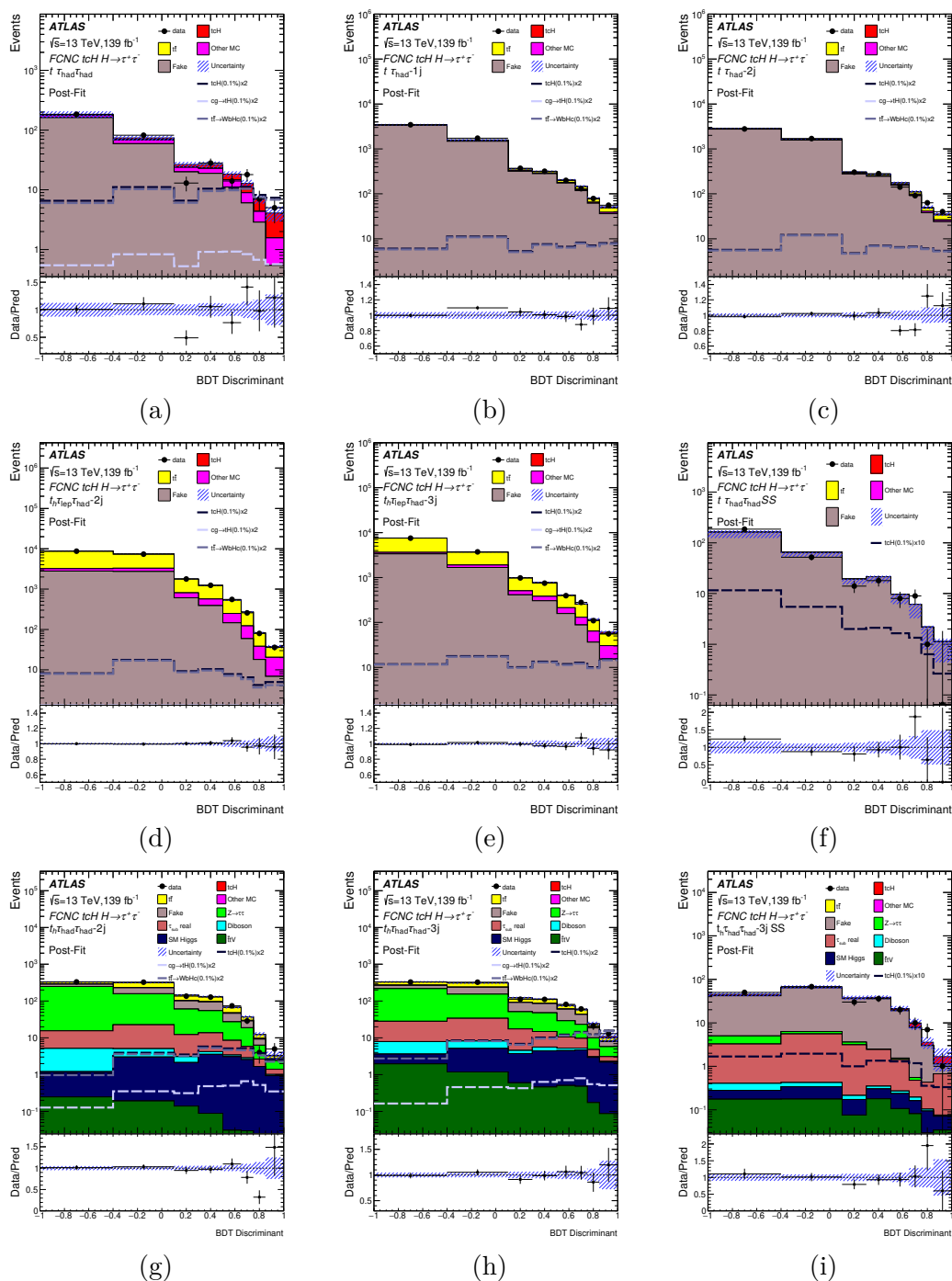


Figure 4. BDT output distributions obtained from a signal+background fit to the data for the tcH search: (a) $t\ell\tau_{\text{had}}\tau_{\text{had}}$, (b) $t\ell\tau_{\text{had}}\text{-1j}$, (c) $t\ell\tau_{\text{had}}\text{-2j}$, (d) $t_h\tau_{\text{lep}}\tau_{\text{had}}\text{-2j}$, (e) $t_h\tau_{\text{lep}}\tau_{\text{had}}\text{-3j}$, (f) $t\ell\tau_{\text{had}}\tau_{\text{had}}\text{-SS}$, (g) $t_h\tau_{\text{had}}\tau_{\text{had}}\text{-2j}$, (h) $t_h\tau_{\text{had}}\tau_{\text{had}}\text{-3j}$ and (i) $t_h\tau_{\text{had}}\tau_{\text{had}}\text{-3j SS}$. The total statistical and systematic uncertainty is indicated by the hatched band. The signal shapes of $tt(cH)$, tH , and their sum are also shown using a normalisation of $2 \times \mathcal{B}(t \rightarrow cH)$ of 0.1%.

	$t_\ell \tau_{\text{had}}\text{-1j}$	$t_\ell \tau_{\text{had}}\text{-2j}$	$t_h \tau_{\text{lep}} \tau_{\text{had}}\text{-3j}$	$t_h \tau_{\text{lep}} \tau_{\text{had}}\text{-2j}$	$t_\ell \tau_{\text{had}} \tau_{\text{had}}$
Double Fake	—	—	—	—	73 ± 24
$t\bar{t}V$	9.3 ± 1.2	22.6 ± 2.8	23.5 ± 3.0	13.7 ± 1.7	2.57 ± 0.35
SM Higgs	5.8 ± 0.8	13.7 ± 1.7	32.8 ± 3.5	13.5 ± 2.5	16.7 ± 1.9
Diboson	32.6 ± 3.4	19.9 ± 2.1	36 ± 4	46 ± 5	13.2 ± 1.4
Other MC	35.6 ± 3.1	15.9 ± 1.7	226 ± 21	620 ± 40	6.7 ± 0.6
$Z \rightarrow \tau\tau$	0 ± 6	9.1 ± 2.2	500 ± 60	880 ± 90	2.1 ± 0.7
Lep. Fake	212 ± 30	80 ± 10	292 ± 26	490 ± 70	0.9 ± 0.4
QCD Fake	670 ± 200	310 ± 90	180 ± 70	330 ± 110	—
b Fake	960 ± 140	1250 ± 230	710 ± 140	710 ± 130	82 ± 13
W -jet Fake	970 ± 200	1090 ± 240	3300 ± 500	3800 ± 600	5.5 ± 1.8
Other Fake	3020 ± 260	2470 ± 160	1420 ± 220	1320 ± 320	129 ± 14
$t\bar{t}$	281 ± 14	195 ± 24	7100 ± 400	11800 ± 500	7.7 ± 2.7
Total background	6200 ± 170	5480 ± 100	13820 ± 140	20000 ± 170	339 ± 27
tcH	30 ± 5	27 ± 4	51 ± 8	34 ± 6	36 ± 5
tuH	36 ± 8	32 ± 5	63 ± 10	45 ± 7	48 ± 7
Data	6353	5410	13804	20000	351

	$t_h \tau_{\text{had}} \tau_{\text{had}}\text{-2j}$	$t_h \tau_{\text{had}} \tau_{\text{had}}\text{-3j}$
$t\bar{t}V$	0.7 ± 0.4	5.5 ± 1.0
Diboson	8.4 ± 1.6	10.8 ± 1.5
Rare	17.9 ± 3.1	10.2 ± 2.6
SM Higgs	17.4 ± 2.5	25.9 ± 3.1
only τ_{sub} real	56 ± 30	80 ± 50
$t\bar{t}$	221 ± 28	220 ± 40
Fake τ	220 ± 70	270 ± 70
$Z \rightarrow \tau\tau$	490 ± 50	420 ± 50
Total background	1040 ± 35	1040 ± 40
tcH	15.6 ± 2.5	42 ± 8
tuH	23 ± 4	52 ± 10
Data	1033	1052

Table 6. Predicted and observed yields in each of the analysis regions considered. The background prediction is shown after a background-only fit is applied to the data. Also shown are the expected signals for $t\bar{t} \rightarrow WbHc$ and $t\bar{t} \rightarrow WbHu$ assuming $\mathcal{B}(t \rightarrow cH) = 0.1\%$ and $\mathcal{B}(t \rightarrow uH) = 0.1\%$ respectively. The contributions with real τ_{had} candidates from $t\bar{t}$ and $Z \rightarrow \ell^+ \ell^-$ ($\ell = e, \mu$), diboson, $t\bar{t}V$, $t\bar{t}H$, single-top-quark, and other small backgrounds are combined into a single background source referred to as ‘Other MC’ in the leptonic channels, whereas single-top-quark and the small contributions are combined into ‘Rare’ in the hadronic channels. The quoted uncertainties are the sum in quadrature of the statistical and systematic uncertainties of the yields.

Source of uncertainty	$\Delta\mathcal{B} [10^{-5}]$	
	$t \rightarrow uH$	$t \rightarrow cH$
Lepton ID	0.6	0.8
E_T^{miss}	0.7	0.7
Fake lepton modeling	1.2	1.7
JES and JER	2.5	3.3
Flavour tagging	2.7	3.7
$t\bar{t}$ modeling	2.6	3.9
Other MC modeling	2.1	3.0
Fake τ modeling	3.3	4.7
Signal modeling including $\text{Br}(H \rightarrow \tau\tau)$	1.8	1.5
τ ID	3.3	4.4
Luminosity and Pileup	1.7	2.4
MC statistics	5.1	7.1
Total systematic uncertainty	10.1	14.1
Data statistical uncertainty	14.9	19.4
Total uncertainties	18	24

Table 7. Absolute uncertainties on $\mathcal{B}(t \rightarrow qH)$ ($q = u, c$) obtained from the combined fit to the data. The uncertainties are symmetrised and grouped into the categories described in the section 9.

τ_{had} candidates have the same charge. In this VR the signal contribution is negligible in the highest BDT bins and the background shape is well reproduced by the data.

Upper limits on $\mathcal{B}(t \rightarrow cH)$ and $\mathcal{B}(t \rightarrow uH)$ are derived using the CL_s method [119, 120], and the observed (expected) 95% CL limits are $\mathcal{B}(t \rightarrow cH) < 9.4 \times 10^{-4}$ ($4.8_{-1.4}^{+2.2} \times 10^{-4}$), assuming $\mathcal{B}(t \rightarrow uH) = 0$, and $\mathcal{B}(t \rightarrow uH) < 6.9 \times 10^{-4}$ ($3.5_{-1.0}^{+1.5} \times 10^{-4}$), assuming $\mathcal{B}(t \rightarrow cH) = 0$. These results are dominated by the leptonic channels, whose sensitivity is a factor of two better than that of the hadronic channels. The expected sensitivity is a factor of five better than that of the previous ATLAS search, which was based on 36 fb^{-1} of data and used $H \rightarrow \tau\tau$ decays [32]. A factor of 2 improvement in sensitivity comes from the larger dataset, and a further factor of 2.5 comes from including additional leptonic channels, tH production, and improved techniques.

In both cases, the results are dominated by the statistical uncertainty. The main contributions to the total systematic uncertainty arise from the size of the MC samples, the uncertainties in the τ_{had} identification efficiency, the renormalisation and factorisation scales, the b -tagging efficiency, the choice of parton shower and hadronisation schemes for $t\bar{t}$ modelling, and the fake- τ_{had} background estimation in the hadronic channels. Their absolute impacts on the signal strength are summarised in table 7. A summary of the upper limits, significance and best-fit values of the branching ratios obtained by the individual searches, as well as their combination, is given in table 8 and in figures 5(a) and 5(b).

Upper limits on the branching ratios $\mathcal{B}(t \rightarrow qH)$ ($q = u, c$) can be translated into upper limits on the dimension-6 (D6) operator Wilson coefficients ($C_{u\phi}^{i3}, C_{u\phi}^{3i}$) appearing in

Signal Region	$t \rightarrow cH$			$t \rightarrow uH$		
	95% CL upper limit [10^{-3}]	Significance	$\mathcal{B}[10^{-3}]$	95% CL upper limit [10^{-3}]	Significance	$\mathcal{B}[10^{-3}]$
	Observed (Expected)			Observed (Expected)		
$t_h \tau_{\text{had}} \tau_{\text{had}}\text{-}2\text{j}$	1.80 ($2.72^{+1.18}_{-0.76}$)	−0.96 (0.78)	$-1.03^{+1.03}_{-1.03}$	1.07 ($1.60^{+0.71}_{-0.45}$)	−0.90 (1.31)	$-0.55^{+0.58}_{-0.58}$
$t_h \tau_{\text{had}} \tau_{\text{had}}\text{-}3\text{j}$	1.14 ($1.02^{+0.45}_{-0.29}$)	0.34 (1.87)	$0.16^{+0.47}_{-0.47}$	0.97 ($0.86^{+0.38}_{-0.24}$)	0.36 (2.25)	$0.14^{+0.40}_{-0.40}$
Hadronic combination	1.00 ($0.95^{+0.42}_{-0.27}$)	0.26 (1.99)	$0.11^{+0.43}_{-0.43}$	0.76 ($0.76^{+0.33}_{-0.21}$)	0.12 (2.52)	$0.04^{+0.34}_{-0.34}$
$t_\ell \tau_{\text{had}}\text{-}2\text{j}$	4.77 ($4.23^{+1.72}_{-1.18}$)	0.41 (0.47)	$0.85^{+2.06}_{-2.06}$	3.84 ($3.48^{+1.42}_{-0.97}$)	0.36 (0.58)	$0.61^{+1.68}_{-1.68}$
$t_\ell \tau_{\text{had}}\text{-}1\text{j}$	3.80 ($3.56^{+1.51}_{-0.99}$)	0.22 (0.58)	$0.36^{+1.70}_{-1.70}$	2.98 ($2.78^{+1.17}_{-0.78}$)	0.22 (0.73)	$0.29^{+1.33}_{-1.33}$
$t_h \tau_{\text{lep}} \tau_{\text{had}}\text{-}2\text{j}$	4.71 ($5.71^{+2.68}_{-1.60}$)	−0.52 (0.38)	$-1.36^{+2.56}_{-2.56}$	2.50 ($2.97^{+1.25}_{-0.83}$)	−0.47 (0.70)	$-0.66^{+1.38}_{-1.38}$
$t_h \tau_{\text{lep}} \tau_{\text{had}}\text{-}3\text{j}$	2.71 ($2.71^{+1.25}_{-0.76}$)	−0.03 (0.77)	$-0.03^{+1.26}_{-1.26}$	2.02 ($2.03^{+0.86}_{-0.57}$)	−0.05 (0.99)	$-0.03^{+0.98}_{-0.98}$
$t_\ell \tau_{\text{had}} \tau_{\text{had}}$	1.35 ($0.61^{+0.27}_{-0.17}$)	2.64 (3.31)	$0.74^{+0.33}_{-0.33}$	0.97 ($0.44^{+0.19}_{-0.12}$)	2.64 (4.38)	$0.53^{+0.24}_{-0.24}$
Leptonic combination	1.25 ($0.58^{+0.25}_{-0.16}$)	2.61 (3.46)	$0.69^{+0.31}_{-0.31}$	0.88 ($0.41^{+0.18}_{-0.11}$)	2.60 (4.62)	$0.49^{+0.22}_{-0.22}$
Combination	0.94 ($0.48^{+0.20}_{-0.14}$)	2.34 (4.02)	$0.51^{+0.24}_{-0.24}$	0.69 ($0.35^{+0.15}_{-0.10}$)	2.31 (5.18)	$0.37^{+0.18}_{-0.18}$

Table 8. Summary of 95% CL upper limits on $\mathcal{B}(t \rightarrow cH)$ and $\mathcal{B}(t \rightarrow uH)$, significance and best-fit branching ratio in the signal regions with a benchmark branching ratio of $\mathcal{B}(t \rightarrow qH) = 0.1\%$. The expected significance is obtained from an Asimov fit [121] with a signal injection corresponding to a branching ratio of 0.1%.

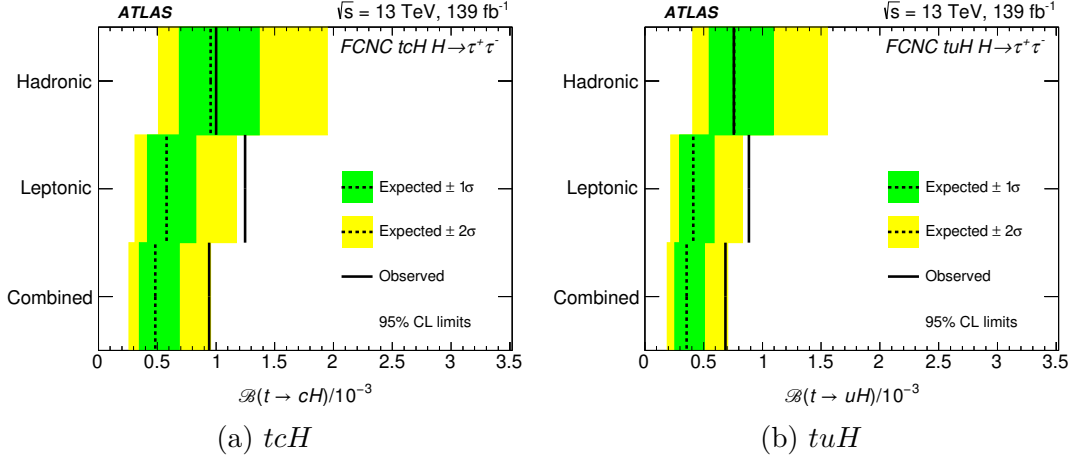


Figure 5. (a) This figure shows 95% CL upper limits on $\mathcal{B}(t \rightarrow cH)$ for the individual searches as well as their combination, assuming $\mathcal{B}(t \rightarrow uH) = 0$. (b) This figure shows 95% CL upper limits on $\mathcal{B}(t \rightarrow uH)$ for the individual searches as well as their combination, assuming $\mathcal{B}(t \rightarrow cH) = 0$. The observed limits (solid lines) are compared with the expected (median) limits under the background-only hypothesis (dotted lines). The surrounding shaded bands correspond to the 68% and 95% CL intervals around the expected limits, denoted by $\pm 1\sigma$ and $\pm 2\sigma$ respectively.

the effective field theory Lagrangian for the tqH interaction [76]:

$$\mathcal{L}_{\text{EFT}} = \frac{C_{u\phi}^{i3}}{\Lambda^2} (\phi^\dagger \phi) (\bar{q}_i t) \tilde{\phi} + \frac{C_{u\phi}^{3i}}{\Lambda^2} (\phi^\dagger \phi) (\bar{t} q_i) \tilde{\phi}$$

where the subscript $i = 1, 2$ represents the generation of the light-quark fields ($q = u, c$). The branching ratio $\mathcal{B}(t \rightarrow qH)$ is estimated as the ratio of its partial width to the SM $t \rightarrow Wb$ partial width including next-to-leading-order QCD corrections. The coefficients can be extracted as $C_{q\phi} = \sqrt{1946.6 \mathcal{B}(t \rightarrow qH)}$ [76]. The $C_{q\phi}$ coefficient corresponds to

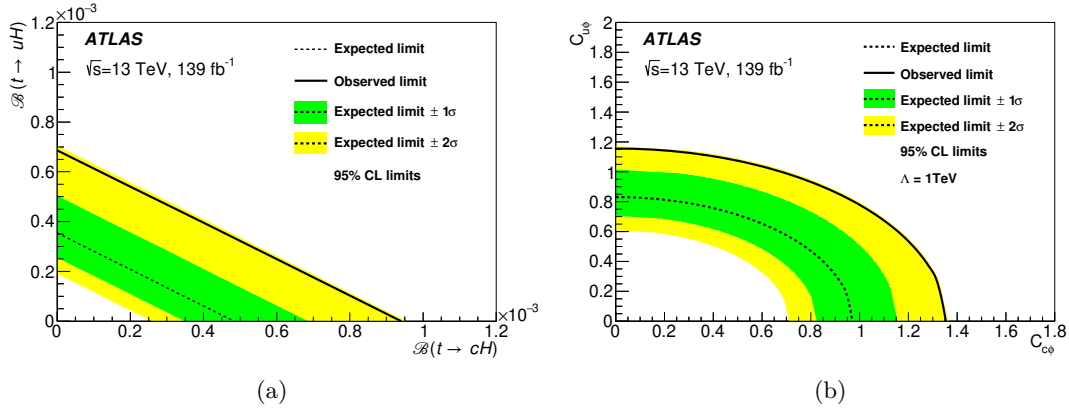


Figure 6. 95% CL upper limits (a) in the $\mathcal{B}(t \rightarrow cH)$ versus $\mathcal{B}(t \rightarrow uH)$ plane and (b) in the $C_{c\phi}$ versus $C_{u\phi}$ plane for the combination of the searches. The observed limits (solid lines) are compared with the expected (median) limits under the background-only hypothesis (dotted lines). The surrounding shaded bands correspond to the 68% and 95% CL intervals around the expected limits, denoted by $\pm 1\sigma$ and $\pm 2\sigma$ respectively.

the sum in quadrature of the coefficients relative to the two possible chirality combinations of the quark fields, $C_{q\phi} = \sqrt{(C_{q\phi}^{i3})^2 + (C_{q\phi}^{3i})^2}$ [76]. The observed (expected) upper limits on the D6 Wilson coefficients from the combination of the search results are $C_{c\phi} < 1.35$ (0.97) and $C_{u\phi} < 1.16$ (0.82) for a new-physics scale $\Lambda = 1$ TeV.

A similar set of results can be obtained by simultaneously varying both branching ratios in the likelihood function. Figure 6(a) shows the 95% CL upper limits on the branching ratios in the $\mathcal{B}(t \rightarrow uH)$ versus $\mathcal{B}(t \rightarrow cH)$ plane. The corresponding upper limits on the D6 Wilson coefficient couplings in the $C_{u\phi}$ versus $C_{c\phi}$ plane are shown in figure 6(b).

12 Conclusion

A search for flavour-changing neutral current processes involving a top quark, another up-type quark ($q = u, c$), and a SM Higgs boson is presented. The search uses 139 fb^{-1} of 13 TeV pp collisions recorded by the ATLAS detector at the LHC. Evidence of FCNC tqH interactions is sought in both the $t\bar{t}$ decay mode, where one top quark decays via SM processes and the other one decays through $t \rightarrow qH$, and the production mode ($pp \rightarrow tH$), where a single top quark produced via the FCNC interaction decays as $t \rightarrow Wb$. A slight excess of data is observed above background, with a significance of 2.3σ . Upper limits at the 95% confidence level are set on the $t \rightarrow qH$ branching ratios and the corresponding dimension-6 operator Wilson coefficients in the effective tqH couplings. The observed (expected) 95% CL upper limits set on the $t \rightarrow cH$ and $t \rightarrow uH$ branching ratios are 9.4×10^{-4} ($4.8_{-1.4}^{+2.2} \times 10^{-4}$) and 6.9×10^{-4} ($3.5_{-1.0}^{+1.5} \times 10^{-4}$), respectively. The corresponding combined observed (expected) upper limits on the dimension-6 operator Wilson coefficients in the effective tqH couplings, for a new-physics scale Λ of 1 TeV, are $C_{c\phi} < 1.35$ (0.97) and $C_{u\phi} < 1.16$ (0.82). These results improve significantly upon the previously published ATLAS studies in this channel and provide more stringent limits than the previous combination of ATLAS $t \rightarrow qH$ results.

Acknowledgments

We thank CERN for the very successful operation of the LHC, as well as the support staff from our institutions without whom ATLAS could not be operated efficiently.

We acknowledge the support of ANPCyT, Argentina; YerPhI, Armenia; ARC, Australia; BMWFW and FWF, Austria; ANAS, Azerbaijan; CNPq and FAPESP, Brazil; NSERC, NRC and CFI, Canada; CERN; ANID, Chile; CAS, MOST and NSFC, China; Minciencias, Colombia; MEYS CR, Czech Republic; DNRF and DNSRC, Denmark; IN2P3-CNRS and CEA-DRF/IRFU, France; SRNSFG, Georgia; BMBF, HGF and MPG, Germany; GSRI, Greece; RGC and Hong Kong SAR, China; ISF and Benoziyo Center, Israel; INFN, Italy; MEXT and JSPS, Japan; CNRST, Morocco; NWO, Netherlands; RCN, Norway; MEiN, Poland; FCT, Portugal; MNE/IFA, Romania; MESTD, Serbia; MSSR, Slovakia; ARRS and MIZŠ, Slovenia; DSI/NRF, South Africa; MICINN, Spain; SRC and Wallenberg Foundation, Sweden; SERI, SNSF and Cantons of Bern and Geneva, Switzerland; MOST, Taiwan; TENMAK, Türkiye; STFC, United Kingdom; DOE and NSF, United States of America. In addition, individual groups and members have received support from BCKDF, CANARIE, Compute Canada and CRC, Canada; PRIMUS 21/SCI/017 and UNCE SCI/013, Czech Republic; COST, ERC, ERDF, Horizon 2020 and Marie Skłodowska-Curie Actions, European Union; Investissements d’Avenir Labex, Investissements d’Avenir Idex and ANR, France; DFG and AvH Foundation, Germany; Herakleitos, Thales and Aristeia programmes co-financed by EU-ESF and the Greek NSRF, Greece; BSF-NSF and MINERVA, Israel; Norwegian Financial Mechanism 2014-2021, Norway; NCN and NAWA, Poland; La Caixa Banking Foundation, CERCA Programme Generalitat de Catalunya and PROMETEO and GenT Programmes Generalitat Valenciana, Spain; Göran Gustafssons Stiftelse, Sweden; The Royal Society and Leverhulme Trust, United Kingdom.

The crucial computing support from all WLCG partners is acknowledged gratefully, in particular from CERN, the ATLAS Tier-1 facilities at TRIUMF (Canada), NDGF (Denmark, Norway, Sweden), CC-IN2P3 (France), KIT/GridKA (Germany), INFN-CNAF (Italy), NL-T1 (Netherlands), PIC (Spain), ASGC (Taiwan), RAL (UK) and BNL (USA), the Tier-2 facilities worldwide and large non-WLCG resource providers. Major contributors of computing resources are listed in ref. [122].

A Fake- τ_{had} scale factor calibration in the CRtt

Figure 7 presents the post-fit distributions of the leading τ_{had} p_T in the CRtt. These show good agreement between the data and the fitted background model. Tables 9 and 10 summarise the scale factors for 1-prong and 3-prong fake τ decays derived from the CRtt including both the statistical and systematic uncertainties. However, the interpretation of these scale factors is difficult due to their large correlations.

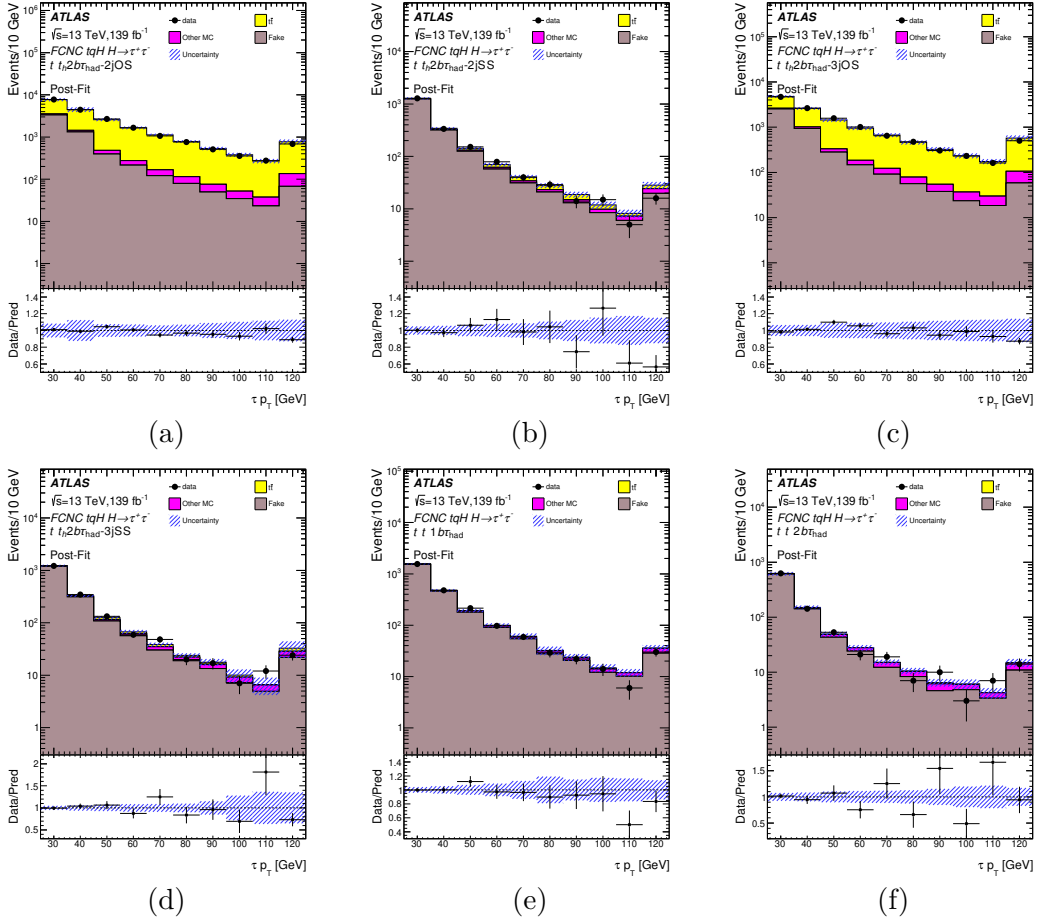


Figure 7. Leading $\tau_{\text{had}} p_T$ distributions obtained after the fit to data (‘Post-Fit’) for the fake- τ_{had} scale factors in the following CRtt: (a) $t_{\ell} t_h 2b \tau_{\text{had}}\text{-}2j$ OS, (b) $t_{\ell} t_h 2b \tau_{\text{had}}\text{-}2j$ SS, (c) $t_{\ell} t_h 2b \tau_{\text{had}}\text{-}3j$ OS, (d) $t_{\ell} t_h 2b \tau_{\text{had}}\text{-}3j$ SS, (e) $t_{\ell} t_h 1b \tau_{\text{had}}\text{-}nj$ and (f) $t_{\ell} t_h 2b \tau_{\text{had}}\text{-}nj$. The total statistical and systematic uncertainty of the background prediction is indicated by the hatched band. Overflow events are included in the last bin. The lower panels show the ratio of data to prediction.

Fake- τ types	1-prong τ decay		
$\tau_{\text{had}} p_T$	25–35 GeV	35–45 GeV	> 45 GeV
Type-1	$0.71 \pm 0.01 \pm 0.03$	$0.61 \pm 0.02 \pm 0.04$	$0.38 \pm 0.02 \pm 0.05$
Type-2	$0.76 \pm 0.06 \pm 0.04$	$0.37 \pm 0.08 \pm 0.02$	$0.74 \pm 0.08 \pm 0.02$
Type-3	$0.62 \pm 0.10 \pm 0.03$	$0.83 \pm 0.09 \pm 0.03$	$0.94 \pm 0.07 \pm 0.02$
Type-4	$1.20 \pm 0.02 \pm 0.01$	$1.01 \pm 0.04 \pm 0.02$	$0.76 \pm 0.03 \pm 0.03$

Table 9. Summary of fake- τ (1-prong) scale factors derived in the CRtt. The numbers are shown as central values, statistical uncertainties, and systematics uncertainties.

Fake- τ types	3-prong τ decays		
$\tau_{\text{had}} p_{\text{T}}$	25–35 GeV	35–45 GeV	> 45 GeV
Type-1	$1.01 \pm 0.03 \pm 0.04$	$1.09 \pm 0.04 \pm 0.05$	$0.30 \pm 0.05 \pm 0.07$
Type-2	$0.93 \pm 0.10 \pm 0.04$	$1.05 \pm 0.09 \pm 0.03$	$0.79 \pm 0.09 \pm 0.04$
Type-3	$1.07 \pm 0.13 \pm 0.03$	$1.39 \pm 0.12 \pm 0.03$	$1.26 \pm 0.10 \pm 0.04$
Type-4	$1.28 \pm 0.07 \pm 0.02$	$0.66 \pm 0.08 \pm 0.01$	$0.71 \pm 0.07 \pm 0.02$

Table 10. Summary of fake- τ (3-prong) scale factors derived in the CRtt. The numbers are shown as central values, statistical uncertainties, and systematics uncertainties.

Open Access. This article is distributed under the terms of the Creative Commons Attribution License ([CC-BY 4.0](https://creativecommons.org/licenses/by/4.0/)), which permits any use, distribution and reproduction in any medium, provided the original author(s) and source are credited. SCOAP³ supports the goals of the International Year of Basic Sciences for Sustainable Development.

References

- [1] ATLAS collaboration, *Observation of a new particle in the search for the Standard Model Higgs boson with the ATLAS detector at the LHC*, *Phys. Lett. B* **716** (2012) 1 [[arXiv:1207.7214](https://arxiv.org/abs/1207.7214)] [[INSPIRE](#)].
- [2] CMS collaboration, *Observation of a new boson at a mass of 125 GeV with the CMS experiment at the LHC*, *Phys. Lett. B* **716** (2012) 30 [[arXiv:1207.7235](https://arxiv.org/abs/1207.7235)] [[INSPIRE](#)].
- [3] ATLAS and CMS collaborations, *Combined Measurement of the Higgs Boson Mass in pp Collisions at $\sqrt{s} = 7$ and 8 TeV with the ATLAS and CMS Experiments*, *Phys. Rev. Lett.* **114** (2015) 191803 [[arXiv:1503.07589](https://arxiv.org/abs/1503.07589)] [[INSPIRE](#)].
- [4] K. Agashe, *Working Group Report: Top Quark*, [arXiv:1311.2028](https://arxiv.org/abs/1311.2028) [[INSPIRE](#)].
- [5] S.L. Glashow, J. Iliopoulos and L. Maiani, *Weak Interactions with Lepton-Hadron Symmetry*, *Phys. Rev. D* **2** (1970) 1285 [[INSPIRE](#)].
- [6] G. Eilam, J.L. Hewett and A. Soni, *Rare decays of the top quark in the standard and two Higgs doublet models*, *Phys. Rev. D* **44** (1991) 1473 [Erratum *ibid.* **59** (1999) 039901] [[INSPIRE](#)].
- [7] B. Mele, S. Petrarca and A. Soddu, *A New evaluation of the $t \rightarrow cH$ decay width in the standard model*, *Phys. Lett. B* **435** (1998) 401 [[hep-ph/9805498](https://arxiv.org/abs/hep-ph/9805498)] [[INSPIRE](#)].
- [8] J.A. Aguilar-Saavedra, *Top flavor-changing neutral interactions: Theoretical expectations and experimental detection*, *Acta Phys. Polon. B* **35** (2004) 2695 [[hep-ph/0409342](https://arxiv.org/abs/hep-ph/0409342)] [[INSPIRE](#)].
- [9] C. Zhang and F. Maltoni, *Top-quark decay into Higgs boson and a light quark at next-to-leading order in QCD*, *Phys. Rev. D* **88** (2013) 054005 [[arXiv:1305.7386](https://arxiv.org/abs/1305.7386)] [[INSPIRE](#)].
- [10] J.A. Aguilar-Saavedra, *Effects of mixing with quark singlets*, *Phys. Rev. D* **67** (2003) 035003 [Erratum *ibid.* **69** (2004) 099901] [[hep-ph/0210112](https://arxiv.org/abs/hep-ph/0210112)] [[INSPIRE](#)].
- [11] G.C. Branco et al., *Theory and phenomenology of two-Higgs-doublet models*, *Phys. Rept.* **516** (2012) 1 [[arXiv:1106.0034](https://arxiv.org/abs/1106.0034)] [[INSPIRE](#)].

- [12] S. Bejar, J. Guasch and J. Sola, *Loop induced flavor changing neutral decays of the top quark in a general two Higgs doublet model*, *Nucl. Phys. B* **600** (2001) 21 [[hep-ph/0011091](#)] [[INSPIRE](#)].
- [13] J. Guasch and J. Sola, *FCNC top quark decays: a door to SUSY physics in high luminosity colliders?*, *Nucl. Phys. B* **562** (1999) 3 [[hep-ph/9906268](#)] [[INSPIRE](#)].
- [14] J.J. Cao et al., *SUSY-induced FCNC top-quark processes at the large hadron collider*, *Phys. Rev. D* **75** (2007) 075021 [[hep-ph/0702264](#)] [[INSPIRE](#)].
- [15] J. Cao et al., *SUSY induced top quark FCNC decay $t \rightarrow ch$ after Run I of LHC*, *Eur. Phys. J. C* **74** (2014) 3058 [[arXiv:1404.1241](#)] [[INSPIRE](#)].
- [16] G. Eilam et al., *Top quark rare decay $t \rightarrow ch$ in R-parity violating SUSY*, *Phys. Lett. B* **510** (2001) 227 [[hep-ph/0102037](#)] [[INSPIRE](#)].
- [17] A. Azatov, G. Panico, G. Perez and Y. Soreq, *On the Flavor Structure of Natural Composite Higgs Models & Top Flavor Violation*, *JHEP* **12** (2014) 082 [[arXiv:1408.4525](#)] [[INSPIRE](#)].
- [18] A. Azatov, M. Toharia and L. Zhu, *Higgs mediated flavor changing neutral currents in warped extra dimensions*, *Phys. Rev. D* **80** (2009) 035016 [[arXiv:0906.1990](#)] [[INSPIRE](#)].
- [19] T.P. Cheng and M. Sher, *Mass matrix ansatz and flavor nonconservation in models with multiple Higgs doublets*, *Phys. Rev. D* **35** (1987) 3484 [[INSPIRE](#)].
- [20] I. Baum, G. Eilam and S. Bar-Shalom, *Scalar flavor changing neutral currents and rare top quark decays in a two Higgs doublet model ‘for the top quark’*, *Phys. Rev. D* **77** (2008) 113008 [[arXiv:0802.2622](#)] [[INSPIRE](#)].
- [21] K.-F. Chen, W.-S. Hou, C. Kao and M. Kohda, *When the Higgs meets the Top: Search for $t \rightarrow ch^0$ at the LHC*, *Phys. Lett. B* **725** (2013) 378 [[arXiv:1304.8037](#)] [[INSPIRE](#)].
- [22] C.-W. Chiang, H. Fukuda, M. Takeuchi and T.T. Yanagida, *Flavor-changing neutral-current decays in top-specific variant axion model*, *JHEP* **11** (2015) 057 [[arXiv:1507.04354](#)] [[INSPIRE](#)].
- [23] A. Crivellin, J. Heeck and P. Stoffer, *A perturbed lepton-specific two-Higgs-doublet model facing experimental hints for physics beyond the Standard Model*, *Phys. Rev. Lett.* **116** (2016) 081801 [[arXiv:1507.07567](#)] [[INSPIRE](#)].
- [24] F.J. Botella, G.C. Branco, M. Nebot and M.N. Rebelo, *Flavour Changing higgs couplings in a class of two Higgs doublet models*, *Eur. Phys. J. C* **76** (2016) 161 [[arXiv:1508.05101](#)] [[INSPIRE](#)].
- [25] S. Gori, C. Grojean, A. Juste and A. Paul, *Heavy Higgs searches: flavour matters*, *JHEP* **01** (2018) 108 [[arXiv:1710.03752](#)] [[INSPIRE](#)].
- [26] C.-W. Chiang, H. Fukuda, M. Takeuchi and T.T. Yanagida, *Current status of top-specific variant axion model*, *Phys. Rev. D* **97** (2018) 035015 [[arXiv:1711.02993](#)] [[INSPIRE](#)].
- [27] A. Greljo, J.F. Kamenik and J. Kopp, *Disentangling flavor violation in the top-Higgs sector at the LHC*, *JHEP* **07** (2014) 046 [[arXiv:1404.1278](#)] [[INSPIRE](#)].
- [28] D. Florian, *Handbook of LHC Higgs Cross Sections: 4. Deciphering the Nature of the Higgs Sector*, [arXiv:1610.07922](#) [[DOI:10.23731/CYRM-2017-002](#)] [[INSPIRE](#)].
- [29] ATLAS collaboration, *Search for top quark decays $t \rightarrow qH$ with $H \rightarrow \gamma\gamma$ using the ATLAS detector*, *JHEP* **06** (2014) 008 [[arXiv:1403.6293](#)] [[INSPIRE](#)].
- [30] ATLAS collaboration, *Search for flavour-changing neutral current top quark decays $t \rightarrow Hq$ in pp collisions at $\sqrt{s} = 8$ TeV with the ATLAS detector*, *JHEP* **12** (2015) 061 [[arXiv:1509.06047](#)] [[INSPIRE](#)].

- [31] CMS collaboration, *Search for top quark decays via Higgs-boson-mediated flavor-changing neutral currents in pp collisions at $\sqrt{s} = 8$ TeV*, *JHEP* **02** (2017) 079 [[arXiv:1610.04857](#)] [[INSPIRE](#)].
- [32] ATLAS collaboration, *Search for top-quark decays $t \rightarrow Hq$ with 36 fb^{-1} of pp collision data at $\sqrt{s} = 13$ TeV with the ATLAS detector*, *JHEP* **05** (2019) 123 [[arXiv:1812.11568](#)] [[INSPIRE](#)].
- [33] ATLAS collaboration, *Search for top quark decays $t \rightarrow qH$, with $H \rightarrow \gamma\gamma$, in $\sqrt{s} = 13$ TeV pp collisions using the ATLAS detector*, *JHEP* **10** (2017) 129 [[arXiv:1707.01404](#)] [[INSPIRE](#)].
- [34] ATLAS collaboration, *Search for flavor-changing neutral currents in top quark decays $t \rightarrow Hc$ and $t \rightarrow Hu$ in multilepton final states in proton-proton collisions at $\sqrt{s} = 13$ TeV with the ATLAS detector*, *Phys. Rev. D* **98** (2018) 032002 [[arXiv:1805.03483](#)] [[INSPIRE](#)].
- [35] CMS collaboration, *Search for the flavor-changing neutral current interactions of the top quark and the Higgs boson which decays into a pair of b quarks at $\sqrt{s} = 13$ TeV*, *JHEP* **06** (2018) 102 [[arXiv:1712.02399](#)] [[INSPIRE](#)].
- [36] CMS collaboration, *Search for flavor-changing neutral current interactions of the top quark and the Higgs boson decaying to a bottom quark-antiquark pair at $\sqrt{s} = 13$ TeV*, *JHEP* **02** (2022) 169 [[arXiv:2112.09734](#)] [[INSPIRE](#)].
- [37] CMS collaboration, *Search for Flavor-Changing Neutral Current Interactions of the Top Quark and Higgs Boson in Final States with Two Photons in Proton-Proton Collisions at $\sqrt{s} = 13$ TeV*, *Phys. Rev. Lett.* **129** (2022) 032001 [[arXiv:2111.02219](#)] [[INSPIRE](#)].
- [38] ATLAS collaboration, *The ATLAS Experiment at the CERN Large Hadron Collider*, 2008 *JINST* **3** S08003 [[INSPIRE](#)].
- [39] ATLAS collaboration, *ATLAS Insertable B-Layer Technical Design Report*, [CERN-LHCC-2010-013](#) (2010).
- [40] ATLAS collaboration, *ATLAS Insertable B-Layer Technical Design Report Addendum*, [CERN-LHCC-2012-009](#) (2012).
- [41] B. Abbott, *Production and Integration of the ATLAS Insertable B-Layer*, 2018 *JINST* **13** T05008 [[arXiv:1803.00844](#)] [[INSPIRE](#)].
- [42] ATLAS collaboration, *Performance of the ATLAS Trigger System in 2015*, *Eur. Phys. J. C* **77** (2017) 317 [[arXiv:1611.09661](#)] [[INSPIRE](#)].
- [43] ATLAS collaboration, *The ATLAS Collaboration Software and Firmware*, [ATL-SOFT-PUB-2021-001](#), CERN, Geneva (2021).
- [44] ATLAS collaboration, *ATLAS data quality operations and performance for 2015–2018 data-taking*, 2020 *JINST* **15** P04003 [[arXiv:1911.04632](#)] [[INSPIRE](#)].
- [45] ATLAS collaboration, *Vertex Reconstruction Performance of the ATLAS Detector at $\sqrt{s} = 13$ TeV*, [ATL-PHYS-PUB-2015-026](#), CERN, Geneva (2015).
- [46] ATLAS collaboration, *Electron and photon performance measurements with the ATLAS detector using the 2015–2017 LHC proton-proton collision data*, 2019 *JINST* **14** P12006 [[arXiv:1908.00005](#)] [[INSPIRE](#)].
- [47] ATLAS collaboration, *Electron reconstruction and identification in the ATLAS experiment using the 2015 and 2016 LHC proton-proton collision data at $\sqrt{s} = 13$ TeV*, *Eur. Phys. J. C* **79** (2019) 639 [[arXiv:1902.04655](#)] [[INSPIRE](#)].

- [48] ATLAS collaboration, *Muon reconstruction and identification efficiency in ATLAS using the full Run 2 pp collision data set at $\sqrt{s} = 13$ TeV*, *Eur. Phys. J. C* **81** (2021) 578 [[arXiv:2012.00578](#)] [[INSPIRE](#)].
- [49] ATLAS collaboration, *Muon reconstruction performance of the ATLAS detector in proton–proton collision data at $\sqrt{s} = 13$ TeV*, *Eur. Phys. J. C* **76** (2016) 292 [[arXiv:1603.05598](#)] [[INSPIRE](#)].
- [50] M. Cacciari, G.P. Salam and G. Soyez, *The anti- k_t jet clustering algorithm*, *JHEP* **04** (2008) 063 [[arXiv:0802.1189](#)] [[INSPIRE](#)].
- [51] M. Cacciari, G.P. Salam and G. Soyez, *FastJet user manual*, *Eur. Phys. J. C* **72** (2012) 1896 [[arXiv:1111.6097](#)] [[INSPIRE](#)].
- [52] ATLAS collaboration, *Topological cell clustering in the ATLAS calorimeters and its performance in LHC Run 1*, *Eur. Phys. J. C* **77** (2017) 490 [[arXiv:1603.02934](#)] [[INSPIRE](#)].
- [53] ATLAS collaboration, *Jet reconstruction and performance using particle flow with the ATLAS Detector*, *Eur. Phys. J. C* **77** (2017) 466 [[arXiv:1703.10485](#)] [[INSPIRE](#)].
- [54] ATLAS collaboration, *Jet energy scale measurements and their systematic uncertainties in proton-proton collisions at $\sqrt{s} = 13$ TeV with the ATLAS detector*, *Phys. Rev. D* **96** (2017) 072002 [[arXiv:1703.09665](#)] [[INSPIRE](#)].
- [55] M. Cacciari, G.P. Salam and G. Soyez, *The catchment area of jets*, *JHEP* **04** (2008) 005 [[arXiv:0802.1188](#)] [[INSPIRE](#)].
- [56] ATLAS collaboration, *Selection of jets produced in 13 TeV proton–proton collisions with the ATLAS detector*, [ATLAS-CONF-2015-029](#) (2015).
- [57] ATLAS collaboration, *Performance of pile-up mitigation techniques for jets in pp collisions at $\sqrt{s} = 8$ TeV using the ATLAS detector*, *Eur. Phys. J. C* **76** (2016) 581 [[arXiv:1510.03823](#)] [[INSPIRE](#)].
- [58] ATLAS collaboration, *ATLAS b-jet identification performance and efficiency measurement with $t\bar{t}$ events in pp collisions at $\sqrt{s} = 13$ TeV*, *Eur. Phys. J. C* **79** (2019) 970 [[arXiv:1907.05120](#)] [[INSPIRE](#)].
- [59] ATLAS collaboration, *Optimisation and performance studies of the ATLAS b-tagging algorithms for the 2017-18 LHC run*, [ATL-PHYS-PUB-2017-013](#), CERN, Geneva (2017).
- [60] ATLAS collaboration, *Identification of hadronic tau lepton decays using neural networks in the ATLAS experiment*, [ATL-PHYS-PUB-2019-033](#), CERN, Geneva (2019).
- [61] A. Graves, *Supervised Sequence Labelling*, in *Studies in Computational Intelligence*, Springer (2012), p. 5–13 [[DOI:10.1007/978-3-642-24797-2_2](#)].
- [62] ATLAS collaboration, *Performance of missing transverse momentum reconstruction with the ATLAS detector using proton-proton collisions at $\sqrt{s} = 13$ TeV*, *Eur. Phys. J. C* **78** (2018) 903 [[arXiv:1802.08168](#)] [[INSPIRE](#)].
- [63] ATLAS collaboration, *Performance of electron and photon triggers in ATLAS during LHC Run 2*, *Eur. Phys. J. C* **80** (2020) 47 [[arXiv:1909.00761](#)] [[INSPIRE](#)].
- [64] ATLAS collaboration, *Performance of the ATLAS muon triggers in Run 2, 2020* *JINST* **15** P09015 [[arXiv:2004.13447](#)] [[INSPIRE](#)].
- [65] ATLAS collaboration, *The ATLAS inner detector trigger performance in pp collisions at 13 TeV during LHC Run 2*, *Eur. Phys. J. C* **82** (2022) 206 [[arXiv:2107.02485](#)] [[INSPIRE](#)].
- [66] ATLAS collaboration, *Performance of the ATLAS Level-1 topological trigger in Run 2*, *Eur. Phys. J. C* **82** (2022) 7 [[arXiv:2105.01416](#)] [[INSPIRE](#)].

- [67] S. Frixione, P. Nason and G. Ridolfi, *A Positive-weight next-to-leading-order Monte Carlo for heavy flavour hadroproduction*, *JHEP* **09** (2007) 126 [[arXiv:0707.3088](#)] [[INSPIRE](#)].
- [68] P. Nason, *A New method for combining NLO QCD with shower Monte Carlo algorithms*, *JHEP* **11** (2004) 040 [[hep-ph/0409146](#)] [[INSPIRE](#)].
- [69] S. Frixione, P. Nason and C. Oleari, *Matching NLO QCD computations with Parton Shower simulations: the POWHEG method*, *JHEP* **11** (2007) 070 [[arXiv:0709.2092](#)] [[INSPIRE](#)].
- [70] S. Alioli, P. Nason, C. Oleari and E. Re, *A general framework for implementing NLO calculations in shower Monte Carlo programs: the POWHEG BOX*, *JHEP* **06** (2010) 043 [[arXiv:1002.2581](#)] [[INSPIRE](#)].
- [71] NNPDF collaboration, *Parton distributions for the LHC Run II*, *JHEP* **04** (2015) 040 [[arXiv:1410.8849](#)] [[INSPIRE](#)].
- [72] T. Sjöstrand, S. Mrenna and P.Z. Skands, *A brief introduction to PYTHIA 8.1*, *Comput. Phys. Commun.* **178** (2008) 852 [[arXiv:0710.3820](#)] [[INSPIRE](#)].
- [73] R.D. Ball et al., *Parton distributions with LHC data*, *Nucl. Phys. B* **867** (2013) 244 [[arXiv:1207.1303](#)] [[INSPIRE](#)].
- [74] ATLAS collaboration, *ATLAS Pythia 8 tunes to 7 TeV data*, *ATL-PHYS-PUB-2014-021*, CERN, Geneva (2014).
- [75] J. Alwall et al., *The automated computation of tree-level and next-to-leading order differential cross sections, and their matching to parton shower simulations*, *JHEP* **07** (2014) 079 [[arXiv:1405.0301](#)] [[INSPIRE](#)].
- [76] C. Degrande, F. Maltoni, J. Wang and C. Zhang, *Automatic computations at next-to-leading order in QCD for top-quark flavor-changing neutral processes*, *Phys. Rev. D* **91** (2015) 034024 [[arXiv:1412.5594](#)] [[INSPIRE](#)].
- [77] M. Czakon and A. Mitov, *Top++: a program for the calculation of the top-pair cross-section at hadron colliders*, *Comput. Phys. Commun.* **185** (2014) 2930 [[arXiv:1112.5675](#)] [[INSPIRE](#)].
- [78] M. Cacciari et al., *Top-pair production at hadron colliders with next-to-next-to-leading logarithmic soft-gluon resummation*, *Phys. Lett. B* **710** (2012) 612 [[arXiv:1111.5869](#)] [[INSPIRE](#)].
- [79] P. Bärnreuther, M. Czakon and A. Mitov, *Percent Level Precision Physics at the Tevatron: First Genuine NNLO QCD Corrections to $q\bar{q} \rightarrow t\bar{t} + X$* , *Phys. Rev. Lett.* **109** (2012) 132001 [[arXiv:1204.5201](#)] [[INSPIRE](#)].
- [80] M. Czakon and A. Mitov, *NNLO corrections to top-pair production at hadron colliders: the all-fermionic scattering channels*, *JHEP* **12** (2012) 054 [[arXiv:1207.0236](#)] [[INSPIRE](#)].
- [81] M. Czakon and A. Mitov, *NNLO corrections to top pair production at hadron colliders: the quark-gluon reaction*, *JHEP* **01** (2013) 080 [[arXiv:1210.6832](#)] [[INSPIRE](#)].
- [82] M. Czakon, P. Fiedler and A. Mitov, *Total Top-Quark Pair-Production Cross Section at Hadron Colliders Through $O(\alpha_S^4)$* , *Phys. Rev. Lett.* **110** (2013) 252004 [[arXiv:1303.6254](#)] [[INSPIRE](#)].
- [83] R. Frederix, E. Re and P. Torrielli, *Single-top t -channel hadroproduction in the four-flavour scheme with POWHEG and aMC@NLO*, *JHEP* **09** (2012) 130 [[arXiv:1207.5391](#)] [[INSPIRE](#)].
- [84] S. Frixione, E. Laenen, P. Motylinski and B.R. Webber, *Single-top production in MC@NLO*, *JHEP* **03** (2006) 092 [[hep-ph/0512250](#)] [[INSPIRE](#)].

- [85] T. Sjöstrand, S. Mrenna and P.Z. Skands, *PYTHIA 6.4 physics and manual*, *JHEP* **05** (2006) 026 [[hep-ph/0603175](#)] [[INSPIRE](#)].
- [86] N. Kidonakis, *Next-to-next-to-leading-order collinear and soft gluon corrections for t -channel single top quark production*, *Phys. Rev. D* **83** (2011) 091503 [[arXiv:1103.2792](#)] [[INSPIRE](#)].
- [87] N. Kidonakis, *Two-loop soft anomalous dimensions for single top quark associated production with a W^- or H^-* , *Phys. Rev. D* **82** (2010) 054018 [[arXiv:1005.4451](#)] [[INSPIRE](#)].
- [88] N. Kidonakis, *NNLL resummation for s -channel single top quark production*, *Phys. Rev. D* **81** (2010) 054028 [[arXiv:1001.5034](#)] [[INSPIRE](#)].
- [89] T. Gleisberg et al., *Event generation with SHERPA 1.1*, *JHEP* **02** (2009) 007 [[arXiv:0811.4622](#)] [[INSPIRE](#)].
- [90] T. Gleisberg and S. Höche, *Comix, a new matrix element generator*, *JHEP* **12** (2008) 039 [[arXiv:0808.3674](#)] [[INSPIRE](#)].
- [91] F. Cascioli, P. Maierhöfer and S. Pozzorini, *Scattering Amplitudes with Open Loops*, *Phys. Rev. Lett.* **108** (2012) 111601 [[arXiv:1111.5206](#)] [[INSPIRE](#)].
- [92] S. Schumann and F. Krauss, *A Parton shower algorithm based on Catani-Seymour dipole factorisation*, *JHEP* **03** (2008) 038 [[arXiv:0709.1027](#)] [[INSPIRE](#)].
- [93] S. Höche, F. Krauss, M. Schönherr and F. Siegert, *QCD matrix elements + parton showers. The NLO case*, *JHEP* **04** (2013) 027 [[arXiv:1207.5030](#)] [[INSPIRE](#)].
- [94] C. Anastasiou, L.J. Dixon, K. Melnikov and F. Petriello, *High precision QCD at hadron colliders: Electroweak gauge boson rapidity distributions at NNLO*, *Phys. Rev. D* **69** (2004) 094008 [[hep-ph/0312266](#)] [[INSPIRE](#)].
- [95] D.J. Lange, *The EvtGen particle decay simulation package*, *Nucl. Instrum. Meth. A* **462** (2001) 152 [[INSPIRE](#)].
- [96] ATLAS collaboration, *The Pythia 8 A3 tune description of ATLAS minimum bias and inelastic measurements incorporating the Donnachie-Landshoff diffractive model*, *ATL-PHYS-PUB-2016-017*, CERN, Geneva (2016).
- [97] ATLAS collaboration, *The ATLAS Simulation Infrastructure*, *Eur. Phys. J. C* **70** (2010) 823 [[arXiv:1005.4568](#)] [[INSPIRE](#)].
- [98] GEANT4 collaboration, *GEANT4 — a simulation toolkit*, *Nucl. Instrum. Meth. A* **506** (2003) 250 [[INSPIRE](#)].
- [99] C. ATLAS et al., *The simulation principle and performance of the ATLAS fast calorimeter simulation FastCaloSim*, *ATL-PHYS-PUB-2010-013*, CERN, Geneva (2010).
- [100] X. Chen and L. Xia, *Searching for flavor changing neutral currents in $t \rightarrow Hc$, $H \rightarrow \tau\tau$ decays at the LHC*, *Phys. Rev. D* **93** (2016) 113010 [[arXiv:1509.08149](#)] [[INSPIRE](#)].
- [101] A. Djouadi, J. Kalinowski and M. Spira, *HDECAY: A Program for Higgs boson decays in the standard model and its supersymmetric extension*, *Comput. Phys. Commun.* **108** (1998) 56 [[hep-ph/9704448](#)] [[INSPIRE](#)].
- [102] ATLAS collaboration, *Measurements of Higgs boson production cross-sections in the $H \rightarrow \tau^+\tau^-$ decay channel in pp collisions at $\sqrt{s} = 13$ TeV with the ATLAS detector*, *JHEP* **08** (2022) 175 [[arXiv:2201.08269](#)] [[INSPIRE](#)].
- [103] A. Hocker et al., *TMVA — Toolkit for Multivariate Data Analysis*, [physics/0703039](#) [[INSPIRE](#)].

- [104] ATLAS collaboration, *Luminosity determination in pp collisions at $\sqrt{s} = 8$ TeV using the ATLAS detector at the LHC*, *Eur. Phys. J. C* **76** (2016) 653 [[arXiv:1608.03953](#)] [[INSPIRE](#)].
- [105] G. Avoni et al., *The new LUCID-2 detector for luminosity measurement and monitoring in ATLAS*, *2018 JINST* **13** P07017 [[INSPIRE](#)].
- [106] ATLAS collaboration, *Measurement of the tau lepton reconstruction and identification performance in the ATLAS experiment using pp collisions at $\sqrt{s} = 13$ TeV*, *ATLAS-CONF-2017-029*, CERN, Geneva (2017).
- [107] ATLAS collaboration, *Measurement of b-tagging efficiency of c-jets in $t\bar{t}$ events using a likelihood approach with the ATLAS detector*, *ATLAS-CONF-2018-001*, CERN, Geneva (2018).
- [108] ATLAS collaboration, *Performance of b-jet identification in the ATLAS experiment*, *2016 JINST* **11** P04008 [[arXiv:1512.01094](#)] [[INSPIRE](#)].
- [109] ATLAS collaboration, *Calibration of light-flavour b-jet mistagging rates using ATLAS proton-proton collision data at $\sqrt{s} = 13$ TeV*, *ATLAS-CONF-2018-006*, CERN, Geneva (2018).
- [110] L.A. Harland-Lang, A.D. Martin, P. Motylinski and R.S. Thorne, *Parton distributions in the LHC era: MMHT 2014 PDFs*, *Eur. Phys. J. C* **75** (2015) 204 [[arXiv:1412.3989](#)] [[INSPIRE](#)].
- [111] J. Bellm et al., *Herwig 7.0/Herwig++ 3.0 release note*, *Eur. Phys. J. C* **76** (2016) 196 [[arXiv:1512.01178](#)] [[INSPIRE](#)].
- [112] ATLAS collaboration, *Simulation of top quark production for the ATLAS experiment at $\sqrt{s} = 13$ TeV*, *ATL-PHYS-PUB-2016-004*, CERN, Geneva (2016).
- [113] NNPDF collaboration, *Parton distributions for the LHC Run II*, *JHEP* **04** (2015) 040 [[arXiv:1410.8849](#)] [[INSPIRE](#)].
- [114] H.-L. Lai et al., *New parton distributions for collider physics*, *Phys. Rev. D* **82** (2010) 074024 [[arXiv:1007.2241](#)] [[INSPIRE](#)].
- [115] J. Gao et al., *CT10 next-to-next-to-leading order global analysis of QCD*, *Phys. Rev. D* **89** (2014) 033009 [[arXiv:1302.6246](#)] [[INSPIRE](#)].
- [116] ATLAS collaboration, *Measurements of the inclusive and differential production cross sections of a top-quark-antiquark pair in association with a Z boson at $\sqrt{s} = 13$ TeV with the ATLAS detector*, *Eur. Phys. J. C* **81** (2021) 737 [[arXiv:2103.12603](#)] [[INSPIRE](#)].
- [117] W. Verkerke and D.P. Kirkby, *The RooFit toolkit for data modeling*, *eConf C0303241* (2003) MOLT007 [[physics/0306116](#)] [[INSPIRE](#)].
- [118] W. Verkerke and D. Kirkby, *RooFit users manual*, <http://roofit.sourceforge.net>.
- [119] T. Junk, *Confidence level computation for combining searches with small statistics*, *Nucl. Instrum. Meth. A* **434** (1999) 435 [[hep-ex/9902006](#)] [[INSPIRE](#)].
- [120] A.L. Read, *Presentation of search results: The CL_s technique*, *J. Phys. G* **28** (2002) 2693 [[INSPIRE](#)].
- [121] G. Cowan, K. Cranmer, E. Gross and O. Vitells, *Asymptotic formulae for likelihood-based tests of new physics*, *Eur. Phys. J. C* **71** (2011) 1554 [Erratum *ibid.* **73** (2013) 2501] [[arXiv:1007.1727](#)] [[INSPIRE](#)].
- [122] ATLAS collaboration, *ATLAS computing acknowledgements*, *ATL-SOFT-PUB-2021-003* (2021).

The ATLAS collaboration

G. Aad ^{[101](#)}, B. Abbott ^{[119](#)}, D.C. Abbott ^{[102](#)}, K. Abeling ^{[55](#)}, S.H. Abidi ^{[29](#)},
A. Aboulhorma ^{[35e](#)}, H. Abramowicz ^{[150](#)}, H. Abreu ^{[149](#)}, Y. Abulaiti ^{[116](#)},
A.C. Abusleme Hoffman ^{[136a](#)}, B.S. Acharya ^{[68a,68b,o](#)}, B. Achkar ^{[55](#)}, L. Adam ^{[99](#)},
C. Adam Bourdarios ^{[4](#)}, L. Adamczyk ^{[84a](#)}, L. Adamek ^{[154](#)}, S.V. Addepalli ^{[26](#)},
J. Adelman ^{[114](#)}, A. Adiguzel ^{[21c](#)}, S. Adorni ^{[56](#)}, T. Adye ^{[133](#)}, A.A. Affolder ^{[135](#)}, Y. Afik ^{[36](#)},
M.N. Agaras ^{[13](#)}, J. Agarwala ^{[72a,72b](#)}, A. Aggarwal ^{[99](#)}, C. Agheorghiesei ^{[27c](#)},
J.A. Aguilar-Saavedra ^{[129f](#)}, A. Ahmad ^{[36](#)}, F. Ahmadov ^{[38,w](#)}, W.S. Ahmed ^{[103](#)}, S. Ahuja ^{[94](#)},
X. Ai ^{[48](#)}, G. Aielli ^{[75a,75b](#)}, I. Aizenberg ^{[167](#)}, M. Akbiyik ^{[99](#)}, T.P.A. Åkesson ^{[97](#)},
A.V. Akimov ^{[37](#)}, K. Al Khoury ^{[41](#)}, G.L. Alberghi ^{[23b](#)}, J. Albert ^{[163](#)}, P. Albicocco ^{[53](#)},
M.J. Alconada Verzini ^{[89](#)}, S. Alderweireldt ^{[52](#)}, M. Aleksa ^{[36](#)}, I.N. Aleksandrov ^{[38](#)},
C. Alexa ^{[27b](#)}, T. Alexopoulos ^{[10](#)}, A. Alfonsi ^{[113](#)}, F. Alfonsi ^{[23b](#)}, M. Alhroob ^{[119](#)}, B. Ali ^{[131](#)},
S. Ali ^{[147](#)}, M. Aliev ^{[37](#)}, G. Alimonti ^{[70a](#)}, C. Allaire ^{[36](#)}, B.M.M. Allbrooke ^{[145](#)},
P.P. Allport ^{[20](#)}, A. Aloisio ^{[71a,71b](#)}, F. Alonso ^{[89](#)}, C. Alpigiani ^{[137](#)}, E. Alunno Camelia ^{[75a,75b](#)},
M. Alvarez Estevez ^{[98](#)}, M.G. Alviggi ^{[71a,71b](#)}, Y. Amaral Coutinho ^{[81b](#)}, A. Ambler ^{[103](#)},
C. Amelung ^{[36](#)}, C.G. Ames ^{[108](#)}, D. Amidei ^{[105](#)}, S.P. Amor Dos Santos ^{[129a](#)}, S. Amoroso ^{[48](#)},
K.R. Amos ^{[161](#)}, C.S. Amrouche ^{[56](#)}, V. Ananiev ^{[124](#)}, C. Anastopoulos ^{[138](#)}, N. Andari ^{[134](#)},
T. Andeen ^{[11](#)}, J.K. Anders ^{[19](#)}, S.Y. Andrean ^{[47a,47b](#)}, A. Andreazza ^{[70a,70b](#)}, S. Angelidakis ^{[9](#)},
A. Angerami ^{[41,y](#)}, A.V. Anisenkov ^{[37](#)}, A. Annovi ^{[73a](#)}, C. Antel ^{[56](#)}, M.T. Anthony ^{[138](#)},
E. Antipov ^{[120](#)}, M. Antonelli ^{[53](#)}, D.J.A. Antrim ^{[17a](#)}, F. Anulli ^{[74a](#)}, M. Aoki ^{[82](#)},
J.A. Aparisi Pozo ^{[161](#)}, M.A. Aparo ^{[145](#)}, L. Aperio Bella ^{[48](#)}, C. Appelt ^{[18](#)}, N. Aranzabal ^{[36](#)},
V. Araujo Ferraz ^{[81a](#)}, C. Arcangeletti ^{[53](#)}, A.T.H. Arce ^{[51](#)}, E. Arena ^{[91](#)}, J-F. Arguin ^{[107](#)},
S. Argyropoulos ^{[54](#)}, J.-H. Arling ^{[48](#)}, A.J. Armbruster ^{[36](#)}, O. Arnaez ^{[154](#)}, H. Arnold ^{[113](#)},
Z.P. Arrubarrena Tame ^{[108](#)}, G. Artioni ^{[74a,74b](#)}, H. Asada ^{[110](#)}, K. Asai ^{[117](#)}, S. Asai ^{[152](#)},
N.A. Asbah ^{[61](#)}, E.M. Asimakopoulou ^{[159](#)}, J. Assahsah ^{[35d](#)}, K. Assamagan ^{[29](#)}, R. Astalos ^{[28a](#)},
R.J. Atkin ^{[33a](#)}, M. Atkinson ^{[160](#)}, N.B. Atlay ^{[18](#)}, H. Atmani ^{[62b](#)}, P.A. Atmasiddha ^{[105](#)},
K. Augsten ^{[131](#)}, S. Auricchio ^{[71a,71b](#)}, A.D. Auriol ^{[20](#)}, V.A. Austrup ^{[169](#)}, G. Avner ^{[149](#)},
G. Avolio ^{[36](#)}, K. Axiotis ^{[56](#)}, M.K. Ayoub ^{[14c](#)}, G. Azuelos ^{[107,ab](#)}, D. Babal ^{[28a](#)},
H. Bachacou ^{[134](#)}, K. Bachas ^{[151,q](#)}, A. Bachiu ^{[34](#)}, F. Backman ^{[47a,47b](#)}, A. Badea ^{[61](#)},
P. Bagnaia ^{[74a,74b](#)}, M. Bahmani ^{[18](#)}, A.J. Bailey ^{[161](#)}, V.R. Bailey ^{[160](#)}, J.T. Baines ^{[133](#)},
C. Bakalis ^{[10](#)}, O.K. Baker ^{[170](#)}, P.J. Bakker ^{[113](#)}, E. Bakos ^{[15](#)}, D. Bakshi Gupta ^{[8](#)},
S. Balaji ^{[146](#)}, R. Balasubramanian ^{[113](#)}, E.M. Baldin ^{[37](#)}, P. Balek ^{[132](#)}, E. Ballabene ^{[70a,70b](#)},
F. Balli ^{[134](#)}, L.M. Baltes ^{[63a](#)}, W.K. Balunas ^{[32](#)}, J. Balz ^{[99](#)}, E. Banas ^{[85](#)},
M. Bandieramonte ^{[128](#)}, A. Bandyopadhyay ^{[24](#)}, S. Bansal ^{[24](#)}, L. Barak ^{[150](#)},
E.L. Barberio ^{[104](#)}, D. Barberis ^{[57b,57a](#)}, M. Barbero ^{[101](#)}, G. Barbour ^{[95](#)}, K.N. Barends ^{[33a](#)},
T. Barillari ^{[109](#)}, M-S. Barisits ^{[36](#)}, J. Barkeloo ^{[122](#)}, T. Barklow ^{[142](#)}, R.M. Barnett ^{[17a](#)},
P. Baron ^{[121](#)}, D.A. Baron Moreno ^{[100](#)}, A. Baroncelli ^{[62a](#)}, G. Barone ^{[29](#)}, A.J. Barr ^{[125](#)},
L. Barranco Navarro ^{[47a,47b](#)}, F. Barreiro ^{[98](#)}, J. Barreiro Guimarães da Costa ^{[14a](#)},
U. Barron ^{[150](#)}, M.G. Barros Teixeira ^{[129a](#)}, S. Barsov ^{[37](#)}, F. Bartels ^{[63a](#)}, R. Bartoldus ^{[142](#)},
A.E. Barton ^{[90](#)}, P. Bartos ^{[28a](#)}, A. Basalaeu ^{[48](#)}, A. Basan ^{[99](#)}, M. Baselga ^{[49](#)},
I. Bashta ^{[76a,76b](#)}, A. Bassalat ^{[66,ag](#)}, M.J. Basso ^{[154](#)}, C.R. Basson ^{[100](#)}, R.L. Bates ^{[59](#)},
S. Batlamous ^{[35e](#)}, J.R. Batley ^{[32](#)}, B. Batool ^{[140](#)}, M. Battaglia ^{[135](#)}, M. Bause ^{[74a,74b](#)},

P. Bauer ²⁴, A. Bayirli ^{21a}, J.B. Beacham ⁵¹, T. Beau ¹²⁶, P.H. Beauchemin ¹⁵⁷,
F. Becherer ⁵⁴, P. Bechtle ²⁴, H.P. Beck ^{19,p}, K. Becker ¹⁶⁵, C. Becot ⁴⁸, A.J. Beddall ^{21d},
V.A. Bednyakov ³⁸, C.P. Bee ¹⁴⁴, L.J. Beemster¹⁵, T.A. Beermann ³⁶, M. Begalli ^{81b,81d},
M. Begel ²⁹, A. Behera ¹⁴⁴, J.K. Behr ⁴⁸, C. Beirao Da Cruz E Silva ³⁶, J.F. Beirer ^{55,36},
F. Beisiegel ²⁴, M. Belfkir ^{115b}, G. Bella ¹⁵⁰, L. Bellagamba ^{23b}, A. Bellerive ³⁴,
P. Bellos ²⁰, K. Beloborodov ³⁷, K. Belotskiy ³⁷, N.L. Belyaev ³⁷, D. Benckekroun ^{35a},
F. Bendebba ^{35a}, Y. Benhammou ¹⁵⁰, D.P. Benjamin ²⁹, M. Benoit ²⁹, J.R. Bensinger ²⁶,
S. Bentvelsen ¹¹³, L. Beresford ³⁶, M. Beretta ⁵³, D. Berge ¹⁸, E. Bergeas Kuutmann ¹⁵⁹,
N. Berger ⁴, B. Bergmann ¹³¹, J. Beringer ^{17a}, S. Berlendis ⁷, G. Bernardi ⁵,
C. Bernius ¹⁴², F.U. Bernlochner ²⁴, T. Berry ⁹⁴, P. Berta ¹³², A. Berthold ⁵⁰,
I.A. Bertram ⁹⁰, O. Bessidskaia Bylund ¹⁶⁹, S. Bethke ¹⁰⁹, A. Betti ^{74a,74b}, A.J. Bevan ⁹³,
M. Bhamjee ^{33c}, S. Bhatta ¹⁴⁴, D.S. Bhattacharya ¹⁶⁴, P. Bhattacharai ²⁶, V.S. Bhopatkar ⁶,
R. Bi¹²⁸, R. Bi^{29,ae}, R.M. Bianchi ¹²⁸, O. Biebel ¹⁰⁸, R. Bielski ¹²², N.V. Biesuz ^{73a,73b},
M. Biglietti ^{76a}, T.R.V. Billoud ¹³¹, M. Bindi ⁵⁵, A. Bingul ^{21b}, C. Bini ^{74a,74b},
S. Biondi ^{23b,23a}, A. Biondini ⁹¹, C.J. Birch-sykes ¹⁰⁰, G.A. Bird ^{20,133}, M. Birman ¹⁶⁷,
T. Bisanz ³⁶, D. Biswas ^{168,k}, A. Bitadze ¹⁰⁰, K. Bjørke ¹²⁴, I. Bloch ⁴⁸, C. Blocker ²⁶,
A. Blue ⁵⁹, U. Blumenschein ⁹³, J. Blumenthal ⁹⁹, G.J. Bobbink ¹¹³, V.S. Bobrovnikov ³⁷,
M. Boehler ⁵⁴, D. Bogavac ³⁶, A.G. Bogdanchikov ³⁷, C. Bohm ^{47a}, V. Boisvert ⁹⁴,
P. Bokan ⁴⁸, T. Bold ^{84a}, M. Bomben ⁵, M. Bona ⁹³, M. Boonekamp ¹³⁴, C.D. Booth ⁹⁴,
A.G. Borbély ⁵⁹, H.M. Borecka-Bielska ¹⁰⁷, L.S. Borgna ⁹⁵, G. Borissov ⁹⁰,
D. Bortoletto ¹²⁵, D. Boscherini ^{23b}, M. Bosman ¹³, J.D. Bossio Sola ³⁶, K. Bouaouda ^{35a},
J. Boudreau ¹²⁸, E.V. Bouhova-Thacker ⁹⁰, D. Boumediene ⁴⁰, R. Bouquet ⁵,
A. Boveia ¹¹⁸, J. Boyd ³⁶, D. Boye ²⁹, I.R. Boyko ³⁸, J. Bracinek ²⁰, N. Brahimi ^{62d,62c},
G. Brandt ¹⁶⁹, O. Brandt ³², F. Braren ⁴⁸, B. Brau ¹⁰², J.E. Brau ¹²²,
W.D. Breaden Madden ⁵⁹, K. Brendlinger ⁴⁸, R. Brenner ¹⁶⁷, L. Brenner ³⁶, R. Brenner ¹⁵⁹,
S. Bressler ¹⁶⁷, B. Brickwedde ⁹⁹, D. Britton ⁵⁹, D. Britzger ¹⁰⁹, I. Brock ²⁴,
G. Brooijmans ⁴¹, W.K. Brooks ^{136f}, E. Brost ²⁹, P.A. Bruckman de Renstrom ⁸⁵,
B. Brüers ⁴⁸, D. Bruncko ^{28b,*}, A. Bruni ^{23b}, G. Bruni ^{23b}, M. Bruschi ^{23b},
N. Bruscino ^{74a,74b}, L. Bryngemark ¹⁴², T. Buanes ¹⁶, Q. Buat ¹³⁷, P. Buchholz ¹⁴⁰,
A.G. Buckley ⁵⁹, I.A. Budagov ^{38,*}, M.K. Bugge ¹²⁴, O. Bulekov ³⁷, B.A. Bullard ⁶¹,
S. Burdin ⁹¹, C.D. Burgard ⁴⁸, A.M. Burger ⁴⁰, B. Burghgrave ⁸, J.T.P. Burr ³²,
C.D. Burton ¹¹, J.C. Burzynski ¹⁴¹, E.L. Busch ⁴¹, V. Büscher ⁹⁹, P.J. Bussey ⁵⁹,
J.M. Butler ²⁵, C.M. Buttar ⁵⁹, J.M. Butterworth ⁹⁵, W. Buttinger ¹³³,
C.J. Buxo Vazquez ¹⁰⁶, A.R. Buzykaev ³⁷, G. Cabras ^{23b}, S. Cabrera Urbán ¹⁶¹,
D. Caforio ⁵⁸, H. Cai ¹²⁸, Y. Cai ^{14a,14d}, V.M.M. Cairo ³⁶, O. Cakir ^{3a}, N. Calace ³⁶,
P. Calafiura ^{17a}, G. Calderini ¹²⁶, P. Calfayan ⁶⁷, G. Callea ⁵⁹, L.P. Caloba ^{81b},
D. Calvet ⁴⁰, S. Calvet ⁴⁰, T.P. Calvet ¹⁰¹, M. Calvetti ^{73a,73b}, R. Camacho Toro ¹²⁶,
S. Camarda ³⁶, D. Camarero Munoz ⁹⁸, P. Camarri ^{75a,75b}, M.T. Camerlingo ^{76a,76b},
D. Cameron ¹²⁴, C. Camincher ¹⁶³, M. Campanelli ⁹⁵, A. Camplani ⁴², V. Canale ^{71a,71b},
A. Canesse ¹⁰³, M. Cano Bret ⁷⁹, J. Cantero ¹⁶¹, Y. Cao ¹⁶⁰, F. Capocasa ²⁶,
M. Capua ^{43b,43a}, A. Carbone ^{70a,70b}, R. Cardarelli ^{75a}, J.C.J. Cardenas ⁸, F. Cardillo ¹⁶¹,
T. Carli ³⁶, G. Carlino ^{71a}, B.T. Carlson ^{128,r}, E.M. Carlson ^{163,155a}, L. Carminati ^{70a,70b},
M. Carnesale ^{74a,74b}, S. Caron ¹¹², E. Carquin ^{136f}, S. Carrá ^{70a,70b}, G. Carratta ^{23b,23a},

F. Carrio Argos ^{[133g](#)}, J.W.S. Carter ^{[154](#)}, T.M. Carter ^{[52](#)}, M.P. Casado ^{[13,h](#)}, A.F. Casha ^{[154](#)}, E.G. Castiglia ^{[170](#)}, F.L. Castillo ^{[63a](#)}, L. Castillo Garcia ^{[13](#)}, V. Castillo Gimenez ^{[161](#)}, N.F. Castro ^{[129a,129e](#)}, A. Catinaccio ^{[36](#)}, J.R. Catmore ^{[124](#)}, V. Cavaliere ^{[29](#)}, N. Cavalli ^{[23b,23a](#)}, V. Cavasinni ^{[73a,73b](#)}, E. Celebi ^{[21a](#)}, F. Celli ^{[125](#)}, M.S. Centonze ^{[69a,69b](#)}, K. Cerny ^{[121](#)}, A.S. Cerqueira ^{[81a](#)}, A. Cerri ^{[145](#)}, L. Cerrito ^{[75a,75b](#)}, F. Cerutti ^{[17a](#)}, A. Cervelli ^{[23b](#)}, S.A. Cetin ^{[21d](#)}, Z. Chadi ^{[35a](#)}, D. Chakraborty ^{[114](#)}, M. Chala ^{[129f](#)}, J. Chan ^{[168](#)}, W.S. Chan ^{[113](#)}, W.Y. Chan ^{[152](#)}, J.D. Chapman ^{[32](#)}, B. Chargeishvili ^{[148b](#)}, D.G. Charlton ^{[20](#)}, T.P. Charman ^{[93](#)}, M. Chatterjee ^{[19](#)}, S. Chekanov ^{[6](#)}, S.V. Chekulaev ^{[155a](#)}, G.A. Chelkov ^{[38,a](#)}, A. Chen ^{[105](#)}, B. Chen ^{[150](#)}, B. Chen ^{[163](#)}, C. Chen ^{[62a](#)}, H. Chen ^{[14c](#)}, H. Chen ^{[29](#)}, J. Chen ^{[62c](#)}, J. Chen ^{[26](#)}, S. Chen ^{[152](#)}, S.J. Chen ^{[14c](#)}, X. Chen ^{[62c](#)}, X. Chen ^{[14b,aa](#)}, Y. Chen ^{[62a](#)}, C.L. Cheng ^{[168](#)}, H.C. Cheng ^{[64a](#)}, A. Cheplakov ^{[38](#)}, E. Cheremushkina ^{[48](#)}, E. Cherepanova ^{[113](#)}, R. Cherkaoui El Moursli ^{[35e](#)}, E. Cheu ^{[7](#)}, K. Cheung ^{[65](#)}, L. Chevalier ^{[134](#)}, V. Chiarella ^{[53](#)}, G. Chiarelli ^{[73a](#)}, G. Chiodini ^{[69a](#)}, A.S. Chisholm ^{[20](#)}, A. Chitan ^{[27b](#)}, Y.H. Chiu ^{[163](#)}, M.V. Chizhov ^{[38](#)}, K. Choi ^{[11](#)}, A.R. Chomont ^{[74a,74b](#)}, Y. Chou ^{[102](#)}, E.Y.S. Chow ^{[113](#)}, T. Chowdhury ^{[33g](#)}, L.D. Christopher ^{[33g](#)}, K.L. Chu ^{[64a](#)}, M.C. Chu ^{[64a](#)}, X. Chu ^{[14a,14d](#)}, J. Chudoba ^{[130](#)}, J.J. Chwastowski ^{[85](#)}, D. Cieri ^{[109](#)}, K.M. Ciesla ^{[84a](#)}, V. Cindro ^{[92](#)}, A. Ciocio ^{[17a](#)}, F. Ciotto ^{[71a,71b](#)}, Z.H. Citron ^{[167,l](#)}, M. Citterio ^{[70a](#)}, D.A. Ciubotaru ^{[27b](#)}, B.M. Ciungu ^{[154](#)}, A. Clark ^{[56](#)}, P.J. Clark ^{[52](#)}, J.M. Clavijo Columbie ^{[48](#)}, S.E. Clawson ^{[100](#)}, C. Clement ^{[47a,47b](#)}, J. Clercx ^{[48](#)}, L. Clissa ^{[23b,23a](#)}, Y. Coadou ^{[101](#)}, M. Cobal ^{[68a,68c](#)}, A. Coccaro ^{[57b](#)}, R.F. Coelho Barrue ^{[129a](#)}, R. Coelho Lopes De Sa ^{[102](#)}, S. Coelli ^{[70a](#)}, H. Cohen ^{[150](#)}, A.E.C. Coimbra ^{[70a,70b](#)}, B. Cole ^{[41](#)}, J. Collot ^{[60](#)}, P. Conde Muno ^{[129a,129g](#)}, S.H. Connell ^{[33c](#)}, I.A. Connelly ^{[59](#)}, E.I. Conroy ^{[125](#)}, F. Conventi ^{[71a,ac](#)}, H.G. Cooke ^{[20](#)}, A.M. Cooper-Sarkar ^{[125](#)}, F. Cormier ^{[162](#)}, L.D. Corpe ^{[36](#)}, M. Corradi ^{[74a,74b](#)}, E.E. Corrigan ^{[97](#)}, F. Corriveau ^{[103,v](#)}, A. Cortes-Gonzalez ^{[18](#)}, M.J. Costa ^{[161](#)}, F. Costanza ^{[4](#)}, D. Costanzo ^{[138](#)}, B.M. Cote ^{[118](#)}, G. Cowan ^{[94](#)}, J.W. Cowley ^{[32](#)}, K. Cranmer ^{[116](#)}, S. Cr p -Renaudin ^{[60](#)}, F. Crescioli ^{[126](#)}, M. Cristinziani ^{[140](#)}, M. Cristoforetti ^{[77a,77b,c](#)}, V. Croft ^{[157](#)}, G. Crosetti ^{[43b,43a](#)}, A. Cueto ^{[36](#)}, T. Cuhadar Donszelmann ^{[158](#)}, H. Cui ^{[14a,14d](#)}, Z. Cui ^{[7](#)}, A.R. Cukierman ^{[142](#)}, W.R. Cunningham ^{[59](#)}, F. Curcio ^{[43b,43a](#)}, P. Czodrowski ^{[36](#)}, M.M. Czurylo ^{[63b](#)}, M.J. Da Cunha Sargedas De Sousa ^{[62a](#)}, J.V. Da Fonseca Pinto ^{[81b](#)}, C. Da Via ^{[100](#)}, W. Dabrowski ^{[84a](#)}, T. Dado ^{[49](#)}, S. Dahbi ^{[33g](#)}, T. Dai ^{[105](#)}, C. Dallapiccola ^{[102](#)}, M. Dam ^{[42](#)}, G. D'amen ^{[29](#)}, V. D'Amico ^{[76a,76b](#)}, J. Damp ^{[99](#)}, J.R. Dandoy ^{[127](#)}, M.F. Daneri ^{[30](#)}, M. Danninger ^{[141](#)}, V. Dao ^{[36](#)}, G. Darbo ^{[57b](#)}, S. Darmora ^{[6](#)}, S.J. Das ^{[29,ae](#)}, A. Dattagupta ^{[122](#)}, S. D'Auria ^{[70a,70b](#)}, C. David ^{[155b](#)}, T. Davidek ^{[132](#)}, D.R. Davis ^{[51](#)}, B. Davis-Purcell ^{[34](#)}, I. Dawson ^{[93](#)}, K. De ^{[8](#)}, R. De Asmundis ^{[71a](#)}, M. De Beurs ^{[113](#)}, S. De Castro ^{[23b,23a](#)}, N. De Groot ^{[112](#)}, P. de Jong ^{[113](#)}, H. De la Torre ^{[106](#)}, A. De Maria ^{[14c](#)}, A. De Salvo ^{[74a](#)}, U. De Sanctis ^{[75a,75b](#)}, M. De Santis ^{[75a,75b](#)}, A. De Santo ^{[145](#)}, J.B. De Vivie De Regie ^{[60](#)}, D.V. Dedovich ^{[38](#)}, J. Degens ^{[113](#)}, A.M. Deiana ^{[44](#)}, F. Del Corso ^{[23b,23a](#)}, J. Del Peso ^{[98](#)}, F. Del Rio ^{[63a](#)}, F. Deliot ^{[134](#)}, C.M. Delitzsch ^{[49](#)}, M. Della Pietra ^{[71a,71b](#)}, D. Della Volpe ^{[56](#)}, A. Dell'Acqua ^{[36](#)}, L. Dell'Asta ^{[70a,70b](#)}, M. Delmastro ^{[4](#)}, P.A. Delsart ^{[60](#)}, S. Demers ^{[170](#)}, M. Demichev ^{[38](#)}, S.P. Denisov ^{[37](#)}, L. D'Eramo ^{[114](#)}, D. Derendarz ^{[85](#)}, F. Derue ^{[126](#)}, P. Dervan ^{[91](#)}, K. Desch ^{[24](#)}, K. Dette ^{[154](#)}, C. Deutsch ^{[24](#)}, P.O. Deviveiros ^{[36](#)},

F.A. Di Bello [ID](#)^{74a,74b}, A. Di Ciaccio [ID](#)^{75a,75b}, L. Di Ciaccio [ID](#)⁴, A. Di Domenico [ID](#)^{74a,74b},
C. Di Donato [ID](#)^{71a,71b}, A. Di Girolamo [ID](#)³⁶, G. Di Gregorio [ID](#)^{73a,73b}, A. Di Luca [ID](#)^{77a,77b},
B. Di Micco [ID](#)^{76a,76b}, R. Di Nardo [ID](#)^{76a,76b}, C. Diaconu [ID](#)¹⁰¹, F.A. Dias [ID](#)¹¹³,
T. Dias Do Vale [ID](#)¹⁴¹, M.A. Diaz [ID](#)^{136a,136b}, F.G. Diaz Capriles [ID](#)²⁴, M. Didenko [ID](#)¹⁶¹,
E.B. Diehl [ID](#)¹⁰⁵, L. Diehl [ID](#)⁵⁴, S. Díez Cornell [ID](#)⁴⁸, C. Díez Pardos [ID](#)¹⁴⁰, C. Dimitriadis [ID](#)^{24,159},
A. Dimitrievska [ID](#)^{17a}, W. Ding [ID](#)^{14b}, J. Dingfelder [ID](#)²⁴, I-M. Dinu [ID](#)^{27b}, S.J. Dittmeier [ID](#)^{63b},
F. Dittus [ID](#)³⁶, F. Djama [ID](#)¹⁰¹, T. Djobava [ID](#)^{148b}, J.I. Djuvsland [ID](#)¹⁶, D. Dodsworth [ID](#)²⁶,
C. Doglioni [ID](#)^{100,97}, J. Dolejsi [ID](#)¹³², Z. Dolezal [ID](#)¹³², M. Donadelli [ID](#)^{81c}, B. Dong [ID](#)^{62c},
J. Donini [ID](#)⁴⁰, A. D’Onofrio [ID](#)^{14c}, M. D’Onofrio [ID](#)⁹¹, J. Dopke [ID](#)¹³³, A. Doria [ID](#)^{71a},
M.T. Dova [ID](#)⁸⁹, A.T. Doyle [ID](#)⁵⁹, M.A. Draguet [ID](#)¹²⁵, E. Drechsler [ID](#)¹⁴¹, E. Dreyer [ID](#)¹⁶⁷,
I. Drivas-koulouris [ID](#)¹⁰, A.S. Drobac [ID](#)¹⁵⁷, D. Du [ID](#)^{62a}, T.A. du Pree [ID](#)¹¹³, F. Dubinin [ID](#)³⁷,
M. Dubovsky [ID](#)^{28a}, E. Duchovni [ID](#)¹⁶⁷, G. Duckeck [ID](#)¹⁰⁸, O.A. Ducu [ID](#)³⁶, D. Duda [ID](#)¹⁰⁹,
A. Dudarev [ID](#)³⁶, M. D’uffizi [ID](#)¹⁰⁰, L. Duflot [ID](#)⁶⁶, M. Dührssen [ID](#)³⁶, C. Dülsen [ID](#)¹⁶⁹,
A.E. Dumitriu [ID](#)^{27b}, M. Dunford [ID](#)^{63a}, S. Dungs [ID](#)⁴⁹, K. Dunne [ID](#)^{47a,47b}, A. Duperrin [ID](#)¹⁰¹,
H. Duran Yildiz [ID](#)^{3a}, M. Düren [ID](#)⁵⁸, A. Durglishvili [ID](#)^{148b}, B.L. Dwyer [ID](#)¹¹⁴, G.I. Dyckes [ID](#)^{17a},
M. Dyndal [ID](#)^{84a}, S. Dysch [ID](#)¹⁰⁰, B.S. Dziedzic [ID](#)⁸⁵, Z.O. Earnshaw [ID](#)¹⁴⁵, B. Eckerova [ID](#)^{28a},
M.G. Eggleston [ID](#)⁵¹, E. Egidio Purcino De Souza [ID](#)^{81b}, L.F. Ehrke [ID](#)⁵⁶, G. Eigen [ID](#)¹⁶,
K. Einsweiler [ID](#)^{17a}, T. Ekelof [ID](#)¹⁵⁹, P.A. Ekman [ID](#)⁹⁷, Y. El Ghazali [ID](#)^{35b}, H. El Jarrari [ID](#)^{35e,147},
A. El Moussaouy [ID](#)^{35a}, V. Ellajosyula [ID](#)¹⁵⁹, M. Ellert [ID](#)¹⁵⁹, F. Ellinghaus [ID](#)¹⁶⁹, A.A. Elliot [ID](#)⁹³,
N. Ellis [ID](#)³⁶, J. Elmsheuser [ID](#)²⁹, M. Elsing [ID](#)³⁶, D. Emelianov [ID](#)¹³³, A. Emerman [ID](#)⁴¹,
Y. Enari [ID](#)¹⁵², I. Ene [ID](#)^{17a}, S. Epari [ID](#)¹³, J. Erdmann [ID](#)⁴⁹, A. Ereditato [ID](#)¹⁹, P.A. Erland [ID](#)⁸⁵,
M. Errenst [ID](#)¹⁶⁹, M. Escalier [ID](#)⁶⁶, C. Escobar [ID](#)¹⁶¹, E. Etzion [ID](#)¹⁵⁰, G. Evans [ID](#)^{129a}, H. Evans [ID](#)⁶⁷,
M.O. Evans [ID](#)¹⁴⁵, A. Ezhilov [ID](#)³⁷, S. Ezzarqtouni [ID](#)^{35a}, F. Fabbri [ID](#)⁵⁹, L. Fabbri [ID](#)^{23b,23a},
G. Facini [ID](#)⁹⁵, V. Fadeyev [ID](#)¹³⁵, R.M. Fakhrutdinov [ID](#)³⁷, S. Falciano [ID](#)^{74a}, P.J. Falke [ID](#)²⁴,
S. Falke [ID](#)³⁶, J. Faltova [ID](#)¹³², Y. Fan [ID](#)^{14a}, Y. Fang [ID](#)^{14a,14d}, G. Fanourakis [ID](#)⁴⁶, M. Fanti [ID](#)^{70a,70b},
M. Faraj [ID](#)^{68a,68b}, A. Farbin [ID](#)⁸, A. Farilla [ID](#)^{76a}, T. Farooque [ID](#)¹⁰⁶, S.M. Farrington [ID](#)⁵²,
F. Fassi [ID](#)^{35e}, D. Fassouliotis [ID](#)⁹, M. Fauci Giannelli [ID](#)^{75a,75b}, W.J. Fawcett [ID](#)³², L. Fayard [ID](#)⁶⁶,
O.L. Fedin [ID](#)^{37,a}, G. Fedotov [ID](#)³⁷, M. Feickert [ID](#)¹⁶⁰, L. Feligioni [ID](#)¹⁰¹, A. Fell [ID](#)¹³⁸,
D.E. Fellers [ID](#)¹²², C. Feng [ID](#)^{62b}, M. Feng [ID](#)^{14b}, M.J. Fenton [ID](#)¹⁵⁸, A.B. Fenyuk [ID](#)³⁷, L. Ferencz [ID](#)⁴⁸,
S.W. Ferguson [ID](#)⁴⁵, J. Ferrando [ID](#)⁴⁸, A. Ferrari [ID](#)¹⁵⁹, P. Ferrari [ID](#)¹¹³, R. Ferrari [ID](#)^{72a},
D. Ferrere [ID](#)⁵⁶, C. Ferretti [ID](#)¹⁰⁵, F. Fiedler [ID](#)⁹⁹, A. Filipčič [ID](#)⁹², E.K. Filmer [ID](#)¹, F. Filthaut [ID](#)¹¹²,
M.C.N. Fiolhais [ID](#)^{129a,129c,b}, L. Fiorini [ID](#)¹⁶¹, F. Fischer [ID](#)¹⁴⁰, W.C. Fisher [ID](#)¹⁰⁶, T. Fitschen [ID](#)^{20,66},
I. Fleck [ID](#)¹⁴⁰, P. Fleischmann [ID](#)¹⁰⁵, T. Flick [ID](#)¹⁶⁹, L. Flores [ID](#)¹²⁷, M. Flores [ID](#)^{33d,ah},
L.R. Flores Castillo [ID](#)^{64a}, F.M. Follega [ID](#)^{77a,77b}, N. Fomin [ID](#)¹⁶, J.H. Foo [ID](#)¹⁵⁴, B.C. Forland [ID](#)⁶⁷,
A. Formica [ID](#)¹³⁴, A.C. Forti [ID](#)¹⁰⁰, E. Fortin [ID](#)¹⁰¹, A.W. Fortman [ID](#)⁶¹, M.G. Foti [ID](#)^{17a},
L. Fountas [ID](#)^{9,i}, D. Fournier [ID](#)⁶⁶, H. Fox [ID](#)⁹⁰, P. Francavilla [ID](#)^{73a,73b}, S. Francescato [ID](#)⁶¹,
M. Franchini [ID](#)^{23b,23a}, S. Franchino [ID](#)^{63a}, D. Francis [ID](#)³⁶, L. Franco [ID](#)¹¹², L. Franconi [ID](#)¹⁹,
M. Franklin [ID](#)⁶¹, G. Frattari [ID](#)²⁶, A.C. Freegard [ID](#)⁹³, P.M. Freeman [ID](#)²⁰, W.S. Freund [ID](#)^{81b},
N. Fritzsche [ID](#)⁵⁰, A. Froch [ID](#)⁵⁴, D. Froidevaux [ID](#)³⁶, J.A. Frost [ID](#)¹²⁵, Y. Fu [ID](#)^{62a}, M. Fujimoto [ID](#)¹¹⁷,
E. Fullana Torregrosa [ID](#)^{161,*}, J. Fuster [ID](#)¹⁶¹, A. Gabrielli [ID](#)^{23b,23a}, A. Gabrielli [ID](#)³⁶, P. Gadow [ID](#)⁴⁸,
G. Gagliardi [ID](#)^{57b,57a}, L.G. Gagnon [ID](#)^{17a}, G.E. Gallardo [ID](#)¹²⁵, E.J. Gallas [ID](#)¹²⁵, B.J. Gallop [ID](#)¹³³,
R. Gamboa Goni [ID](#)⁹³, K.K. Gan [ID](#)¹¹⁸, S. Ganguly [ID](#)¹⁵², J. Gao [ID](#)^{62a}, Y. Gao [ID](#)⁵²,
F.M. Garay Walls [ID](#)^{136a,136b}, B. Garcia [ID](#)^{29,ae}, C. García [ID](#)¹⁶¹, J.E. García Navarro [ID](#)¹⁶¹,

J.A. García Pascual [14a](#), M. Garcia-Sciveres [17a](#), R.W. Gardner [39](#), D. Garg [79](#),
R.B. Garg [142,ai](#), S. Gargiulo [54](#), C.A. Garner [154](#), V. Garonne [29](#), S.J. Gasiorowski [137](#),
P. Gaspar [81b](#), G. Gaudio [72a](#), V. Gautam [13](#), P. Gauzzi [74a,74b](#), I.L. Gavrilenko [37](#),
A. Gavriluk [37](#), C. Gay [162](#), G. Gaycken [48](#), E.N. Gazis [10](#), A.A. Geanta [27b](#),
C.M. Gee [135](#), J. Geisen [97](#), M. Geisen [99](#), C. Gemme [57b](#), M.H. Genest [60](#),
S. Gentile [74a,74b](#), S. George [94](#), W.F. George [20](#), T. Geralis [46](#), L.O. Gerlach [55](#),
P. Gessinger-Befurt [36](#), M. Ghasemi Bostanabad [163](#), M. Ghneimat [140](#), A. Ghosal [140](#),
A. Ghosh [158](#), A. Ghosh [7](#), B. Giacobbe [23b](#), S. Giagu [74a,74b](#), N. Giangiacomi [154](#),
P. Giannetti [73a](#), A. Giannini [62a](#), S.M. Gibson [94](#), M. Gignac [135](#), D.T. Gil [84b](#),
A.K. Gilbert [84a](#), B.J. Gilbert [41](#), D. Gillberg [34](#), G. Gilles [113](#), N.E.K. Gillwald [48](#),
L. Ginabat [126](#), D.M. Gingrich [2,ab](#), M.P. Giordani [68a,68c](#), P.F. Giraud [134](#),
G. Giugliarelli [68a,68c](#), D. Giugni [70a](#), F. Giuli [36](#), I. Gkialas [9,i](#), L.K. Gladilin [37](#),
C. Glasman [98](#), G.R. Gledhill [122](#), M. Glisic [122](#), I. Gnesi [43b,e](#), Y. Go [29,ae](#),
M. Goblirsch-Kolb [26](#), D. Godin [107](#), S. Goldfarb [104](#), T. Golling [56](#), M.G.D. Gololo [33g](#),
D. Golubkov [37](#), J.P. Gombas [106](#), A. Gomes [129a,129b](#), G. Gomes Da Silva [140](#),
A.J. Gomez Delegido [161](#), R. Goncalves Gama [55](#), R. Gonçalo [129a,129c](#), G. Gonella [122](#),
L. Gonella [20](#), A. Gongadze [38](#), F. Gonnella [20](#), J.L. Gonski [41](#), R.Y. González Andana [52](#),
S. González de la Hoz [161](#), S. Gonzalez Fernandez [13](#), R. Gonzalez Lopez [91](#),
C. Gonzalez Renteria [17a](#), R. Gonzalez Suarez [159](#), S. Gonzalez-Sevilla [56](#),
G.R. Gonzalvo Rodriguez [161](#), L. Goossens [36](#), N.A. Gorasia [20](#), P.A. Gorbounov [37](#),
B. Gorini [36](#), E. Gorini [69a,69b](#), A. Gorišek [92](#), A.T. Goshaw [51](#), M.I. Gostkin [38](#),
C.A. Gottardo [112](#), M. Goughri [35b](#), V. Goumarre [48](#), A.G. Goussiou [137](#), N. Govender [33c](#),
C. Goy [4](#), I. Grabowska-Bold [84a](#), K. Graham [34](#), E. Gramstad [124](#), S. Grancagnolo [18](#),
M. Grandi [145](#), V. Gratchev [37,*](#), P.M. Gravila [27f](#), F.G. Gravili [69a,69b](#), H.M. Gray [17a](#),
M. Greco [69a,69b](#), C. Greife [24](#), I.M. Gregor [48](#), P. Grenier [142](#), C. Grieco [13](#),
A.A. Grillo [135](#), K. Grimm [31,m](#), S. Grinstein [13,t](#), J.-F. Grivaz [66](#), E. Gross [167](#),
J. Grosse-Knetter [55](#), C. Grud [105](#), A. Grummer [111](#), J.C. Grundy [125](#), L. Guan [105](#),
W. Guan [168](#), C. Gubbels [162](#), J.G.R. Guerrero Rojas [161](#), G. Guerrieri [68a,68c](#),
F. Guescini [109](#), R. Gugel [99](#), J.A.M. Guhit [105](#), A. Guida [48](#), T. Guillemin [4](#),
E. Guilloton [165,133](#), S. Guindon [36](#), F. Guo [14a,14d](#), J. Guo [62c](#), L. Guo [66](#), Y. Guo [105](#),
R. Gupta [48](#), S. Gurbuz [24](#), S.S. Gurdasani [54](#), G. Gustavino [36](#), M. Guth [56](#),
P. Gutierrez [119](#), L.F. Gutierrez Zagazeta [127](#), C. Gutsche [95](#), C. Guyot [134](#),
C. Gwenlan [125](#), C.B. Gwilliam [91](#), E.S. Haaland [124](#), A. Haas [116](#), M. Habedank [48](#),
C. Haber [17a](#), H.K. Hadavand [8](#), A. Hadeef [99](#), S. Hadzic [109](#), M. Haleem [164](#), J. Haley [120](#),
J.J. Hall [138](#), G.D. Hallowell [101](#), L. Halser [19](#), K. Hamano [163](#), H. Hamdaoui [35e](#),
M. Hamer [24](#), G.N. Hamity [52](#), J. Han [62b](#), K. Han [62a](#), L. Han [14c](#), L. Han [62a](#),
S. Han [17a](#), Y.F. Han [154](#), K. Hanagaki [82](#), M. Hance [135](#), D.A. Hangal [41,y](#), M.D. Hank [39](#),
R. Hankache [100](#), J.B. Hansen [42](#), J.D. Hansen [42](#), P.H. Hansen [42](#), K. Hara [156](#),
D. Harada [56](#), T. Harenberg [169](#), S. Harkusha [37](#), Y.T. Harris [125](#), N.M. Harrison [118](#),
P.F. Harrison [165](#), N.M. Hartman [142](#), N.M. Hartmann [108](#), Y. Hasegawa [139](#), A. Hasib [52](#),
S. Haug [19](#), R. Hauser [106](#), M. Havranek [131](#), C.M. Hawkes [20](#), R.J. Hawkins [36](#),
S. Hayashida [110](#), D. Hayden [106](#), C. Hayes [105](#), R.L. Hayes [162](#), C.P. Hays [125](#),
J.M. Hays [93](#), H.S. Hayward [91](#), F. He [62a](#), Y. He [153](#), Y. He [126](#), M.P. Heath [52](#),


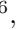

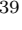

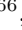
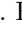
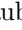
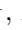

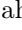
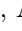


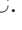
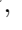
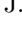

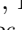

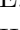






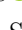
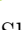

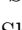

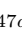

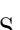
V. Hedberg ⁹⁷, A.L. Heggelund ¹²⁴, N.D. Hehir ⁹³, C. Heidegger ⁵⁴, K.K. Heidegger ⁵⁴, W.D. Heidorn ⁸⁰, J. Heilman ³⁴, S. Heim ⁴⁸, T. Heim ^{17a}, J.G. Heinlein ¹²⁷, J.J. Heinrich ¹²², L. Heinrich ³⁶, J. Hejbal ¹³⁰, L. Helary ⁴⁸, A. Held ¹¹⁶, S. Hellesund ¹²⁴, C.M. Helling ¹⁶², S. Hellman ^{47a,47b}, C. Helsens ³⁶, R.C.W. Henderson ⁹⁰, L. Henkelmann ³², A.M. Henriques Correia ³⁶, H. Herde ¹⁴², Y. Hernández Jiménez ¹⁴⁴, H. Herr ⁹⁹, M.G. Herrmann ¹⁰⁸, T. Herrmann ⁵⁰, G. Herten ⁵⁴, R. Hertenberger ¹⁰⁸, L. Hervas ³⁶, N.P. Hessey ^{155a}, H. Hibi ⁸³, E. Higón-Rodríguez ¹⁶¹, S.J. Hillier ²⁰, I. Hinchliffe ^{17a}, F. Hinterkeuser ²⁴, M. Hirose ¹²³, S. Hirose ¹⁵⁶, D. Hirschbuehl ¹⁶⁹, T.G. Hitchings ¹⁰⁰, B. Hiti ⁹², J. Hobbs ¹⁴⁴, R. Hobincu ^{27e}, N. Hod ¹⁶⁷, M.C. Hodgkinson ¹³⁸, B.H. Hodgkinson ³², A. Hoecker ³⁶, J. Hofer ⁴⁸, D. Hohn ⁵⁴, T. Holm ²⁴, M. Holzbock ¹⁰⁹, L.B.A.H. Hommels ³², B.P. Honan ¹⁰⁰, J. Hong ^{62c}, T.M. Hong ¹²⁸, Y. Hong ⁵⁵, J.C. Honig ⁵⁴, A. Hönle ¹⁰⁹, B.H. Hooberman ¹⁶⁰, W.H. Hopkins ⁶, Y. Horii ¹¹⁰, S. Hou ¹⁴⁷, A.S. Howard ⁹², J. Howarth ⁵⁹, J. Hoya ⁸⁹, M. Hrabovsky ¹²¹, A. Hrynevich ³⁷, T. Hryn'ova ⁴, P.J. Hsu ⁶⁵, S.-C. Hsu ¹³⁷, Q. Hu ^{41,y}, Y.F. Hu ^{14a,14d,ad}, D.P. Huang ⁹⁵, S. Huang ^{64b}, X. Huang ^{14c}, Y. Huang ^{62a}, Y. Huang ^{14a}, Z. Huang ¹⁰⁰, Z. Hubacek ¹³¹, M. Huebner ²⁴, F. Huegging ²⁴, T.B. Huffman ¹²⁵, M. Huhtinen ³⁶, S.K. Huiberts ¹⁶, R. Hulsken ¹⁰³, N. Huseynov ^{12,a}, J. Huston ¹⁰⁶, J. Huth ⁶¹, R. Hyneman ¹⁴², S. Hyrych ^{28a}, G. Iacobucci ⁵⁶, G. Iakovidis ²⁹, I. Ibragimov ¹⁴⁰, L. Iconomidou-Fayard ⁶⁶, P. Iengo ^{71a,71b}, R. Iguchi ¹⁵², T. Iizawa ⁵⁶, Y. Ikegami ⁸², A. Ilg ¹⁹, N. Ilic ¹⁵⁴, H. Imam ^{35a}, T. Ingebrechtsen Carlson ^{47a,47b}, G. Introzzi ^{72a,72b}, M. Iodice ^{76a}, V. Ippolito ^{74a,74b}, M. Ishino ¹⁵², W. Islam ¹⁶⁸, C. Issever ^{18,48}, S. Istin ^{21a,af}, H. Ito ¹⁶⁶, J.M. Iturbe Ponce ^{64a}, R. Iuppa ^{77a,77b}, A. Ivina ¹⁶⁷, J.M. Izen ⁴⁵, V. Izzo ^{71a}, P. Jacka ^{130,131}, P. Jackson ¹, R.M. Jacobs ⁴⁸, B.P. Jaeger ¹⁴¹, C.S. Jagfeld ¹⁰⁸, G. Jäkel ¹⁶⁹, K. Jakobs ⁵⁴, T. Jakoubek ¹⁶⁷, J. Jamieson ⁵⁹, K.W. Janas ^{84a}, G. Jarlskog ⁹⁷, A.E. Jaspan ⁹¹, T. Javůrek ³⁶, M. Javurkova ¹⁰², F. Jeanneau ¹³⁴, L. Jeanty ¹²², J. Jejelava ^{148a,x}, P. Jenni ^{54,f}, C.E. Jessiman ³⁴, S. Jézéquel ⁴, J. Jia ¹⁴⁴, X. Jia ⁶¹, X. Jia ^{14a,14d}, Z. Jia ^{14c}, Y. Jiang ^{62a}, S. Jiggins ⁵², J. Jimenez Pena ¹⁰⁹, S. Jin ^{14c}, A. Jinaru ^{27b}, O. Jinnouchi ¹⁵³, H. Jivan ^{33g}, P. Johansson ¹³⁸, K.A. Johns ⁷, C.A. Johnson ⁶⁷, D.M. Jones ³², E. Jones ¹⁶⁵, P. Jones ³², R.W.L. Jones ⁹⁰, T.J. Jones ⁹¹, J. Jovicevic ¹⁵, X. Ju ^{17a}, J.J. Junggeburth ³⁶, A. Juste Rozas ^{13,t}, S. Kabana ^{136e}, A. Kaczmarska ⁸⁵, M. Kado ^{74a,74b}, H. Kagan ¹¹⁸, M. Kagan ¹⁴², A. Kahn ⁴¹, A. Kahn ¹²⁷, C. Kahra ⁹⁹, T. Kaji ¹⁶⁶, E. Kajomovitz ¹⁴⁹, N. Kakati ¹⁶⁷, C.W. Kalderon ²⁹, A. Kamenshchikov ¹⁵⁴, N.J. Kang ¹³⁵, Y. Kano ¹¹⁰, D. Kar ^{33g}, K. Karava ¹²⁵, M.J. Kareem ^{155b}, E. Karentzos ⁵⁴, I. Karkanias ¹⁵¹, S.N. Karpov ³⁸, Z.M. Karpova ³⁸, V. Kartvelishvili ⁹⁰, A.N. Karyukhin ³⁷, E. Kasimi ¹⁵¹, C. Kato ^{62d}, J. Katzy ⁴⁸, S. Kaur ³⁴, K. Kawade ¹³⁹, K. Kawagoe ⁸⁸, T. Kawaguchi ¹¹⁰, T. Kawamoto ¹³⁴, G. Kawamura ⁵⁵, E.F. Kay ¹⁶³, F.I. Kaya ¹⁵⁷, S. Kazakos ¹³, V.F. Kazanin ³⁷, Y. Ke ¹⁴⁴, J.M. Keaveney ^{33a}, R. Keeler ¹⁶³, G.V. Kehris ⁶¹, J.S. Keller ³⁴, A.S. Kelly ⁹⁵, D. Kelsey ¹⁴⁵, J.J. Kempster ²⁰, J. Kendrick ²⁰, K.E. Kennedy ⁴¹, O. Kepka ¹³⁰, B.P. Kerridge ¹⁶⁵, S. Kersten ¹⁶⁹, B.P. Kerševan ⁹², L. Keszeghova ^{28a}, S. Ketabchi Haghighat ¹⁵⁴, M. Khandoga ¹²⁶, A. Khanov ¹²⁰, A.G. Kharlamov ³⁷, T. Kharlamova ³⁷, E.E. Khoda ¹³⁷, T.J. Khoo ¹⁸, G. Khoraiuli ¹⁶⁴, J. Khubua ^{148b}, Y.A.R. Khwaira ⁶⁶, M. Kiehn ³⁶, A. Kilgallon ¹²², D.W. Kim ^{47a,47b},

E. Kim ¹⁵³, Y.K. Kim ³⁹, N. Kimura ⁹⁵, A. Kirchhoff ⁵⁵, D. Kirchmeier ⁵⁰, C. Kirfel ²⁴, J. Kirk ¹³³, A.E. Kiryunin ¹⁰⁹, T. Kishimoto ¹⁵², D.P. Kisliuk ¹⁵⁴, C. Kitsaki ¹⁰, O. Kivernyk ²⁴, M. Klassen ^{63a}, C. Klein ³⁴, L. Klein ¹⁶⁴, M.H. Klein ¹⁰⁵, M. Klein ⁹¹, U. Klein ⁹¹, P. Klimek ³⁶, A. Klimentov ²⁹, F. Klimpel ¹⁰⁹, T. Klingl ²⁴, T. Klioutchnikova ³⁶, F.F. Klitzner ¹⁰⁸, P. Kluit ¹¹³, S. Kluth ¹⁰⁹, E. Kneringer ⁷⁸, T.M. Knight ¹⁵⁴, A. Knue ⁵⁴, D. Kobayashi ⁸⁸, R. Kobayashi ⁸⁶, M. Kocian ¹⁴², T. Kodama ¹⁵², P. Kodyš ¹³², D.M. Koeck ¹⁴⁵, P.T. Koenig ²⁴, T. Koffas ³⁴, N.M. Köhler ³⁶, M. Kolb ¹³⁴, I. Koletsou ⁴, T. Komarek ¹²¹, K. Köneke ⁵⁴, A.X.Y. Kong ¹, T. Kono ¹¹⁷, N. Konstantinidis ⁹⁵, B. Konya ⁹⁷, R. Kopeliansky ⁶⁷, S. Koperny ^{84a}, K. Korcyl ⁸⁵, K. Kordas ¹⁵¹, G. Koren ¹⁵⁰, A. Korn ⁹⁵, S. Korn ⁵⁵, I. Korolkov ¹³, N. Korotkova ³⁷, B. Kortman ¹¹³, O. Kortner ¹⁰⁹, S. Kortner ¹⁰⁹, W.H. Kostecka ¹¹⁴, V.V. Kostyukhin ¹⁴⁰, A. Kotsokechagia ⁶⁶, A. Kotwal ⁵¹, A. Koulouris ³⁶, A. Kourkumeli-Charalampidi ^{72a,72b}, C. Kourkumelis ⁹, E. Kourlitis ⁶, O. Kovanda ¹⁴⁵, R. Kowalewski ¹⁶³, W. Kozanecki ¹³⁴, A.S. Kozhin ³⁷, V.A. Kramarenko ³⁷, G. Kramberger ⁹², P. Kramer ⁹⁹, M.W. Krasny ¹²⁶, A. Krasznahorkay ³⁶, J.A. Kremer ⁹⁹, T. Kresse ⁵⁰, J. Kretzschmar ⁹¹, K. Kreul ¹⁸, P. Krieger ¹⁵⁴, F. Krieter ¹⁰⁸, S. Krishnamurthy ¹⁰², A. Krishnan ^{63b}, M. Krivos ¹³², K. Krizka ^{17a}, K. Kroeninger ⁴⁹, H. Kroha ¹⁰⁹, J. Kroll ¹³⁰, J. Kroll ¹²⁷, K.S. Krowpman ¹⁰⁶, U. Kruchonak ³⁸, H. Krüger ²⁴, N. Krumnack ⁸⁰, M.C. Kruse ⁵¹, J.A. Krzysiak ⁸⁵, A. Kubota ¹⁵³, O. Kuchinskaia ³⁷, S. Kудay ^{3a}, D. Kuechler ⁴⁸, J.T. Kuechler ⁴⁸, S. Kuehn ³⁶, T. Kuhl ⁴⁸, V. Kukhtin ³⁸, Y. Kulchitsky ^{37a}, S. Kuleshov ^{136d,136b}, M. Kumar ^{33g}, N. Kumari ¹⁰¹, M. Kuna ⁶⁰, A. Kupco ¹³⁰, T. Kupfer ⁴⁹, A. Kupich ³⁷, O. Kuprash ⁵⁴, H. Kurashige ⁸³, L.L. Kurchaninov ^{155a}, Y.A. Kurochkin ³⁷, A. Kurova ³⁷, E.S. Kuwertz ³⁶, M. Kuze ¹⁵³, A.K. Kvam ¹⁰², J. Kvita ¹²¹, T. Kwan ¹⁰³, K.W. Kwok ^{64a}, C. Lacasta ¹⁶¹, F. Lacava ^{74a,74b}, H. Lacker ¹⁸, D. Lacour ¹²⁶, N.N. Lad ⁹⁵, E. Ladygin ³⁸, B. Laforge ¹²⁶, T. Lagouri ^{136e}, S. Lai ⁵⁵, I.K. Lakomic ^{84a}, N. Lalloue ⁶⁰, J.E. Lambert ¹¹⁹, S. Lammers ⁶⁷, W. Lampl ⁷, C. Lampoudis ¹⁵¹, A.N. Lancaster ¹¹⁴, E. Lançon ²⁹, U. Landgraf ⁵⁴, M.P.J. Landon ⁹³, V.S. Lang ⁵⁴, R.J. Langenberg ¹⁰², A.J. Lankford ¹⁵⁸, F. Lanni ²⁹, K. Lantzsch ²⁴, A. Lanza ^{72a}, A. Lapertosa ^{57b,57a}, J.F. Laporte ¹³⁴, T. Lari ^{70a}, F. Lasagni Manghi ^{23b}, M. Lassnig ³⁶, V. Latonova ¹³⁰, T.S. Lau ^{64a}, A. Laudrain ⁹⁹, A. Laurier ³⁴, S.D. Lawlor ⁹⁴, Z. Lawrence ¹⁰⁰, M. Lazzaroni ^{70a,70b}, B. Le ¹⁰⁰, B. Leban ⁹², A. Lebedev ⁸⁰, M. LeBlanc ³⁶, T. LeCompte ⁶, F. Ledroit-Guillon ⁶⁰, A.C.A. Lee ⁹⁵, G.R. Lee ¹⁶, L. Lee ⁶¹, S.C. Lee ¹⁴⁷, S. Lee ^{47a,47b}, L.L. Leeuw ^{33c}, H.P. Lefebvre ⁹⁴, M. Lefebvre ¹⁶³, C. Leggett ^{17a}, K. Lehmann ¹⁴¹, G. Lehmann Miotto ³⁶, W.A. Leight ¹⁰², A. Leisos ^{151,s}, M.A.L. Leite ^{81c}, C.E. Leitgeb ⁴⁸, R. Leitner ¹³², K.J.C. Leney ⁴⁴, T. Lenz ²⁴, S. Leone ^{73a}, C. Leonidopoulos ⁵², A. Leopold ¹⁴³, C. Leroy ¹⁰⁷, R. Les ¹⁰⁶, C.G. Lester ³², M. Levchenko ³⁷, J. Levêque ⁴, D. Levin ¹⁰⁵, L.J. Levinson ¹⁶⁷, D.J. Lewis ²⁰, B. Li ^{14b}, B. Li ^{62b}, C. Li ^{62a}, C-Q. Li ^{62c,62d}, H. Li ^{62a}, H. Li ^{62b}, H. Li ^{14c}, H. Li ^{62b}, J. Li ^{62c}, K. Li ¹³⁷, L. Li ^{62c}, M. Li ^{14a,14d}, Q.Y. Li ^{62a}, S. Li ^{62d,62c,d}, T. Li ^{62b}, X. Li ¹⁰³, Z. Li ^{62b}, Z. Li ¹²⁵, Z. Li ¹⁰³, Z. Li ⁹¹, Z. Liang ^{14a}, M. Liberatore ⁴⁸, B. Liberti ^{75a}, K. Lie ^{64c}, J. Lieber Marin ^{81b}, K. Lin ¹⁰⁶, R.A. Linck ⁶⁷, R.E. Lindley ⁷, J.H. Lindon ², A. Linss ⁴⁸, E. Lipeles ¹²⁷, A. Lipniacka ¹⁶, T.M. Liss ^{160,z}, A. Lister ¹⁶², J.D. Little ⁴, B. Liu ^{14a}, B.X. Liu ¹⁴¹, D. Liu ^{62d,62c}, J.B. Liu ^{62a},

J.K.K. Liu ³², K. Liu ^{62d,62c}, M. Liu ^{62a}, M.Y. Liu ^{62a}, P. Liu ^{14a}, Q. Liu ^{62d,137,62c},
X. Liu ^{62a}, Y. Liu ⁴⁸, Y. Liu ^{14c,14d}, Y.L. Liu ¹⁰⁵, Y.W. Liu ^{62a}, M. Livan ^{72a,72b},
J. Llorente Merino ¹⁴¹, S.L. Lloyd ⁹³, E.M. Lobodzinska ⁴⁸, P. Loch ⁷, S. Loffredo ^{75a,75b},
T. Lohse ¹⁸, K. Lohwasser ¹³⁸, M. Lokajicek ¹³⁰, J.D. Long ¹⁶⁰, I. Longarini ^{74a,74b},
L. Longo ^{69a,69b}, R. Longo ¹⁶⁰, I. Lopez Paz ³⁶, A. Lopez Solis ⁴⁸, J. Lorenz ¹⁰⁸,
N. Lorenzo Martinez ⁴, A.M. Lory ¹⁰⁸, A. Lösle ⁵⁴, X. Lou ^{47a,47b}, X. Lou ^{14a,14d},
A. Lounis ⁶⁶, J. Love ⁶, P.A. Love ⁹⁰, J.J. Lozano Bahilo ¹⁶¹, G. Lu ^{14a,14d}, M. Lu ⁷⁹,
S. Lu ¹²⁷, Y.J. Lu ⁶⁵, H.J. Lubatti ¹³⁷, C. Luci ^{74a,74b}, F.L. Lucio Alves ^{14c},
A. Lucotte ⁶⁰, F. Luehring ⁶⁷, I. Luise ¹⁴⁴, O. Lukianchuk ⁶⁶, O. Lundberg ¹⁴³,
B. Lund-Jensen ¹⁴³, N.A. Luongo ¹²², M.S. Lutz ¹⁵⁰, D. Lynn ²⁹, H. Lyons ⁹¹, R. Lysak ¹³⁰,
E. Lytken ⁹⁷, F. Lyu ^{14a}, V. Lyubushkin ³⁸, T. Lyubushkina ³⁸, H. Ma ²⁹, L.L. Ma ^{62b},
Y. Ma ⁹⁵, D.M. Mac Donell ¹⁶³, G. Maccarrone ⁵³, J.C. MacDonald ¹³⁸, R. Madar ⁴⁰,
W.F. Mader ⁵⁰, J. Maeda ⁸³, T. Maeno ²⁹, M. Maerker ⁵⁰, V. Magerl ⁵⁴, J. Magro ^{68a,68c},
H. Maguire ¹³⁸, D.J. Mahon ⁴¹, C. Maidantchik ^{81b}, A. Maio ^{129a,129b,129d}, K. Maj ^{84a},
O. Majersky ^{28a}, S. Majewski ¹²², N. Makovec ⁶⁶, V. Maksimovic ¹⁵, B. Malaescu ¹²⁶,
Pa. Malecki ⁸⁵, V.P. Maleev ³⁷, F. Malek ⁶⁰, D. Malito ^{43b,43a}, U. Mallik ⁷⁹,
C. Malone ³², S. Maltezos ¹⁰, S. Malyukov ³⁸, J. Mamuzic ¹³, G. Mancini ⁵³,
G. Manco ^{72a,72b}, J.P. Mandalia ⁹³, I. Mandić ⁹², L. Manhaes de Andrade Filho ^{81a},
I.M. Maniatis ¹⁵¹, M. Manisha ¹³⁴, J. Manjarres Ramos ⁵⁰, D.C. Mankad ¹⁶⁷,
K.H. Mankinen ⁹⁷, A. Mann ¹⁰⁸, A. Manousos ⁷⁸, B. Mansoulie ¹³⁴, S. Manzoni ³⁶,
A. Marantis ^{151,s}, G. Marchiori ⁵, M. Marcisovsky ¹³⁰, L. Marcoccia ^{75a,75b}, C. Marcon ⁹⁷,
M. Marinescu ²⁰, M. Marjanovic ¹¹⁹, Z. Marshall ^{17a}, S. Marti-Garcia ¹⁶¹, T.A. Martin ¹⁶⁵,
V.J. Martin ⁵², B. Martin dit Latour ¹⁶, L. Martinelli ^{74a,74b}, M. Martinez ^{13,t},
P. Martinez Agullo ¹⁶¹, V.I. Martinez Outschoorn ¹⁰², P. Martinez Suarez ¹³,
S. Martin-Haugh ¹³³, V.S. Martoiu ^{27b}, A.C. Martyniuk ⁹⁵, A. Marzin ³⁶,
S.R. Maschek ¹⁰⁹, L. Masetti ⁹⁹, T. Mashimo ¹⁵², J. Masik ¹⁰⁰, A.L. Maslennikov ³⁷,
L. Massa ^{23b}, P. Massarotti ^{71a,71b}, P. Mastrandrea ^{73a,73b}, A. Mastroberardino ^{43b,43a},
T. Masubuchi ¹⁵², T. Mathisen ¹⁵⁹, A. Matic ¹⁰⁸, N. Matsuzawa ¹⁵², J. Maurer ^{27b},
B. Maček ⁹², D.A. Maximov ³⁷, R. Mazini ¹⁴⁷, I. Maznas ¹⁵¹, M. Mazza ¹⁰⁶,
S.M. Mazza ¹³⁵, C. Mc Ginn ^{29,ae}, J.P. Mc Gowan ¹⁰³, S.P. Mc Kee ¹⁰⁵,
T.G. McCarthy ¹⁰⁹, W.P. McCormack ^{17a}, E.F. McDonald ¹⁰⁴, A.E. McDougall ¹¹³,
J.A. Mcfayden ¹⁴⁵, G. Mchedlidze ^{148b}, R.P. McKenzie ^{33g}, T.C. McLachlan ⁴⁸,
D.J. McLaughlin ⁹⁵, K.D. McLean ¹⁶³, S.J. McMahon ¹³³, P.C. McNamara ¹⁰⁴,
R.A. McPherson ^{163,v}, J.E. Mdhluli ^{33g}, S. Meehan ³⁶, T. Megy ⁴⁰, S. Mehlhase ¹⁰⁸,
A. Mehta ⁹¹, B. Meirose ⁴⁵, D. Melini ¹⁴⁹, B.R. Mellado Garcia ^{33g}, A.H. Melo ⁵⁵,
F. Meloni ⁴⁸, E.D. Mendes Gouveia ^{129a}, A.M. Mendes Jacques Da Costa ²⁰, H.Y. Meng ¹⁵⁴,
L. Meng ⁹⁰, S. Menke ¹⁰⁹, M. Mentink ³⁶, E. Meoni ^{43b,43a}, C. Merlassino ¹²⁵,
L. Merola ^{71a,71b}, C. Meroni ^{70a}, G. Merz ¹⁰⁵, O. Meshkov ³⁷, J.K.R. Meshreki ¹⁴⁰,
J. Metcalfe ⁶, A.S. Mete ⁶, C. Meyer ⁶⁷, J-P. Meyer ¹³⁴, M. Michetti ¹⁸,
R.P. Middleton ¹³³, L. Mijović ⁵², G. Mikenberg ¹⁶⁷, M. Mikestikova ¹³⁰, M. Mikuž ⁹²,
H. Mildner ¹³⁸, A. Milic ¹⁵⁴, C.D. Milke ⁴⁴, D.W. Miller ³⁹, L.S. Miller ³⁴, A. Milov ¹⁶⁷,
D.A. Milstead ^{47a,47b}, T. Min ^{14c}, A.A. Minaenko ³⁷, I.A. Minashvili ^{148b}, L. Mince ⁵⁹,
A.I. Mincer ¹¹⁶, B. Mindur ^{84a}, M. Mineev ³⁸, Y. Minegishi ¹⁵², Y. Mino ⁸⁶, L.M. Mir ¹³,




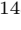
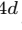
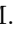

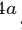


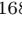


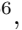


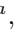







M. Miralles Lopez ^{[161](#)}, M. Mironova ^{[125](#)}, T. Mitani ^{[166](#)}, A. Mitra ^{[165](#)}, V.A. Mitsou ^{[161](#)},
O. Miu ^{[154](#)}, P.S. Miyagawa ^{[93](#)}, Y. Miyazaki ^{[88](#)}, A. Mizukami ^{[82](#)}, J.U. Mjörnmark ^{[97](#)},
T. Mkrtchyan ^{[63a](#)}, M. Mlynarikova ^{[114](#)}, T. Moa ^{[47a,47b](#)}, S. Mobius ^{[55](#)}, K. Mochizuki ^{[107](#)},
P. Moder ^{[48](#)}, P. Mogg ^{[108](#)}, A.F. Mohammed ^{[14a,14d](#)}, S. Mohapatra ^{[41](#)},
G. Mokgatitswane ^{[33g](#)}, B. Mondal ^{[140](#)}, S. Mondal ^{[131](#)}, K. Mönig ^{[48](#)}, E. Monnier ^{[101](#)},
L. Monsonis Romero ^{[161](#)}, J. Montejo Berlingen ^{[36](#)}, M. Montella ^{[118](#)}, F. Monticelli ^{[89](#)},
N. Morange ^{[66](#)}, A.L. Moreira De Carvalho ^{[129a](#)}, M. Moreno Llácer ^{[161](#)},
C. Moreno Martinez ^{[13](#)}, P. Morettini ^{[57b](#)}, S. Morgenstern ^{[165](#)}, M. Morii ^{[61](#)},
M. Morinaga ^{[152](#)}, V. Morisbak ^{[124](#)}, A.K. Morley ^{[36](#)}, F. Morodei ^{[74a,74b](#)}, L. Morvaj ^{[36](#)},
P. Moschovakos ^{[36](#)}, B. Moser ^{[36](#)}, M. Mosidze ^{[148b](#)}, T. Moskalets ^{[54](#)}, P. Moskvitina ^{[112](#)},
J. Moss ^{[31,n](#)}, E.J.W. Moyse ^{[102](#)}, S. Muanza ^{[101](#)}, J. Mueller ^{[128](#)}, D. Muenstermann ^{[90](#)},
R. Müller ^{[19](#)}, G.A. Mullier ^{[97](#)}, J.J. Mullin ^{[127](#)}, D.P. Mungo ^{[70a,70b](#)}, J.L. Munoz Martinez ^{[13](#)},
D. Munoz Perez ^{[161](#)}, F.J. Munoz Sanchez ^{[100](#)}, M. Murin ^{[100](#)}, W.J. Murray ^{[165,133](#)},
A. Murrone ^{[70a,70b](#)}, J.M. Muse ^{[119](#)}, M. Muškinja ^{[17a](#)}, C. Mwewa ^{[29](#)}, A.G. Myagkov ^{[37,a](#)},
A.J. Myers ^{[8](#)}, A.A. Myers ^{[128](#)}, G. Myers ^{[67](#)}, M. Myska ^{[131](#)}, B.P. Nachman ^{[17a](#)},
O. Nackenhorst ^{[49](#)}, A. Nag ^{[50](#)}, K. Nagai ^{[125](#)}, K. Nagano ^{[82](#)}, J.L. Nagle ^{[29,ae](#)}, E. Nagy ^{[101](#)},
A.M. Nairz ^{[36](#)}, Y. Nakahama ^{[82](#)}, K. Nakamura ^{[82](#)}, H. Nanjo ^{[123](#)}, R. Narayan ^{[44](#)},
E.A. Narayanan ^{[111](#)}, I. Naryshkin ^{[37](#)}, M. Naseri ^{[34](#)}, C. Nass ^{[24](#)}, G. Navarro ^{[22a](#)},
J. Navarro-Gonzalez ^{[161](#)}, R. Nayak ^{[150](#)}, P.Y. Nechaeva ^{[37](#)}, F. Nechansky ^{[48](#)}, T.J. Neep ^{[20](#)},
A. Negri ^{[72a,72b](#)}, M. Negrini ^{[23b](#)}, C. Nellist ^{[112](#)}, C. Nelson ^{[103](#)}, K. Nelson ^{[105](#)},
S. Nemecek ^{[130](#)}, M. Nessi ^{[36,g](#)}, M.S. Neubauer ^{[160](#)}, F. Neuhaus ^{[99](#)}, J. Neundorff ^{[48](#)},
R. Newhouse ^{[162](#)}, P.R. Newman ^{[20](#)}, C.W. Ng ^{[128](#)}, Y.S. Ng ^{[18](#)}, Y.W.Y. Ng ^{[158](#)}, B. Ngair ^{[35e](#)},
H.D.N. Nguyen ^{[107](#)}, R.B. Nickerson ^{[125](#)}, R. Nicolaidou ^{[134](#)}, J. Nielsen ^{[135](#)}, M. Niemeyer ^{[55](#)},
N. Nikiforou ^{[36](#)}, V. Nikolaenko ^{[37,a](#)}, I. Nikolic-Audit ^{[126](#)}, K. Nikolopoulos ^{[20](#)}, P. Nilsson ^{[29](#)},
H.R. Nindhito ^{[56](#)}, A. Nisati ^{[74a](#)}, N. Nishu ^{[2](#)}, R. Nisius ^{[109](#)}, J-E. Nitschke ^{[50](#)},
E.K. Nkadimeng ^{[33g](#)}, S.J. Noacco Rosende ^{[89](#)}, T. Nobe ^{[152](#)}, D.L. Noel ^{[32](#)}, Y. Noguchi ^{[86](#)},
T. Nommensen ^{[146](#)}, M.A. Nomura ^{[29](#)}, M.B. Norfolk ^{[138](#)}, R.R.B. Norisam ^{[95](#)}, B.J. Norman ^{[34](#)},
J. Novak ^{[92](#)}, T. Novak ^{[48](#)}, O. Novgorodova ^{[50](#)}, L. Novotny ^{[131](#)}, R. Novotny ^{[111](#)},
L. Nozka ^{[121](#)}, K. Ntekas ^{[158](#)}, E. Nurse ^{[95](#)}, F.G. Oakham ^{[34,ab](#)}, J. Ocariz ^{[126](#)}, A. Ochi ^{[83](#)},
I. Ochoa ^{[129a](#)}, S. Oda ^{[88](#)}, S. Oerdek ^{[159](#)}, A. Ogrodnik ^{[84a](#)}, A. Oh ^{[100](#)}, C.C. Ohm ^{[143](#)},
H. Oide ^{[153](#)}, R. Oishi ^{[152](#)}, M.L. Ojeda ^{[48](#)}, Y. Okazaki ^{[86](#)}, M.W. O’Keefe ^{[91](#)}, Y. Okumura ^{[152](#)},
A. Olariu ^{[27b](#)}, L.F. Oleiro Seabra ^{[129a](#)}, S.A. Olivares Pino ^{[136e](#)}, D. Oliveira Damazio ^{[29](#)},
D. Oliveira Goncalves ^{[81a](#)}, J.L. Oliver ^{[158](#)}, M.J.R. Olsson ^{[158](#)}, A. Olszewski ^{[85](#)},
J. Olszowska ^{[85,*](#)}, Ö.O. Öncel ^{[54](#)}, D.C. O’Neil ^{[141](#)}, A.P. O’Neill ^{[19](#)}, A. Onofre ^{[129a,129e](#)},
P.U.E. Onyisi ^{[11](#)}, M.J. Oreglia ^{[39](#)}, G.E. Orellana ^{[89](#)}, D. Orestano ^{[76a,76b](#)}, N. Orlando ^{[13](#)},
R.S. Orr ^{[154](#)}, V. O’Shea ^{[59](#)}, R. Ospanov ^{[62a](#)}, G. Otero y Garzon ^{[30](#)}, H. Otono ^{[88](#)},
P.S. Ott ^{[63a](#)}, G.J. Ottino ^{[17a](#)}, M. Ouchrif ^{[35d](#)}, J. Ouellette ^{[29,ae](#)}, F. Ould-Saada ^{[124](#)},
M. Owen ^{[59](#)}, R.E. Owen ^{[133](#)}, K.Y. Oyulmaz ^{[21a](#)}, V.E. Ozcan ^{[21a](#)}, N. Ozturk ^{[8](#)},
S. Ozturk ^{[21d](#)}, J. Pacalt ^{[121](#)}, H.A. Pacey ^{[32](#)}, K. Pachal ^{[51](#)}, A. Pacheco Pages ^{[13](#)},
C. Padilla Aranda ^{[13](#)}, G. Padovano ^{[74a,74b](#)}, S. Pagan Griso ^{[17a](#)}, G. Palacino ^{[67](#)},
A. Palazzo ^{[69a,69b](#)}, S. Palazzo ^{[52](#)}, S. Palestini ^{[36](#)}, M. Palka ^{[84b](#)}, J. Pan ^{[170](#)}, T. Pan ^{[64a](#)},
D.K. Panchal ^{[11](#)}, C.E. Pandini ^{[113](#)}, J.G. Panduro Vazquez ^{[94](#)}, H. Pang ^{[14b](#)}, P. Pani ^{[48](#)},
G. Panizzo ^{[68a,68c](#)}, L. Paolozzi ^{[56](#)}, C. Papadatos ^{[107](#)}, S. Parajuli ^{[44](#)}, A. Paramonov ^{[6](#)},

C. Paraskevopoulos ¹⁰, D. Paredes Hernandez ^{64b}, T.H. Park ¹⁵⁴, M.A. Parker ³²,
F. Parodi ^{57b,57a}, E.W. Parrish ¹¹⁴, V.A. Parrish ⁵², J.A. Parsons ⁴¹, U. Parzefall ⁵⁴,
B. Pascual Dias ¹⁰⁷, L. Pascual Dominguez ¹⁵⁰, V.R. Pascuzzi ^{17a}, F. Pasquali ¹¹³,
E. Pasqualucci ^{74a}, S. Passaggio ^{57b}, F. Pastore ⁹⁴, P. Pasuwan ^{47a,47b}, J.R. Pater ¹⁰⁰,
J. Patton ⁹¹, T. Pauly ³⁶, J. Pearkes ¹⁴², M. Pedersen ¹²⁴, R. Pedro ^{129a},
S.V. Peleganchuk ³⁷, O. Penc ¹³⁰, C. Peng ^{64b}, H. Peng ^{62a}, M. Penzin ³⁷,
B.S. Peralva ^{81a,81d}, A.P. Pereira Peixoto ⁶⁰, L. Pereira Sanchez ^{47a,47b},
D.V. Perepelitsa ^{29,ae}, E. Perez Codina ^{155a}, M. Perganti ¹⁰, L. Perini ^{70a,70b,*},
H. Pernegger ³⁶, S. Perrella ³⁶, A. Perrevoort ¹¹², O. Perrin ⁴⁰, K. Peters ⁴⁸,
R.F.Y. Peters ¹⁰⁰, B.A. Petersen ³⁶, T.C. Petersen ⁴², E. Petit ¹⁰¹, V. Petousis ¹³¹,
C. Petridou ¹⁵¹, A. Petrukhin ¹⁴⁰, M. Pettee ^{17a}, N.E. Pettersson ³⁶, A. Petukhov ³⁷,
K. Petukhova ¹³², A. Peyaud ¹³⁴, R. Pezoa ^{136f}, L. Pezzotti ³⁶, G. Pezzullo ¹⁷⁰,
T. Pham ¹⁰⁴, P.W. Phillips ¹³³, M.W. Phipps ¹⁶⁰, G. Piacquadio ¹⁴⁴, E. Pianori ^{17a},
F. Piazza ^{70a,70b}, R. Piegai ³⁰, D. Pietreanu ^{27b}, A.D. Pilkington ¹⁰⁰,
M. Pinamonti ^{68a,68c}, J.L. Pinfold ², B.C. Pinheiro Pereira ^{129a}, C. Pitman Donaldson ⁹⁵,
D.A. Pizzi ³⁴, L. Pizzimento ^{75a,75b}, A. Pizzini ¹¹³, M.-A. Pleier ²⁹, V. Plesanovs ⁵⁴,
V. Pleskot ¹³², E. Plotnikova ³⁸, G. Poddar ⁴, R. Poettgen ⁹⁷, R. Poggi ⁵⁶, L. Poggioli ¹²⁶,
I. Pogrebnyak ¹⁰⁶, D. Pohl ²⁴, I. Pokharel ⁵⁵, S. Polacek ¹³², G. Polesello ^{72a},
A. Poley ^{141,155a}, R. Polifka ¹³¹, A. Polini ^{23b}, C.S. Pollard ¹²⁵, Z.B. Pollock ¹¹⁸,
V. Polychronakos ²⁹, D. Ponomarenko ³⁷, L. Pontecorvo ³⁶, S. Popa ^{27a},
G.A. Popeneciu ^{27d}, D.M. Portillo Quintero ^{155a}, S. Pospisil ¹³¹, P. Postolache ^{27c},
K. Potamianos ¹²⁵, I.N. Potrap ³⁸, C.J. Potter ³², H. Potti ¹, T. Poulsen ⁴⁸, J. Poveda ¹⁶¹,
G. Pownall ⁴⁸, M.E. Pozo Astigarraga ³⁶, A. Prades Ibanez ¹⁶¹, M.M. Prapa ⁴⁶,
J. Pretel ⁵⁴, D. Price ¹⁰⁰, M. Primavera ^{69a}, M.A. Principe Martin ⁹⁸, M.L. Proffitt ¹³⁷,
N. Proklova ³⁷, K. Prokofiev ^{64c}, G. Proto ^{75a,75b}, S. Protopopescu ²⁹, J. Proudfoot ⁶,
M. Przybycien ^{84a}, J.E. Puddefoot ¹³⁸, D. Pudzha ³⁷, P. Puzo ⁶⁶, D. Pyatizhyantseva ³⁷,
J. Qian ¹⁰⁵, Y. Qin ¹⁰⁰, T. Qiu ⁹³, A. Quadt ⁵⁵, M. Queitsch-Maitland ²⁴,
G. Rabanal Bolanos ⁶¹, D. Rafanoharana ⁵⁴, F. Ragusa ^{70a,70b}, J.L. Rainbolt ³⁹,
J.A. Raine ⁵⁶, S. Rajagopalan ²⁹, E. Ramakoti ³⁷, K. Ran ^{14a,14d}, V. Raskina ¹²⁶,
D.F. Rassloff ^{63a}, S. Rave ⁹⁹, B. Ravina ⁵⁹, I. Ravinovich ¹⁶⁷, M. Raymond ³⁶,
A.L. Read ¹²⁴, N.P. Readioff ¹³⁸, D.M. Rebuffi ^{72a,72b}, G. Redlinger ²⁹, K. Reeves ⁴⁵,
J.A. Reidelsturz ¹⁶⁹, D. Reikher ¹⁵⁰, A. Reiss ⁹⁹, A. Rej ¹⁴⁰, C. Rembser ³⁶, A. Renardi ⁴⁸,
M. Renda ^{27b}, M.B. Rendel ¹⁰⁹, A.G. Rennie ⁵⁹, S. Resconi ^{70a}, M. Ressegotti ^{57b,57a},
E.D. Resseguie ^{17a}, S. Rettie ⁹⁵, B. Reynolds ¹¹⁸, E. Reynolds ^{17a}, M. Rezaei Estabragh ¹⁶⁹,
O.L. Rezanova ³⁷, P. Reznicek ¹³², E. Ricci ^{77a,77b}, R. Richter ¹⁰⁹, S. Richter ^{47a,47b},
E. Richter-Was ^{84b}, M. Ridel ¹²⁶, P. Rieck ¹¹⁶, P. Riedler ³⁶, M. Rijssenbeek ¹⁴⁴,
A. Rimoldi ^{72a,72b}, M. Rimoldi ⁴⁸, L. Rinaldi ^{23b,23a}, T.T. Rinn ²⁹, M.P. Rinnagel ¹⁰⁸,
G. Ripellino ¹⁴³, I. Riu ¹³, P. Rivadeneira ⁴⁸, J.C. Rivera Vergara ¹⁶³, F. Rizatdinova ¹²⁰,
E. Rizvi ⁹³, C. Rizzi ⁵⁶, B.A. Roberts ¹⁶⁵, B.R. Roberts ^{17a}, S.H. Robertson ^{103,v},
M. Robin ⁴⁸, D. Robinson ³², C.M. Robles Gajardo ^{136f}, M. Robles Manzano ⁹⁹,
A. Robson ⁵⁹, A. Rocchi ^{75a,75b}, C. Roda ^{73a,73b}, S. Rodriguez Bosca ^{63a},
Y. Rodriguez Garcia ^{22a}, A. Rodriguez Rodriguez ⁵⁴, A.M. Rodríguez Vera ^{155b}, S. Roe ³⁶,
J.T. Roemer ¹⁵⁸, A.R. Roepe-Gier ¹¹⁹, J. Roggel ¹⁶⁹, O. Røhne ¹²⁴, R.A. Rojas ¹⁶³,

B. Roland ⁵⁴, C.P.A. Roland ⁶⁷, J. Roloff ²⁹, A. Romaniouk ³⁷, E. Romano ^{72a,72b},
M. Romano ^{23b}, A.C. Romero Hernandez ¹⁶⁰, N. Rompotis ⁹¹, L. Roos ¹²⁶, S. Rosati ^{74a},
B.J. Rosser ³⁹, E. Rossi ⁴, E. Rossi ^{71a,71b}, L.P. Rossi ^{57b}, L. Rossini ⁴⁸, R. Rosten ¹¹⁸,
M. Rotaru ^{27b}, B. Rottler ⁵⁴, D. Rousseau ⁶⁶, D. Rousso ³², G. Rovelli ^{72a,72b}, A. Roy ¹⁶⁰,
A. Rozanov ¹⁰¹, Y. Rozen ¹⁴⁹, X. Ruan ^{33g}, A. Rubio Jimenez ¹⁶¹, A.J. Ruby ⁹¹,
T.A. Ruggeri ¹, F. Rühr ⁵⁴, A. Ruiz-Martinez ¹⁶¹, A. Rummeler ³⁶, Z. Rurikova ⁵⁴,
N.A. Rusakovich ³⁸, H.L. Russell ¹⁶³, J.P. Rutherford ⁷, E.M. Rüttinger ¹³⁸, K. Rybacki ⁹⁰,
M. Rybar ¹³², E.B. Rye ¹²⁴, A. Ryzhov ³⁷, J.A. Sabater Iglesias ⁵⁶, P. Sabatini ¹⁶¹,
L. Sabetta ^{74a,74b}, H.F-W. Sadrozinski ¹³⁵, F. Safai Tehrani ^{74a}, B. Safarzadeh Samani ¹⁴⁵,
M. Safdari ¹⁴², S. Saha ¹⁰³, M. Sahinsoy ¹⁰⁹, M. Saimpert ¹³⁴, M. Saito ¹⁵², T. Saito ¹⁵²,
D. Salamani ³⁶, G. Salamanna ^{76a,76b}, A. Salnikov ¹⁴², J. Salt ¹⁶¹, A. Salvador Salas ¹³,
D. Salvatore ^{43b,43a}, F. Salvatore ¹⁴⁵, A. Salzburger ³⁶, D. Sammel ⁵⁴, D. Sampsonidis ¹⁵¹,
D. Sampsonidou ^{62d,62c}, J. Sánchez ¹⁶¹, A. Sanchez Pineda ⁴, V. Sanchez Sebastian ¹⁶¹,
H. Sandaker ¹²⁴, C.O. Sander ⁴⁸, J.A. Sandesara ¹⁰², M. Sandhoff ¹⁶⁹, C. Sandoval ^{22b},
D.P.C. Sankey ¹³³, A. Sansoni ⁵³, L. Santi ^{74a,74b}, C. Santoni ⁴⁰, H. Santos ^{129a,129b},
S.N. Santpur ^{17a}, A. Santra ¹⁶⁷, K.A. Saoucha ¹³⁸, J.G. Saraiva ^{129a,129d}, J. Sardain ¹⁰¹,
O. Sasaki ⁸², K. Sato ¹⁵⁶, C. Sauer ^{63b}, F. Sauerburger ⁵⁴, E. Sauvan ⁴, P. Savard ^{154,ab},
R. Sawada ¹⁵², C. Sawyer ¹³³, L. Sawyer ⁹⁶, I. Sayago Galvan ¹⁶¹, C. Sbarra ^{23b},
A. Sbrizzi ^{23b,23a}, T. Scanlon ⁹⁵, J. Schaarschmidt ¹³⁷, P. Schacht ¹⁰⁹, D. Schaefer ³⁹,
U. Schäfer ⁹⁹, A.C. Schaffer ⁶⁶, D. Schaile ¹⁰⁸, R.D. Schamberger ¹⁴⁴, E. Schanet ¹⁰⁸,
C. Scharf ¹⁸, V.A. Schegelsky ³⁷, D. Scheirich ¹³², F. Schenck ¹⁸, M. Schernau ¹⁵⁸,
C. Scheulen ⁵⁵, C. Schiavi ^{57b,57a}, Z.M. Schillaci ²⁶, E.J. Schioppa ^{69a,69b},
M. Schioppa ^{43b,43a}, B. Schlag ⁹⁹, K.E. Schleicher ⁵⁴, S. Schlenker ³⁶, K. Schmieden ⁹⁹,
C. Schmitt ⁹⁹, S. Schmitt ⁴⁸, L. Schoeffel ¹³⁴, A. Schoening ^{63b}, P.G. Scholer ⁵⁴,
E. Schopf ¹²⁵, M. Schott ⁹⁹, J. Schovancova ³⁶, S. Schramm ⁵⁶, F. Schroeder ¹⁶⁹,
H-C. Schultz-Coulon ^{63a}, M. Schumacher ⁵⁴, B.A. Schumm ¹³⁵, Ph. Schune ¹³⁴,
A. Schwartzman ¹⁴², T.A. Schwarz ¹⁰⁵, Ph. Schwemling ¹³⁴, R. Schwienhorst ¹⁰⁶,
A. Sciandra ¹³⁵, G. Sciolla ²⁶, F. Scuri ^{73a}, F. Scutti ¹⁰⁴, C.D. Sebastiani ⁹¹,
K. Sedlaczek ⁴⁹, P. Seema ¹⁸, S.C. Seidel ¹¹¹, A. Seiden ¹³⁵, B.D. Seidlitz ⁴¹, T. Seiss ³⁹,
C. Seitz ⁴⁸, J.M. Seixas ^{81b}, G. Sekhniaidze ^{71a}, S.J. Sekula ⁴⁴, L. Selem ⁴,
N. Semprini-Cesari ^{23b,23a}, S. Sen ⁵¹, D. Sengupta ⁵⁶, V. Senthilkumar ¹⁶¹, L. Serin ⁶⁶,
L. Serkin ^{68a,68b}, M. Sessa ^{76a,76b}, H. Severini ¹¹⁹, S. Sevova ¹⁴², F. Sforza ^{57b,57a},
A. Sfyrly ⁵⁶, E. Shabalina ⁵⁵, R. Shaheen ¹⁴³, J.D. Shahinian ¹²⁷, N.W. Shaikh ^{47a,47b},
D. Shaked Renous ¹⁶⁷, L.Y. Shan ^{14a}, M. Shapiro ^{17a}, A. Sharma ³⁶, A.S. Sharma ¹⁶²,
P. Sharma ⁷⁹, S. Sharma ⁴⁸, P.B. Shatalov ³⁷, K. Shaw ¹⁴⁵, S.M. Shaw ¹⁰⁰, Q. Shen ^{62c},
P. Sherwood ⁹⁵, L. Shi ⁹⁵, C.O. Shimmin ¹⁷⁰, Y. Shimogama ¹⁶⁶, J.D. Shinner ⁹⁴,
I.P.J. Shipsey ¹²⁵, S. Shirabe ⁶⁰, M. Shiyakova ³⁸, J. Shlomi ¹⁶⁷, M.J. Shochet ³⁹,
J. Shojaii ¹⁰⁴, D.R. Shope ¹⁴³, S. Shrestha ¹¹⁸, E.M. Shrif ^{33g}, M.J. Shroff ¹⁶³,
P. Sicho ¹³⁰, A.M. Sickles ¹⁶⁰, E. Sideras Haddad ^{33g}, O. Sidiropoulou ³⁶, A. Sidoti ^{23b},
F. Siegert ⁵⁰, Dj. Sijacki ¹⁵, R. Sikora ^{84a}, F. Sili ⁸⁹, J.M. Silva ²⁰, M.V. Silva Oliveira ³⁶,
S.B. Silverstein ^{47a}, S. Simion ⁶⁶, R. Simoniello ³⁶, E.L. Simpson ⁵⁹, N.D. Simpson ⁹⁷,
S. Simsek ^{21d}, S. Sindhu ⁵⁵, P. Sinervo ¹⁵⁴, V. Sinetckii ³⁷, S. Singh ¹⁴¹, S. Singh ¹⁵⁴,
S. Sinha ⁴⁸, S. Sinha ^{33g}, M. Sioli ^{23b,23a}, I. Siral ¹²², S.Yu. Sivoklov ^{37,*},

J. Sjölin^{47a,47b}, A. Skaf⁵⁵, E. Skorda⁹⁷, P. Skubic¹¹⁹, M. Slawinska⁸⁵, V. Smakhtin¹⁶⁷, B.H. Smart¹³³, J. Smiesko¹³², S.Yu. Smirnov³⁷, Y. Smirnov³⁷, L.N. Smirnova^{37,a}, O. Smirnova⁹⁷, E.A. Smith³⁹, H.A. Smith¹²⁵, J.L. Smith⁹¹, R. Smith¹⁴², M. Smizanska⁹⁰, K. Smolek¹³¹, A. Smykiewicz⁸⁵, A.A. Snesev³⁷, H.L. Snoek¹¹³, S. Snyder²⁹, R. Sobie^{163,v}, A. Soffer¹⁵⁰, C.A. Solans Sanchez³⁶, E.Yu. Soldatov³⁷, U. Soldevila¹⁶¹, A.A. Solodkov³⁷, S. Solomon⁵⁴, A. Soloshenko³⁸, K. Solovieva⁵⁴, O.V. Solovyanov³⁷, V. Solovyev³⁷, P. Sommer³⁶, A. Sonay¹³, W.Y. Song^{155b}, A. Sopczak¹³¹, A.L. Sopio⁹⁵, F. Sopkova^{28b}, V. Sothilingam^{63a}, S. Sottocornola^{72a,72b}, R. Soualah^{115c}, Z. Soumami^{35e}, D. South⁴⁸, S. Spagnolo^{69a,69b}, M. Spalla¹⁰⁹, F. Spanò⁹⁴, D. Sperlich⁵⁴, G. Spigo³⁶, M. Spina¹⁴⁵, S. Spinali⁹⁰, D.P. Spiteri⁵⁹, M. Spousta¹³², E.J. Staats³⁴, A. Stabile^{70a,70b}, R. Stamen^{63a}, M. Stamenkovic¹¹³, A. Stampekis²⁰, M. Standke²⁴, E. Stanecka⁸⁵, B. Stanislaus^{17a}, M.M. Stanitzki⁴⁸, M. Stankaityte¹²⁵, B. Stapf⁴⁸, E.A. Starchenko³⁷, G.H. Stark¹³⁵, J. Stark^{101,aj}, D.M. Starko^{155b}, P. Staroba¹³⁰, P. Starovoitov^{63a}, S. Stärz¹⁰³, R. Staszewski⁸⁵, G. Stavropoulos⁴⁶, J. Steentoft¹⁵⁹, P. Steinberg²⁹, A.L. Steinhelb¹²², B. Stelzer^{141,155a}, H.J. Stelzer¹²⁸, O. Stelzer-Chilton^{155a}, H. Stenzel⁵⁸, T.J. Stevenson¹⁴⁵, G.A. Stewart³⁶, M.C. Stockton³⁶, G. Stoicea^{27b}, M. Stolarski^{129a}, S. Stonjek¹⁰⁹, A. Straessner⁵⁰, J. Strandberg¹⁴³, S. Strandberg^{47a,47b}, M. Strauss¹¹⁹, T. Streblor¹⁰¹, P. Strizenc^{28b}, R. Ströhmer¹⁶⁴, D.M. Strom¹²², L.R. Strom⁴⁸, R. Stroynowski⁴⁴, A. Strubig^{47a,47b}, S.A. Stucci²⁹, B. Stugu¹⁶, J. Stupak¹¹⁹, N.A. Styles⁴⁸, D. Su¹⁴², S. Su^{62a}, W. Su^{62d,137,62c}, X. Su^{62a,66}, K. Sugizaki¹⁵², V.V. Sulin³⁷, M.J. Sullivan⁹¹, D.M.S. Sultan^{77a,77b}, L. Sultanaliyeva³⁷, S. Sultansoy^{3b}, T. Sumida⁸⁶, S. Sun¹⁰⁵, S. Sun¹⁶⁸, O. Sunneborn Gudnadottir¹⁵⁹, M.R. Sutton¹⁴⁵, M. Svatos¹³⁰, M. Swiatkowski^{155a}, T. Swirski¹⁶⁴, I. Sykora^{28a}, M. Sykora¹³², T. Sykora¹³², D. Ta⁹⁹, K. Tackmann^{48,u}, A. Taffard¹⁵⁸, R. Tafirout^{155a}, J.S. Tafoya Vargas⁶⁶, R.H.M. Taibah¹²⁶, R. Takashima⁸⁷, K. Takeda⁸³, E.P. Takeva⁵², Y. Takubo⁸², M. Talby¹⁰¹, A.A. Talyshev³⁷, K.C. Tam^{64b}, N.M. Tamir¹⁵⁰, A. Tanaka¹⁵², J. Tanaka¹⁵², R. Tanaka⁶⁶, M. Tanasini^{57b,57a}, J. Tang^{62c}, Z. Tao¹⁶², S. Tapia Araya⁸⁰, S. Tapprogge⁹⁹, A. Tarek Abouelfadl Mohamed¹⁰⁶, S. Tarem¹⁴⁹, K. Tariq^{62b}, G. Tarna^{27b}, G.F. Tartarelli^{70a}, P. Tas¹³², M. Tasevsky¹³⁰, E. Tassi^{43b,43a}, A.C. Tate¹⁶⁰, G. Tateno¹⁵², Y. Tayalati^{35e}, G.N. Taylor¹⁰⁴, W. Taylor^{155b}, H. Teagle⁹¹, A.S. Tee¹⁶⁸, R. Teixeira De Lima¹⁴², P. Teixeira-Dias⁹⁴, J.J. Teoh¹⁵⁴, K. Terashi¹⁵², J. Terron⁹⁸, S. Terzo¹³, M. Testa⁵³, R.J. Teuscher^{154,v}, A. Thaler⁷⁸, N. Themistokleous⁵², T. Theveniaux-Pelzer¹⁸, O. Thielmann¹⁶⁹, D.W. Thomas⁹⁴, J.P. Thomas²⁰, E.A. Thompson⁴⁸, P.D. Thompson²⁰, E. Thomson¹²⁷, E.J. Thorpe⁹³, Y. Tian⁵⁵, V. Tikhomirov^{37,a}, Yu.A. Tikhonov³⁷, S. Timoshenko³⁷, E.X.L. Ting¹, P. Tipton¹⁷⁰, S. Tisserant¹⁰¹, S.H. Tlou^{33g}, A. Thourji⁴⁰, K. Todome^{23b,23a}, S. Todorova-Nova¹³², S. Todt⁵⁰, M. Togawa⁸², J. Tojo⁸⁸, S. Tokár^{28a}, K. Tokushuku⁸², R. Tombs³², M. Tomoto^{82,110}, L. Tompkins^{142,ai}, P. Tornambe¹⁰², E. Torrence¹²², H. Torres⁵⁰, E. Torró Pastor¹⁶¹, M. Toscani³⁰, C. Toscari³⁹, D.R. Tovey¹³⁸, A. Traet¹⁶, I.S. Trandafir^{27b}, T. Trefzger¹⁶⁴, A. Tricoli²⁹, I.M. Trigger^{155a}, S. Trincaz-Duvoid¹²⁶, D.A. Trischuk¹⁶², B. Trocmé⁶⁰, A. Trofymov⁶⁶, C. Troncon^{70a}, L. Truong^{33c}, M. Trzebinski⁸⁵, A. Trzupek⁸⁵, F. Tsai¹⁴⁴, M. Tsai¹⁰⁵,

A. Tsiamis¹⁵¹, P.V. Tsiareshka³⁷, S. Tsigaridas^{155a}, A. Tsirigotis^{151,s}, V. Tsiskaridze¹⁴⁴, E.G. Tskhadadze^{148a}, M. Tsopoulou¹⁵¹, Y. Tsujikawa⁸⁶, I.I. Tsukerman³⁷, V. Tsulaia^{17a}, S. Tsuno⁸², O. Tsur¹⁴⁹, D. Tsybychev¹⁴⁴, Y. Tu^{64b}, A. Tudorache^{27b}, V. Tudorache^{27b}, A.N. Tuna³⁶, S. Turchikhin³⁸, I. Turk Cakir^{3a}, R. Turra^{70a}, T. Turtuvshin³⁸, P.M. Tuts⁴¹, S. Tzamarias¹⁵¹, P. Tzanis¹⁰, E. Tzovara⁹⁹, K. Uchida¹⁵², F. Ukegawa¹⁵⁶, P.A. Ulloa Poblete^{136c}, G. Unal³⁶, M. Unal¹¹, A. Undrus²⁹, G. Unel¹⁵⁸, K. Uno¹⁵², J. Urban^{28b}, P. Urquijo¹⁰⁴, G. Usai⁸, R. Ushioda¹⁵³, M. Usman¹⁰⁷, Z. Uysal^{21b}, V. Vacek¹³¹, B. Vachon¹⁰³, K.O.H. Vadla¹²⁴, T. Vafeiadis³⁶, C. Valderanis¹⁰⁸, E. Valdes Santurio^{47a,47b}, M. Valente^{155a}, S. Valentinetti^{23b,23a}, A. Valero¹⁶¹, A. Vallier^{101,aj}, J.A. Valls Ferrer¹⁶¹, T.R. Van Daalen¹³⁷, P. Van Gemmeren⁶, S. Van Stroud⁹⁵, I. Van Vulpen¹¹³, M. Vanadia^{75a,75b}, W. Vandelli³⁶, M. Vandenbroucke¹³⁴, E.R. Vandewall¹²⁰, D. Vannicola¹⁵⁰, L. Vannoli^{57b,57a}, R. Vari^{74a}, E.W. Varnes⁷, C. Varni^{17a}, T. Varol¹⁴⁷, D. Varouchas⁶⁶, L. Varriale¹⁶¹, K.E. Varvell¹⁴⁶, M.E. Vasile^{27b}, L. Vaslin⁴⁰, G.A. Vasquez¹⁶³, F. Vazeille⁴⁰, T. Vazquez Schroeder³⁶, J. Veatch³¹, V. Vecchio¹⁰⁰, M.J. Veen¹¹³, I. Veliscek¹²⁵, L.M. Veloce¹⁵⁴, F. Veloso^{129a,129c}, S. Veneziano^{74a}, A. Ventura^{69a,69b}, A. Verbytskyi¹⁰⁹, M. Verducci^{73a,73b}, C. Vergis²⁴, M. Verissimo De Araujo^{81b}, W. Verkerke¹¹³, J.C. Vermeulen¹¹³, C. Vernieri¹⁴², P.J. Verschuuren⁹⁴, M. Vessella¹⁰², M.L. Vesterbacka¹¹⁶, M.C. Vetterli^{141,ab}, A. Vgenopoulos¹⁵¹, N. Viaux Maira^{136f}, T. Vickey¹³⁸, O.E. Vickey Boeriu¹³⁸, G.H.A. Viehhauser¹²⁵, L. Vigani^{63b}, M. Villa^{23b,23a}, M. Villaplana Perez¹⁶¹, E.M. Villhauer⁵², E. Vilucchi⁵³, M.G. Vinciter³⁴, G.S. Virdee²⁰, A. Vishwakarma⁵², C. Vittori^{23b,23a}, I. Vivarelli¹⁴⁵, V. Vladimirov¹⁶⁵, E. Voevodina¹⁰⁹, F. Vogel¹⁰⁸, P. Vokac¹³¹, J. Von Ahnen⁴⁸, E. Von Toerne²⁴, B. Vormwald³⁶, V. Vorobel¹³², K. Vorobev³⁷, M. Vos¹⁶¹, J.H. Vosseveld⁹¹, M. Vozak¹¹³, L. Vozdecky⁹³, N. Vranjes¹⁵, M. Vranjes Milosavljevic¹⁵, M. Vreeswijk¹¹³, R. Vuillermet³⁶, O. Vujanovic⁹⁹, I. Vukotic³⁹, S. Wada¹⁵⁶, C. Wagner¹⁰², W. Wagner¹⁶⁹, S. Wahdan¹⁶⁹, H. Wahlberg⁸⁹, R. Wakasa¹⁵⁶, M. Wakida¹¹⁰, V.M. Walbrecht¹⁰⁹, J. Walder¹³³, R. Walker¹⁰⁸, W. Walkowiak¹⁴⁰, A.M. Wang⁶¹, A.Z. Wang¹⁶⁸, C. Wang^{62a}, C. Wang^{62c}, H. Wang^{17a}, J. Wang^{64a}, P. Wang⁴⁴, R.-J. Wang⁹⁹, R. Wang⁶¹, R. Wang⁶, S.M. Wang¹⁴⁷, S. Wang^{62b}, T. Wang^{62a}, W.T. Wang⁷⁹, W.X. Wang^{62a}, X. Wang^{14c}, X. Wang¹⁶⁰, X. Wang^{62c}, Y. Wang^{62d}, Y. Wang^{14c}, Z. Wang¹⁰⁵, Z. Wang^{62d,51,62c}, Z. Wang¹⁰⁵, A. Warburton¹⁰³, R.J. Ward²⁰, N. Warrack⁵⁹, A.T. Watson²⁰, M.F. Watson²⁰, G. Watts¹³⁷, B.M. Waugh⁹⁵, A.F. Webb¹¹, C. Weber²⁹, M.S. Weber¹⁹, S.A. Weber³⁴, S.M. Weber^{63a}, C. Wei^{62a}, Y. Wei¹²⁵, A.R. Weidberg¹²⁵, J. Weingarten⁴⁹, M. Weirich⁹⁹, C. Weiser⁵⁴, C.J. Wells⁴⁸, T. Wenaus²⁹, B. Wendland⁴⁹, T. Wengler³⁶, N.S. Wenke¹⁰⁹, N. Vermes²⁴, M. Wessels^{63a}, K. Whalen¹²², A.M. Wharton⁹⁰, A.S. White⁶¹, A. White⁸, M.J. White¹, D. Whiteson¹⁵⁸, L. Wickremasinghe¹²³, W. Wiedenmann¹⁶⁸, C. Wiel⁵⁰, M. Wielers¹³³, N. Wieseotte⁹⁹, C. Wiglesworth⁴², L.A.M. Wiik-Fuchs⁵⁴, D.J. Wilbern¹¹⁹, H.G. Wilkens³⁶, D.M. Williams⁴¹, H.H. Williams¹²⁷, S. Williams³², S. Willocq¹⁰², P.J. Windischhofer¹²⁵, F. Winklmeier¹²², B.T. Winter⁵⁴, M. Wittgen¹⁴², M. Wobisch⁹⁶, A. Wolf⁹⁹, R. Wölker¹²⁵, J. Wollrath¹⁵⁸, M.W. Wolter⁸⁵, H. Wolters^{129a,129c}, V.W.S. Wong¹⁶², A.F. Wongel⁴⁸, S.D. Worm⁴⁸, B.K. Wosiek⁸⁵, K.W. Woźniak⁸⁵,

K. Wraight ⁵⁹, J. Wu ^{14a,14d}, M. Wu ^{64a}, S.L. Wu ¹⁶⁸, X. Wu ⁵⁶, Y. Wu ^{62a},
Z. Wu ^{134,62a}, J. Wuerzinger ¹²⁵, T.R. Wyatt ¹⁰⁰, B.M. Wynne ⁵², S. Xella ⁴², L. Xia ^{14c},
M. Xia ^{14b}, J. Xiang ^{64c}, X. Xiao ¹⁰⁵, M. Xie ^{62a}, X. Xie ^{62a}, J. Xiong ^{17a}, I. Xiotidis ¹⁴⁵,
D. Xu ^{14a}, H. Xu ^{62a}, H. Xu ^{62a}, L. Xu ^{62a}, R. Xu ¹²⁷, T. Xu ¹⁰⁵, W. Xu ¹⁰⁵, Y. Xu ^{14b},
Z. Xu ^{62b}, Z. Xu ¹⁴², B. Yabsley ¹⁴⁶, S. Yacoob ^{33a}, N. Yamaguchi ⁸⁸, Y. Yamaguchi ¹⁵³,
H. Yamauchi ¹⁵⁶, T. Yamazaki ^{17a}, Y. Yamazaki ⁸³, J. Yan ^{62c}, S. Yan ¹²⁵, Z. Yan ²⁵,
H.J. Yang ^{62c,62d}, H.T. Yang ^{17a}, S. Yang ^{62a}, T. Yang ^{64c}, X. Yang ^{62a}, X. Yang ^{14a},
Y. Yang ⁴⁴, Z. Yang ^{62a,105}, W.-M. Yao ^{17a}, Y.C. Yap ⁴⁸, H. Ye ^{14c}, J. Ye ⁴⁴, S. Ye ²⁹,
X. Ye ^{62a}, Y. Yeh ⁹⁵, I. Yeletsikh ³⁸, M.R. Yexley ⁹⁰, P. Yin ⁴¹, K. Yorita ¹⁶⁶,
C.J.S. Young ⁵⁴, C. Young ¹⁴², M. Yuan ¹⁰⁵, R. Yuan ^{62b,j}, L. Yue ⁹⁵, X. Yue ^{63a},
M. Zaazoua ^{35e}, B. Zabinski ⁸⁵, E. Zaid ⁵², T. Zakareishvili ^{148b}, N. Zakharchuk ³⁴,
S. Zambito ⁵⁶, J. Zang ¹⁵², D. Zanzi ⁵⁴, O. Zaplatilek ¹³¹, S.V. Zeißner ⁴⁹, C. Zeitnitz ¹⁶⁹,
J.C. Zeng ¹⁶⁰, D.T. Zenger Jr ²⁶, O. Zenin ³⁷, T. Ženiš ^{28a}, S. Zenz ⁹³, S. Zerradi ^{35a},
D. Zerwas ⁶⁶, B. Zhang ^{14c}, D.F. Zhang ¹³⁸, G. Zhang ^{14b}, J. Zhang ⁶, K. Zhang ^{14a,14d},
L. Zhang ^{14c}, R. Zhang ¹⁶⁸, S. Zhang ¹⁰⁵, T. Zhang ¹⁵², X. Zhang ^{62c}, X. Zhang ^{62b},
Z. Zhang ^{17a}, Z. Zhang ⁶⁶, H. Zhao ¹³⁷, P. Zhao ⁵¹, T. Zhao ^{62b}, Y. Zhao ¹³⁵,
Z. Zhao ^{62a}, A. Zhemchugov ³⁸, Z. Zheng ¹⁴², D. Zhong ¹⁶⁰, B. Zhou ¹⁰⁵, C. Zhou ¹⁶⁸,
H. Zhou ⁷, N. Zhou ^{62c}, Y. Zhou ⁷, C.G. Zhu ^{62b}, C. Zhu ^{14a,14d}, H.L. Zhu ^{62a}, H. Zhu ^{14a},
J. Zhu ¹⁰⁵, Y. Zhu ^{62a}, X. Zhuang ^{14a}, K. Zhukov ³⁷, V. Zhulanov ³⁷, N.I. Zimine ³⁸,
J. Zinsser ^{63b}, M. Ziolkowski ¹⁴⁰, L. Živković ¹⁵, A. Zoccoli ^{23b,23a}, K. Zoch ⁵⁶,
T.G. Zorbas ¹³⁸, O. Zormpa ⁴⁶, W. Zou ⁴¹, L. Zwalinski ³⁶

¹ Department of Physics, University of Adelaide, Adelaide; Australia

² Department of Physics, University of Alberta, Edmonton AB; Canada

³ ^(a) Department of Physics, Ankara University, Ankara; ^(b) Division of Physics, TOBB University of Economics and Technology, Ankara; Türkiye

⁴ LAPP, Université Savoie Mont Blanc, CNRS/IN2P3, Annecy, France

⁵ APC, Université Paris Cité, CNRS/IN2P3, Paris; France

⁶ High Energy Physics Division, Argonne National Laboratory, Argonne IL; United States of America

⁷ Department of Physics, University of Arizona, Tucson AZ; United States of America

⁸ Department of Physics, University of Texas at Arlington, Arlington TX; United States of America

⁹ Physics Department, National and Kapodistrian University of Athens, Athens; Greece

¹⁰ Physics Department, National Technical University of Athens, Zografou; Greece

¹¹ Department of Physics, University of Texas at Austin, Austin TX; United States of America

¹² Institute of Physics, Azerbaijan Academy of Sciences, Baku; Azerbaijan

¹³ Institut de Física d'Altes Energies (IFAE), Barcelona Institute of Science and Technology, Barcelona; Spain

¹⁴ ^(a) Institute of High Energy Physics, Chinese Academy of Sciences, Beijing; ^(b) Physics Department, Tsinghua University, Beijing; ^(c) Department of Physics, Nanjing University, Nanjing; ^(d) University of Chinese Academy of Science (UCAS), Beijing; China

¹⁵ Institute of Physics, University of Belgrade, Belgrade; Serbia

¹⁶ Department for Physics and Technology, University of Bergen, Bergen; Norway

¹⁷ ^(a) Physics Division, Lawrence Berkeley National Laboratory, Berkeley CA; ^(b) University of California, Berkeley CA; United States of America

¹⁸ Institut für Physik, Humboldt Universität zu Berlin, Berlin; Germany

¹⁹ Albert Einstein Center for Fundamental Physics and Laboratory for High Energy Physics, University of Bern, Bern; Switzerland

²⁰ School of Physics and Astronomy, University of Birmingham, Birmingham; United Kingdom

- ²¹ ^(a) Department of Physics, Bogazici University, Istanbul; ^(b) Department of Physics Engineering, Gaziantep University, Gaziantep; ^(c) Department of Physics, Istanbul University, Istanbul; ^(d) Istinye University, Sariyer, Istanbul; Türkiye
- ²² ^(a) Facultad de Ciencias y Centro de Investigaciones, Universidad Antonio Nariño, Bogotá; ^(b) Departamento de Física, Universidad Nacional de Colombia, Bogotá; Colombia
- ²³ ^(a) Dipartimento di Fisica e Astronomia A. Righi, Università di Bologna, Bologna; ^(b) INFN Sezione di Bologna; Italy
- ²⁴ Physikalisches Institut, Universität Bonn, Bonn; Germany
- ²⁵ Department of Physics, Boston University, Boston MA; United States of America
- ²⁶ Department of Physics, Brandeis University, Waltham MA; United States of America
- ²⁷ ^(a) Transilvania University of Brasov, Brasov; ^(b) Horia Hulubei National Institute of Physics and Nuclear Engineering, Bucharest; ^(c) Department of Physics, Alexandru Ioan Cuza University of Iasi, Iasi; ^(d) National Institute for Research and Development of Isotopic and Molecular Technologies, Physics Department, Cluj-Napoca; ^(e) University Politehnica Bucharest, Bucharest; ^(f) West University in Timisoara, Timisoara; ^(g) Faculty of Physics, University of Bucharest, Bucharest; Romania
- ²⁸ ^(a) Faculty of Mathematics, Physics and Informatics, Comenius University, Bratislava; ^(b) Department of Subnuclear Physics, Institute of Experimental Physics of the Slovak Academy of Sciences, Kosice; Slovak Republic
- ²⁹ Physics Department, Brookhaven National Laboratory, Upton NY; United States of America
- ³⁰ Universidad de Buenos Aires, Facultad de Ciencias Exactas y Naturales, Departamento de Física, y CONICET, Instituto de Física de Buenos Aires (IFIBA), Buenos Aires; Argentina
- ³¹ California State University, CA; United States of America
- ³² Cavendish Laboratory, University of Cambridge, Cambridge; United Kingdom
- ³³ ^(a) Department of Physics, University of Cape Town, Cape Town; ^(b) iThemba Labs, Western Cape; ^(c) Department of Mechanical Engineering Science, University of Johannesburg, Johannesburg; ^(d) National Institute of Physics, University of the Philippines Diliman (Philippines); ^(e) University of South Africa, Department of Physics, Pretoria; ^(f) University of Zululand, KwaDlangezwa; ^(g) School of Physics, University of the Witwatersrand, Johannesburg; South Africa
- ³⁴ Department of Physics, Carleton University, Ottawa ON; Canada
- ³⁵ ^(a) Faculté des Sciences Ain Chock, Réseau Universitaire de Physique des Hautes Energies - Université Hassan II, Casablanca; ^(b) Faculté des Sciences, Université Ibn-Tofail, Kénitra; ^(c) Faculté des Sciences Semlalia, Université Cadi Ayyad, LPHEA-Marrakech; ^(d) LPMR, Faculté des Sciences, Université Mohamed Premier, Oujda; ^(e) Faculté des sciences, Université Mohammed V, Rabat; ^(f) Institute of Applied Physics, Mohammed VI Polytechnic University, Ben Guerir; Morocco
- ³⁶ CERN, Geneva; Switzerland
- ³⁷ Affiliated with an institute covered by a cooperation agreement with CERN
- ³⁸ Affiliated with an international laboratory covered by a cooperation agreement with CERN
- ³⁹ Enrico Fermi Institute, University of Chicago, Chicago IL; United States of America
- ⁴⁰ LPC, Université Clermont Auvergne, CNRS/IN2P3, Clermont-Ferrand; France
- ⁴¹ Nevis Laboratory, Columbia University, Irvington NY; United States of America
- ⁴² Niels Bohr Institute, University of Copenhagen, Copenhagen; Denmark
- ⁴³ ^(a) Dipartimento di Fisica, Università della Calabria, Rende; ^(b) INFN Gruppo Collegato di Cosenza, Laboratori Nazionali di Frascati; Italy
- ⁴⁴ Physics Department, Southern Methodist University, Dallas TX; United States of America
- ⁴⁵ Physics Department, University of Texas at Dallas, Richardson TX; United States of America
- ⁴⁶ National Centre for Scientific Research "Demokritos", Agia Paraskevi; Greece
- ⁴⁷ ^(a) Department of Physics, Stockholm University; ^(b) Oskar Klein Centre, Stockholm; Sweden
- ⁴⁸ Deutsches Elektronen-Synchrotron DESY, Hamburg and Zeuthen; Germany
- ⁴⁹ Fakultät Physik, Technische Universität Dortmund, Dortmund; Germany
- ⁵⁰ Institut für Kern- und Teilchenphysik, Technische Universität Dresden, Dresden; Germany
- ⁵¹ Department of Physics, Duke University, Durham NC; United States of America
- ⁵² SUPA - School of Physics and Astronomy, University of Edinburgh, Edinburgh; United Kingdom

- ⁵³ INFN e Laboratori Nazionali di Frascati, Frascati; Italy
- ⁵⁴ Physikalisches Institut, Albert-Ludwigs-Universität Freiburg, Freiburg; Germany
- ⁵⁵ II. Physikalisches Institut, Georg-August-Universität Göttingen, Göttingen; Germany
- ⁵⁶ Département de Physique Nucléaire et Corpusculaire, Université de Genève, Genève; Switzerland
- ⁵⁷ ^(a) Dipartimento di Fisica, Università di Genova, Genova; ^(b) INFN Sezione di Genova; Italy
- ⁵⁸ II. Physikalisches Institut, Justus-Liebig-Universität Giessen, Giessen; Germany
- ⁵⁹ SUPA - School of Physics and Astronomy, University of Glasgow, Glasgow; United Kingdom
- ⁶⁰ LPSC, Université Grenoble Alpes, CNRS/IN2P3, Grenoble INP, Grenoble; France
- ⁶¹ Laboratory for Particle Physics and Cosmology, Harvard University, Cambridge MA; United States of America
- ⁶² ^(a) Department of Modern Physics and State Key Laboratory of Particle Detection and Electronics, University of Science and Technology of China, Hefei; ^(b) Institute of Frontier and Interdisciplinary Science and Key Laboratory of Particle Physics and Particle Irradiation (MOE), Shandong University, Qingdao; ^(c) School of Physics and Astronomy, Shanghai Jiao Tong University, Key Laboratory for Particle Astrophysics and Cosmology (MOE), SKLPPC, Shanghai; ^(d) Tsung-Dao Lee Institute, Shanghai; China
- ⁶³ ^(a) Kirchhoff-Institut für Physik, Ruprecht-Karls-Universität Heidelberg, Heidelberg; ^(b) Physikalisches Institut, Ruprecht-Karls-Universität Heidelberg, Heidelberg; Germany
- ⁶⁴ ^(a) Department of Physics, Chinese University of Hong Kong, Shatin, N.T., Hong Kong; ^(b) Department of Physics, University of Hong Kong, Hong Kong; ^(c) Department of Physics and Institute for Advanced Study, Hong Kong University of Science and Technology, Clear Water Bay, Kowloon, Hong Kong; China
- ⁶⁵ Department of Physics, National Tsing Hua University, Hsinchu; Taiwan
- ⁶⁶ IJCLab, Université Paris-Saclay, CNRS/IN2P3, 91405, Orsay; France
- ⁶⁷ Department of Physics, Indiana University, Bloomington IN; United States of America
- ⁶⁸ ^(a) INFN Gruppo Collegato di Udine, Sezione di Trieste, Udine; ^(b) ICTP, Trieste; ^(c) Dipartimento Politecnico di Ingegneria e Architettura, Università di Udine, Udine; Italy
- ⁶⁹ ^(a) INFN Sezione di Lecce; ^(b) Dipartimento di Matematica e Fisica, Università del Salento, Lecce; Italy
- ⁷⁰ ^(a) INFN Sezione di Milano; ^(b) Dipartimento di Fisica, Università di Milano, Milano; Italy
- ⁷¹ ^(a) INFN Sezione di Napoli; ^(b) Dipartimento di Fisica, Università di Napoli, Napoli; Italy
- ⁷² ^(a) INFN Sezione di Pavia; ^(b) Dipartimento di Fisica, Università di Pavia, Pavia; Italy
- ⁷³ ^(a) INFN Sezione di Pisa; ^(b) Dipartimento di Fisica E. Fermi, Università di Pisa, Pisa; Italy
- ⁷⁴ ^(a) INFN Sezione di Roma; ^(b) Dipartimento di Fisica, Sapienza Università di Roma, Roma; Italy
- ⁷⁵ ^(a) INFN Sezione di Roma Tor Vergata; ^(b) Dipartimento di Fisica, Università di Roma Tor Vergata, Roma; Italy
- ⁷⁶ ^(a) INFN Sezione di Roma Tre; ^(b) Dipartimento di Matematica e Fisica, Università Roma Tre, Roma; Italy
- ⁷⁷ ^(a) INFN-TIFPA; ^(b) Università degli Studi di Trento, Trento; Italy
- ⁷⁸ Universität Innsbruck, Department of Astro and Particle Physics, Innsbruck; Austria
- ⁷⁹ University of Iowa, Iowa City IA; United States of America
- ⁸⁰ Department of Physics and Astronomy, Iowa State University, Ames IA; United States of America
- ⁸¹ ^(a) Departamento de Engenharia Elétrica, Universidade Federal de Juiz de Fora (UFJF), Juiz de Fora; ^(b) Universidade Federal do Rio De Janeiro COPPE/EE/IF, Rio de Janeiro; ^(c) Instituto de Física, Universidade de São Paulo, São Paulo; ^(d) Rio de Janeiro State University, Rio de Janeiro; Brazil
- ⁸² KEK, High Energy Accelerator Research Organization, Tsukuba; Japan
- ⁸³ Graduate School of Science, Kobe University, Kobe; Japan
- ⁸⁴ ^(a) AGH University of Science and Technology, Faculty of Physics and Applied Computer Science, Krakow; ^(b) Marian Smoluchowski Institute of Physics, Jagiellonian University, Krakow; Poland
- ⁸⁵ Institute of Nuclear Physics Polish Academy of Sciences, Krakow; Poland
- ⁸⁶ Faculty of Science, Kyoto University, Kyoto; Japan
- ⁸⁷ Kyoto University of Education, Kyoto; Japan
- ⁸⁸ Research Center for Advanced Particle Physics and Department of Physics, Kyushu University, Fukuoka; Japan

- ⁸⁹ Instituto de Física La Plata, Universidad Nacional de La Plata and CONICET, La Plata; Argentina
- ⁹⁰ Physics Department, Lancaster University, Lancaster; United Kingdom
- ⁹¹ Oliver Lodge Laboratory, University of Liverpool, Liverpool; United Kingdom
- ⁹² Department of Experimental Particle Physics, Jožef Stefan Institute and Department of Physics, University of Ljubljana, Ljubljana; Slovenia
- ⁹³ School of Physics and Astronomy, Queen Mary University of London, London; United Kingdom
- ⁹⁴ Department of Physics, Royal Holloway University of London, Egham; United Kingdom
- ⁹⁵ Department of Physics and Astronomy, University College London, London; United Kingdom
- ⁹⁶ Louisiana Tech University, Ruston LA; United States of America
- ⁹⁷ Fysiska institutionen, Lunds universitet, Lund; Sweden
- ⁹⁸ Departamento de Física Teórica C-15 and CIAFF, Universidad Autónoma de Madrid, Madrid; Spain
- ⁹⁹ Institut für Physik, Universität Mainz, Mainz; Germany
- ¹⁰⁰ School of Physics and Astronomy, University of Manchester, Manchester; United Kingdom
- ¹⁰¹ CPPM, Aix-Marseille Université, CNRS/IN2P3, Marseille; France
- ¹⁰² Department of Physics, University of Massachusetts, Amherst MA; United States of America
- ¹⁰³ Department of Physics, McGill University, Montreal QC; Canada
- ¹⁰⁴ School of Physics, University of Melbourne, Victoria; Australia
- ¹⁰⁵ Department of Physics, University of Michigan, Ann Arbor MI; United States of America
- ¹⁰⁶ Department of Physics and Astronomy, Michigan State University, East Lansing MI; United States of America
- ¹⁰⁷ Group of Particle Physics, University of Montreal, Montreal QC; Canada
- ¹⁰⁸ Fakultät für Physik, Ludwig-Maximilians-Universität München, München; Germany
- ¹⁰⁹ Max-Planck-Institut für Physik (Werner-Heisenberg-Institut), München; Germany
- ¹¹⁰ Graduate School of Science and Kobayashi-Maskawa Institute, Nagoya University, Nagoya; Japan
- ¹¹¹ Department of Physics and Astronomy, University of New Mexico, Albuquerque NM; United States of America
- ¹¹² Institute for Mathematics, Astrophysics and Particle Physics, Radboud University/Nikhef, Nijmegen; Netherlands
- ¹¹³ Nikhef National Institute for Subatomic Physics and University of Amsterdam, Amsterdam; Netherlands
- ¹¹⁴ Department of Physics, Northern Illinois University, DeKalb IL; United States of America
- ¹¹⁵ ^(a) New York University Abu Dhabi, Abu Dhabi; ^(b) United Arab Emirates University, Al Ain; ^(c) University of Sharjah, Sharjah; United Arab Emirates
- ¹¹⁶ Department of Physics, New York University, New York NY; United States of America
- ¹¹⁷ Ochanomizu University, Otsuka, Bunkyo-ku, Tokyo; Japan
- ¹¹⁸ Ohio State University, Columbus OH; United States of America
- ¹¹⁹ Homer L. Dodge Department of Physics and Astronomy, University of Oklahoma, Norman OK; United States of America
- ¹²⁰ Department of Physics, Oklahoma State University, Stillwater OK; United States of America
- ¹²¹ Palacký University, Joint Laboratory of Optics, Olomouc; Czech Republic
- ¹²² Institute for Fundamental Science, University of Oregon, Eugene, OR; United States of America
- ¹²³ Graduate School of Science, Osaka University, Osaka; Japan
- ¹²⁴ Department of Physics, University of Oslo, Oslo; Norway
- ¹²⁵ Department of Physics, Oxford University, Oxford; United Kingdom
- ¹²⁶ LPNHE, Sorbonne Université, Université Paris Cité, CNRS/IN2P3, Paris; France
- ¹²⁷ Department of Physics, University of Pennsylvania, Philadelphia PA; United States of America
- ¹²⁸ Department of Physics and Astronomy, University of Pittsburgh, Pittsburgh PA; United States of America
- ¹²⁹ ^(a) Laboratório de Instrumentação e Física Experimental de Partículas - LIP, Lisboa; ^(b) Departamento de Física, Faculdade de Ciências, Universidade de Lisboa, Lisboa; ^(c) Departamento de Física, Universidade de Coimbra, Coimbra; ^(d) Centro de Física Nuclear da Universidade de Lisboa, Lisboa; ^(e) Departamento de Física, Universidade do Minho, Braga; ^(f) Departamento de Física Teórica y del

- Cosmos, Universidad de Granada, Granada (Spain); ^(g) Departamento de Física, Instituto Superior Técnico, Universidade de Lisboa, Lisboa; Portugal
- ¹³⁰ Institute of Physics of the Czech Academy of Sciences, Prague; Czech Republic
- ¹³¹ Czech Technical University in Prague, Prague; Czech Republic
- ¹³² Charles University, Faculty of Mathematics and Physics, Prague; Czech Republic
- ¹³³ Particle Physics Department, Rutherford Appleton Laboratory, Didcot; United Kingdom
- ¹³⁴ IRFU, CEA, Université Paris-Saclay, Gif-sur-Yvette; France
- ¹³⁵ Santa Cruz Institute for Particle Physics, University of California Santa Cruz, Santa Cruz CA; United States of America
- ¹³⁶ ^(a) Departamento de Física, Pontificia Universidad Católica de Chile, Santiago; ^(b) Millennium Institute for Subatomic physics at high energy frontier (SAPHIR), Santiago; ^(c) Instituto de Investigación Multidisciplinario en Ciencia y Tecnología, y Departamento de Física, Universidad de La Serena; ^(d) Universidad Andres Bello, Department of Physics, Santiago; ^(e) Instituto de Alta Investigación, Universidad de Tarapacá, Arica; ^(f) Departamento de Física, Universidad Técnica Federico Santa María, Valparaíso; Chile
- ¹³⁷ Department of Physics, University of Washington, Seattle WA; United States of America
- ¹³⁸ Department of Physics and Astronomy, University of Sheffield, Sheffield; United Kingdom
- ¹³⁹ Department of Physics, Shinshu University, Nagano; Japan
- ¹⁴⁰ Department Physik, Universität Siegen, Siegen; Germany
- ¹⁴¹ Department of Physics, Simon Fraser University, Burnaby BC; Canada
- ¹⁴² SLAC National Accelerator Laboratory, Stanford CA; United States of America
- ¹⁴³ Department of Physics, Royal Institute of Technology, Stockholm; Sweden
- ¹⁴⁴ Departments of Physics and Astronomy, Stony Brook University, Stony Brook NY; United States of America
- ¹⁴⁵ Department of Physics and Astronomy, University of Sussex, Brighton; United Kingdom
- ¹⁴⁶ School of Physics, University of Sydney, Sydney; Australia
- ¹⁴⁷ Institute of Physics, Academia Sinica, Taipei; Taiwan
- ¹⁴⁸ ^(a) E. Andronikashvili Institute of Physics, Iv. Javakishvili Tbilisi State University, Tbilisi; ^(b) High Energy Physics Institute, Tbilisi State University, Tbilisi; ^(c) University of Georgia, Tbilisi; Georgia
- ¹⁴⁹ Department of Physics, Technion, Israel Institute of Technology, Haifa; Israel
- ¹⁵⁰ Raymond and Beverly Sackler School of Physics and Astronomy, Tel Aviv University, Tel Aviv; Israel
- ¹⁵¹ Department of Physics, Aristotle University of Thessaloniki, Thessaloniki; Greece
- ¹⁵² International Center for Elementary Particle Physics and Department of Physics, University of Tokyo, Tokyo; Japan
- ¹⁵³ Department of Physics, Tokyo Institute of Technology, Tokyo; Japan
- ¹⁵⁴ Department of Physics, University of Toronto, Toronto ON; Canada
- ¹⁵⁵ ^(a) TRIUMF, Vancouver BC; ^(b) Department of Physics and Astronomy, York University, Toronto ON; Canada
- ¹⁵⁶ Division of Physics and Tomonaga Center for the History of the Universe, Faculty of Pure and Applied Sciences, University of Tsukuba, Tsukuba; Japan
- ¹⁵⁷ Department of Physics and Astronomy, Tufts University, Medford MA; United States of America
- ¹⁵⁸ Department of Physics and Astronomy, University of California Irvine, Irvine CA; United States of America
- ¹⁵⁹ Department of Physics and Astronomy, University of Uppsala, Uppsala; Sweden
- ¹⁶⁰ Department of Physics, University of Illinois, Urbana IL; United States of America
- ¹⁶¹ Instituto de Física Corpuscular (IFIC), Centro Mixto Universidad de Valencia - CSIC, Valencia; Spain
- ¹⁶² Department of Physics, University of British Columbia, Vancouver BC; Canada
- ¹⁶³ Department of Physics and Astronomy, University of Victoria, Victoria BC; Canada
- ¹⁶⁴ Fakultät für Physik und Astronomie, Julius-Maximilians-Universität Würzburg, Würzburg; Germany
- ¹⁶⁵ Department of Physics, University of Warwick, Coventry; United Kingdom
- ¹⁶⁶ Waseda University, Tokyo; Japan

¹⁶⁷ *Department of Particle Physics and Astrophysics, Weizmann Institute of Science, Rehovot; Israel*

¹⁶⁸ *Department of Physics, University of Wisconsin, Madison WI; United States of America*

¹⁶⁹ *Fakultät für Mathematik und Naturwissenschaften, Fachgruppe Physik, Bergische Universität Wuppertal, Wuppertal; Germany*

¹⁷⁰ *Department of Physics, Yale University, New Haven CT; United States of America*

^a *Also Affiliated with an institute covered by a cooperation agreement with CERN*

^b *Also at Borough of Manhattan Community College, City University of New York, New York NY; United States of America*

^c *Also at Bruno Kessler Foundation, Trento; Italy*

^d *Also at Center for High Energy Physics, Peking University; China*

^e *Also at Centro Studi e Ricerche Enrico Fermi; Italy*

^f *Also at CERN, Geneva; Switzerland*

^g *Also at Département de Physique Nucléaire et Corpusculaire, Université de Genève, Genève; Switzerland*

^h *Also at Departament de Física de la Universitat Autònoma de Barcelona, Barcelona; Spain*

ⁱ *Also at Department of Financial and Management Engineering, University of the Aegean, Chios; Greece*

^j *Also at Department of Physics and Astronomy, Michigan State University, East Lansing MI; United States of America*

^k *Also at Department of Physics and Astronomy, University of Louisville, Louisville, KY; United States of America*

^l *Also at Department of Physics, Ben Gurion University of the Negev, Beer Sheva; Israel*

^m *Also at Department of Physics, California State University, East Bay; United States of America*

ⁿ *Also at Department of Physics, California State University, Sacramento; United States of America*

^o *Also at Department of Physics, King's College London, London; United Kingdom*

^p *Also at Department of Physics, University of Fribourg, Fribourg; Switzerland*

^q *Also at Department of Physics, University of Thessaly; Greece*

^r *Also at Department of Physics, Westmont College, Santa Barbara; United States of America*

^s *Also at Hellenic Open University, Patras; Greece*

^t *Also at Institutio Catalana de Recerca i Estudis Avancats, ICREA, Barcelona; Spain*

^u *Also at Institut für Experimentalphysik, Universität Hamburg, Hamburg; Germany*

^v *Also at Institute of Particle Physics (IPP); Canada*

^w *Also at Institute of Physics, Azerbaijan Academy of Sciences, Baku; Azerbaijan*

^x *Also at Institute of Theoretical Physics, Ilia State University, Tbilisi; Georgia*

^y *Also at Lawrence Livermore National Laboratory, Livermore; United States of America*

^z *Also at The City College of New York, New York NY; United States of America*

^{aa} *Also at The Collaborative Innovation Center of Quantum Matter (CICQM), Beijing; China*

^{ab} *Also at TRIUMF, Vancouver BC; Canada*

^{ac} *Also at Università di Napoli Parthenope, Napoli; Italy*

^{ad} *Also at University of Chinese Academy of Sciences (UCAS), Beijing; China*

^{ae} *Also at University of Colorado Boulder, Department of Physics, Colorado; United States of America*

^{af} *Also at Yeditepe University, Physics Department, Istanbul; Türkiye*

^{ag} *Also at An-Najah National University, Nablus; Palestine*

^{ah} *Also at National Institute of Physics, University of the Philippines Diliman (Philippines); Philippines*

^{ai} *Also at Department of Physics, Stanford University, Stanford CA; United States of America*

^{aj} *Also at L2IT, Université de Toulouse, CNRS/IN2P3, UPS, Toulouse; France*

^{*} *Deceased*